Infrared Spectra of Propene in Helium Nanodroplets and Solid *para*-Hydrogen

Gregory T. Pullen, Peter R. Franke, Gary E. Douberly, Yuan-Pern Lee

June 21, 2018
RG 04

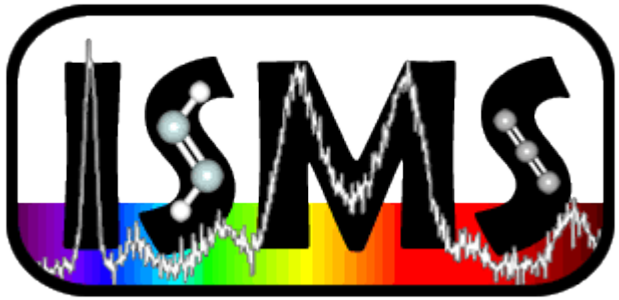

Background

Microwave

Lide, D. R.; Mann, D. E. MICROWAVE SPECTRA OF MOLECULES EXHIBITING INTERNAL ROTATION .1. PROPYLENE. *J. Chem. Phys.* **1957**, *27*, 868-873.

Lide, D. R.; Christensen, D. MOLECULAR STRUCTURE OF PROPYLENE. *J. Chem. Phys.* **1961**, *35*, 1374-&.

Wlodarczak, G.; Demaison, J.; Heineking, N.; Csaszar, A. G. THE ROTATIONAL SPECTRUM OF PROPENE - INTERNAL-ROTATION ANALYSIS AND AB-INITIO AND EXPERIMENTAL CENTRIFUGAL-DISTORTION CONSTANTS. *J. Mol. Spectrosc.* **1994**, *167*, 239-247.

Craig, N. C.; Groner, P.; Conrad, A. R.; Gurusinghe, R.; Tubergen, M. J. Microwave spectra for the three C-13(1) isotopologues of propene and new rotational constants for propene and its C-13(1) isotopologues. *J. Mol. Spectrosc.* **2016**, *328*, 1-6.

Photoelectron

Saethre, L. J.; Svaeren, O.; Svensson, S.; Osborne, S.; Thomas, T. D.; Jauhiainen, J.; Aksela, S. High-resolution C 1s photoelectron spectra of methane, ethene, propene, and 2-methylpropene. *Phys. Rev. A* **1997**, *55*, 2748-2756.

Theory

Jona, P.; Gussoni, M.; Zerbi, G. TRANSFERABILITY OF INFRARED INTENSITY PARAMETERS - APPLICATION TO PROPYLENE. *J. Mol. Struct.* **1982**, *95*, 15-21.

Chhiba, M.; Vergoten, G. THE STRUCTURES AND VIBRATIONAL FREQUENCIES OF A SERIES OF LINEAR ALKENES OBTAINED USING THE SPECTROSCOPIC POTENTIAL SPASIBA. *J. Mol. Struct.* **1994**, *326*, 35-58.

Demaison, J.; Rudolph, H. D. Ab initio anharmonic force field and equilibrium structure of propene. *J. Mol. Spectrosc.* **2008**, *248*, 66-76.

Hickson, K. M.; Wakelam, V.; Loison, J. C. Methylacetylene (CH3CCH) and propene (C3H6) formation in cold dense clouds: A case of dust grain chemistry. *Mol. Astrophys.* **2016**, *3-4*, 1-9.

Infrared

Lord, R. C.; Venkateswarlu, P. THE INFRARED SPECTRA OF PROPYLENE AND PROPYLENE-D6. *Journal of the Optical Society of America* **1953**, *43*, 1079-1085.

Silvi, B.; Labarbe, P.; Perchard, J. P. VIBRATION-SPECTRA AND NORMAL COORDINATES OF 4 ISOTOPES OF PROPENE. *Spectroc. Acta Pt. A-Molec. Biomolec. Spectr.* **1973**, *A 29*, 263-276.

McKean, D. C. CH STRETCHING FREQUENCIES, BOND LENGTHS AND STRENGTHS IN ACETONE, ACETALDEHYDE, PROPENE AND ISOBUTENE. *Spectroc. Acta Pt. A-Molec. Biomolec. Spectr.* **1975**, *31*, 861-870.

Fang, H. L.; Swofford, R. L.; McDevitt, M.; Anderson, A. B. C-H STRETCHING OVERTONE SPECTRUM OF PROPYLENE - MOLECULAR-ORBITAL ANALYSIS IN THE LOCAL-MODE MODEL. *J. Phys. Chem.* **1985**, *89*, 225-229.

Durig, J. R.; Guirgis, G. A.; Bell, S. TORSIONAL SPECTRUM AND ABINITIO CALCULATIONS FOR PROPENE. *J. Phys. Chem.* **1989**, *93*, 3487-3491.

Baylor, L. C.; Weitz, E. OVERTONE SPECTROSCOPY OF CIS-PROPENE-1,2-D2. *J. Phys. Chem.* **1990**, *94*, 6209-6220.

Ainetschian, A.; Fraser, G. T.; Ortigoso, J.; Pate, B. H. CONTAMINATED TORSIONAL TUNNELING SPLITTINGS IN 5 NORMAL-MODE VIBRATIONS OF PROPENE. *J. Chem. Phys.* **1994**, *100*, 729-732.

Zakharieva, O.; Forster, H.; Turneva, M. NORMAL-COORDINATE ANALYSIS OF DEUTERO PROPENES IN THE FREE AND ZEOLITE-ADSORBED STATE. *Spectroc. Acta Pt. A-Molec. Biomolec. Spectr.* **1994**, *50*, 19-28.

Lafferty, W. J.; Flaud, J. M.; Herman, M. Resolved torsional splitting in the v(18) and v(19-) bands of propene. *J. Mol. Struct.* **2006**, *780-81*, 65-69.

Es-sebbar, E. T.; Alrefae, M.; Farooq, A. Infrared cross-sections and integrated band intensities of propylene: Temperature-dependent studies. *J. Quant. Spectrosc. Radiat. Transf.* **2014**, *133*, 559-569.

Buzan, E. M.; Hargreaves, R. J.; Bernath, P. F. High resolution absorption cross sections for propylene in the 3 μm region at high temperatures. *Mol. Astrophys.* **2016**, *3-4*, 16-20.

Sung, K.; Toon, G. C.; Drouin, B. J.; Mantz, A. W.; Smith, M. A. H. FT-IR measurements of cold propene (C3H6) cross-sections at temperatures between 150 and 299 K. *J. Quant. Spectrosc. Radiat. Transf.* **2018**, *213*, 119-132.

Background

Microwave

Lide, D. R.; Mann, D. E. MICROWAVE SPECTRA OF MOLECULES EXHIBITING INTERNAL ROTATION .1. PROPYLENE. *J. Chem. Phys.* **1957**, *27*, 868-873.
Lide, D. R.; Christensen, D. MOLECULAR STRUCTURE OF PROPYLENE. *J. Chem. Phys.* **1961**, *35*, 1374-&.
Wlodarczak, G.; Demaison, J.; Heineking, N.; Csaszar, A. G. THE ROTATIONAL SPECTRUM OF PROPENE - INTERNAL-ROTATION ANALYSIS AND AB-INITIO AND EXPERIMENTAL CENTRIFUGAL-DISTORTION CONSTANTS. *J. Mol. Spectrosc.* **1994**, *167*, 239-247.
Craig, N. C.; Groner, P.; Conrad, A. R.; Gurusinghe, R.; Tubergen, M. J. Microwave spectra for the three C-13(1) isotopologues of propene and new rotational constants for propene and its C-13(1) isotopologues. *J. Mol. Spectrosc.* **2016**, *328*, 1-6.

Photoelectron

Saethre, L. J.; Svaeren, O.; Svensson, S.; Osborne, S.; Thomas, T. D.; Jauhiainen, J.; Aksela, S. High-resolution C 1s photoelectron spectra of methane, ethene, propene, and 2-methylpropene. *Phys. Rev. A* **1997**, *55*, 2748-2756.

Theory

Jona, P.; Gussoni, M.; Zerbi, G. TRANSFERABILITY OF INFRARED INTENSITY PARAMETERS - APPLICATION TO PROPYLENE. *J. Mol. Struct.* **1982**, *95*, 15-21.
Chhiba, M.; Vergoten, G. THE STRUCTURES AND VIBRATIONAL FREQUENCIES OF A SERIES OF LINEAR ALKENES OBTAINED USING THE SPECTROSCOPIC POTENTIAL SPASIBA. *J. Mol. Struct.* **1994**, *326*, 35-58.
Demaison, J.; Rudolph, H. D. Ab initio anharmonic force field and equilibrium structure of propene. *J. Mol. Spectrosc.* **2008**, *248*, 66-76.
Hickson, K. M.; Wakelam, V.; Loison, J. C. Methylacetylene (CH3CCH) and propene (C3H6) formation in cold dense clouds: A case of dust grain chemistry. *Mol. Astrophys.* **2016**, *3-4*, 1-9.

Infrared

Lord, R. C.; Venkateswarlu, P. THE INFRARED SPECTRA OF PROPYLENE AND PROPYLENE-D6. *Journal of the Optical Society of America* **1953**, *43*, 1079-1085.
Silvi, B.; Labarbe, P.; Perchard, J. P. VIBRATION-SPECTRA AND NORMAL COORDINATES OF 4 ISOTOPES OF PROPENE. *Spectroc. Acta Pt. A-Molec. Biomolec. Spectr.* **1973**, *A 29*, 263-276.
McKean, D. C. CH STRETCHING FREQUENCIES, BOND LENGTHS AND STRENGTHS IN ACETONE, ACETALDEHYDE, PROPENE AND ISOBUTENE. *Spectroc. Acta Pt. A-Molec. Biomolec. Spectr.* **1975**, *31*, 861-870.
Fang, H. L.; Swofford, R. L.; McDevitt, M.; Anderson, A. B. C-H STRETCHING OVERTONE SPECTRUM OF PROPYLENE - MOLECULAR-ORBITAL ANALYSIS IN THE LOCAL-MODE MODEL. *J. Phys. Chem.* **1985**, *89*, 225-229.
Durig, J. R.; Guirgis, G. A.; Bell, S. TORSIONAL SPECTRUM AND ABINITIO CALCULATIONS FOR PROPENE. *J. Phys. Chem.* **1989**, *93*, 3487-3491.
Baylor, L. C.; Weitz, E. OVERTONE SPECTROSCOPY OF CIS-PROPENE-1,2-D2. *J. Phys. Chem.* **1990**, *94*, 6209-6220.
Ainetschian, A.; Fraser, G. T.; Ortigoso, J.; Pate, B. H. CONTAMINATED TORSIONAL TUNNELING SPLITTINGS IN 5 NORMAL-MODE VIBRATIONS OF PROPENE. *J. Chem. Phys.* **1994**, *100*, 729-732.
Zakharieva, O.; Forster, H.; Turneva, M. NORMAL-COORDINATE ANALYSIS OF DEUTERO PROPENES IN THE FREE AND ZEOLITE-ADSORBED STATE. *Spectroc. Acta Pt. A-Molec. Biomolec. Spectr.* **1994**, *50*, 19-28.
Lafferty, W. J.; Flaud, J. M.; Herman, M. Resolved torsional splitting in the ν(18) and ν(19) bands of propene. *J. Mol. Struct.* **2006**, *780-81*, 65-69.
Es-sebbar, E. T.; Alrefae, M.; Farooq, A. Infrared cross-sections and integrated band intensities of propylene: Temperature-dependent studies. *J. Quant. Spectrosc. Radiat. Transf.* **2014**, *133*, 559-569.
Buzan, E. M.; Hargreaves, R. J.; Bernath, P. F. High resolution absorption cross sections for propylene in the 3 μm region at high temperatures. *Mol. Astrophys.* **2016**, *3-4*, 16-20.
Sung, K.; Toon, G. C.; Drouin, B. J.; Mantz, A. W.; Smith, M. A. H. FT-IR measurements of cold propene (C3H6) cross-sections at temperatures between 150 and 299 K. *J. Quant. Spectrosc. Radiat. Transf.* **2018**, *213*, 119-132.

Background

Buzan, E. M.; Hargreaves, R. J.; Bernath, P. F. High resolution absorption cross sections for propylene in the 3 µm region at high temperatures. *Mol. Astrophys.* **2016**, *3-4*, 16-20.

Es-sebbar, E. T.; Alrefae, M.; Farooq, A. Infrared cross-sections and integrated band intensities of propylene: Temperature-dependent studies. *J. Quant. Spectrosc. Radiat. Transf.* **2014**, *133*, 559-569.

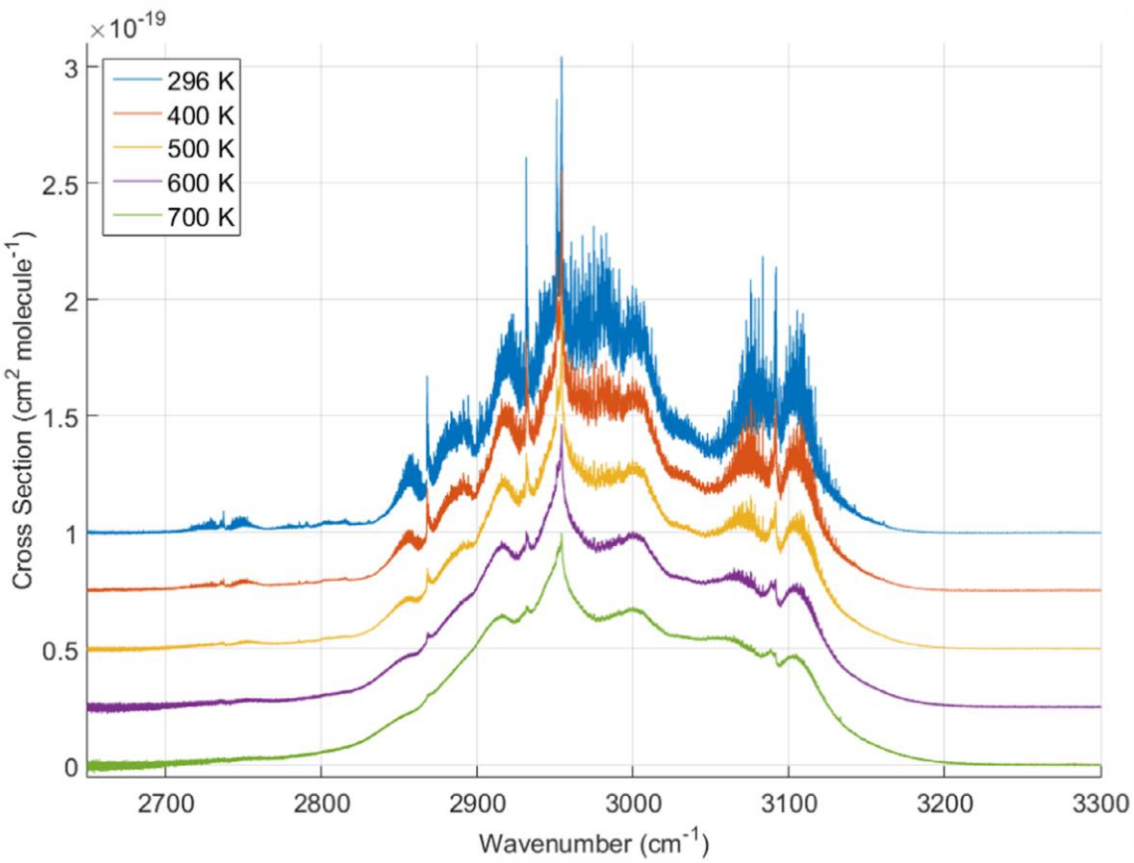

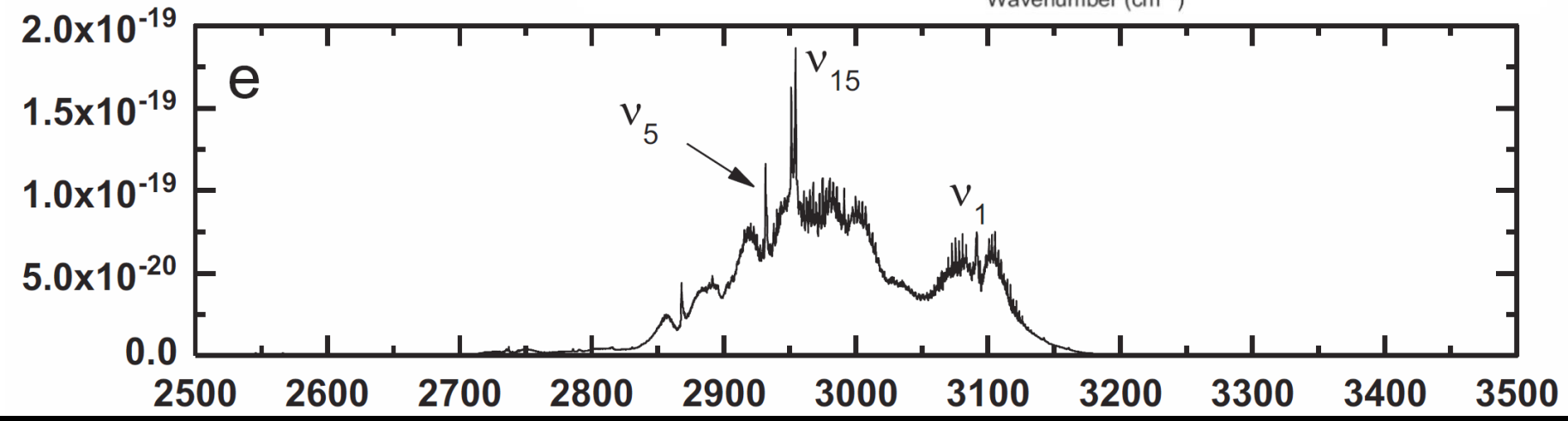

HENDI Setup

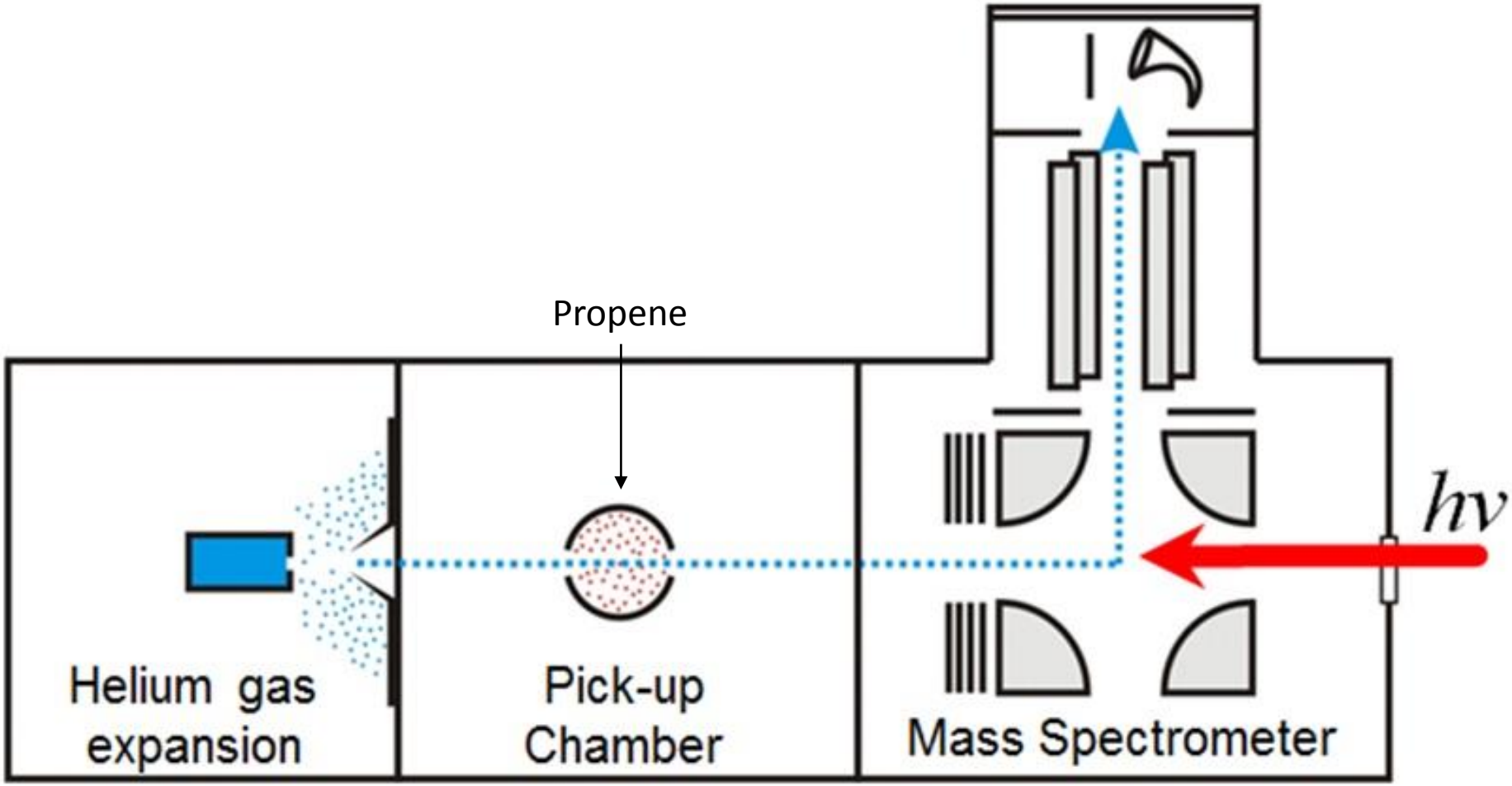
Propene
hv
Helium gas expansion
Pick-up Chamber
Mass Spectrometer

HENDI Setup

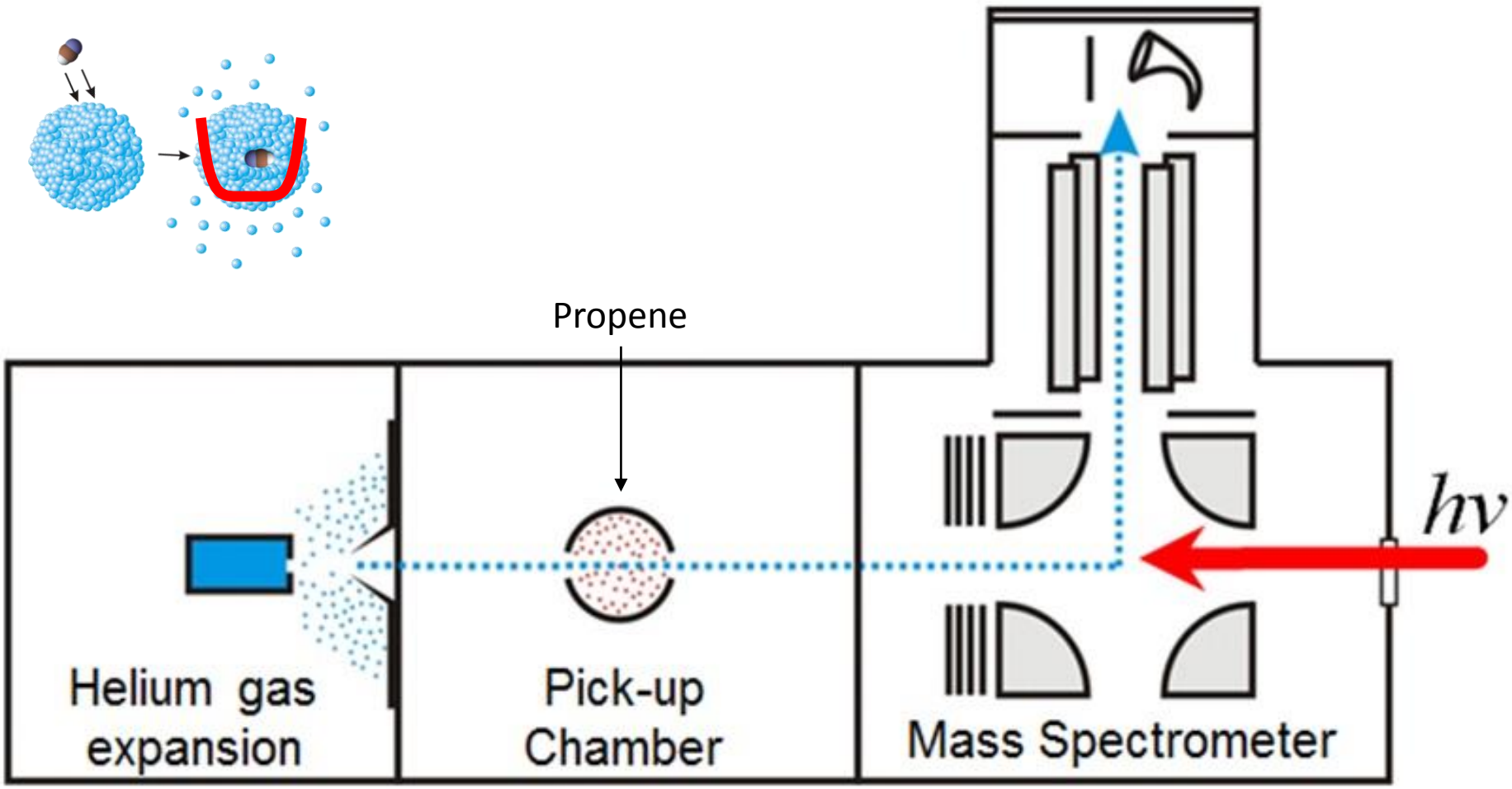
Propene
hv
Helium gas expansion
Pick-up Chamber
Mass Spectrometer

HENDI Setup

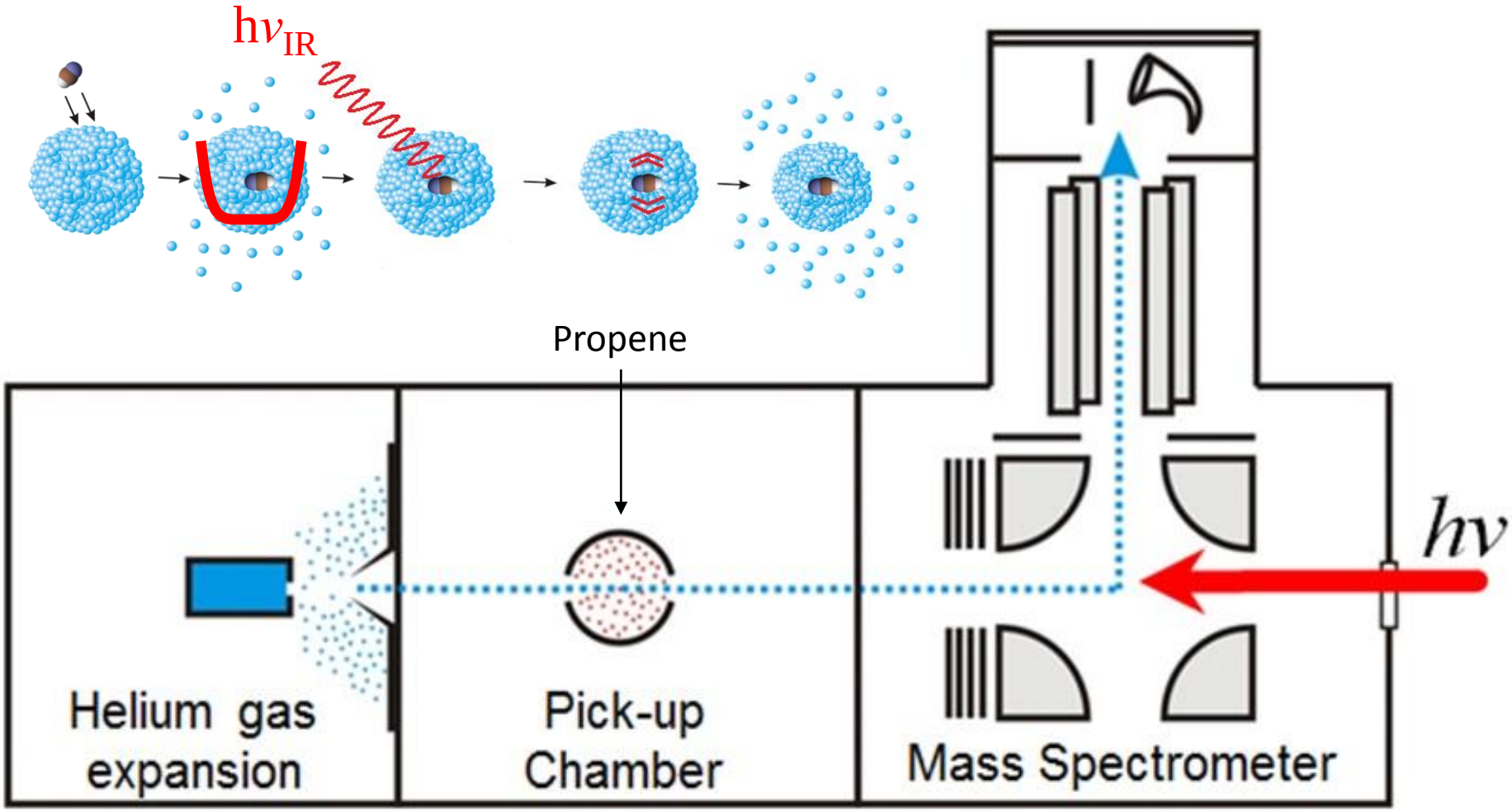
hν_IR
Propene
hν
Helium gas expansion
Pick-up Chamber
Mass Spectrometer

p-H_2 Setup

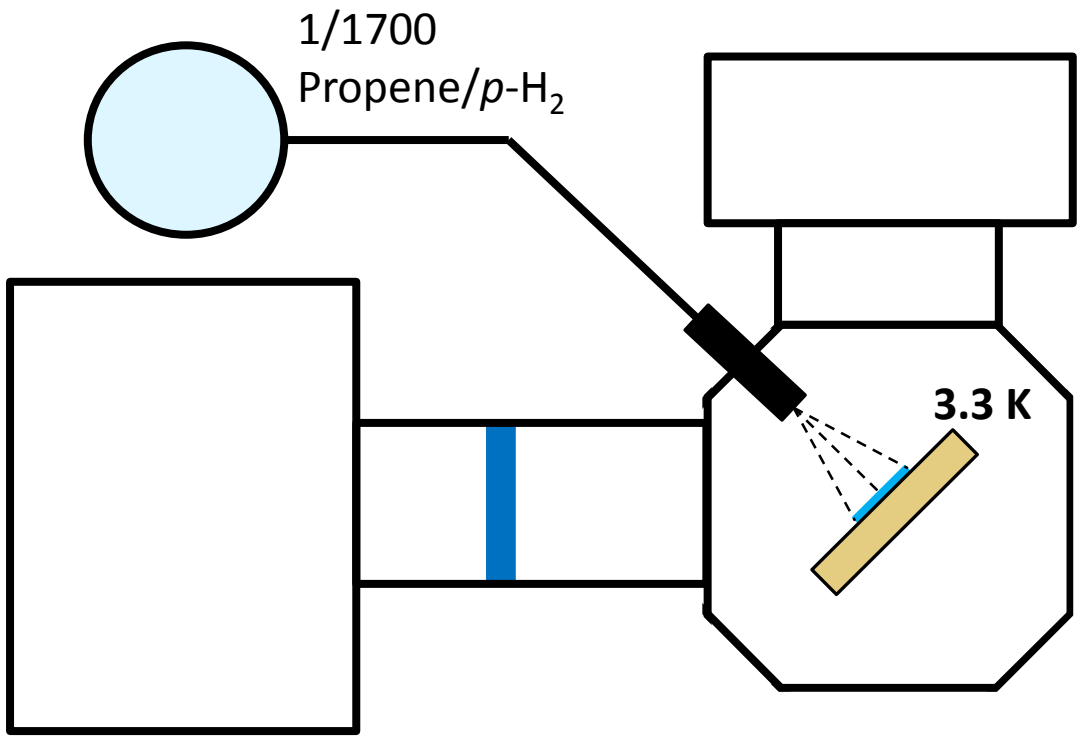

10 hr (~11 mmol/hr)

p-H_2 Setup

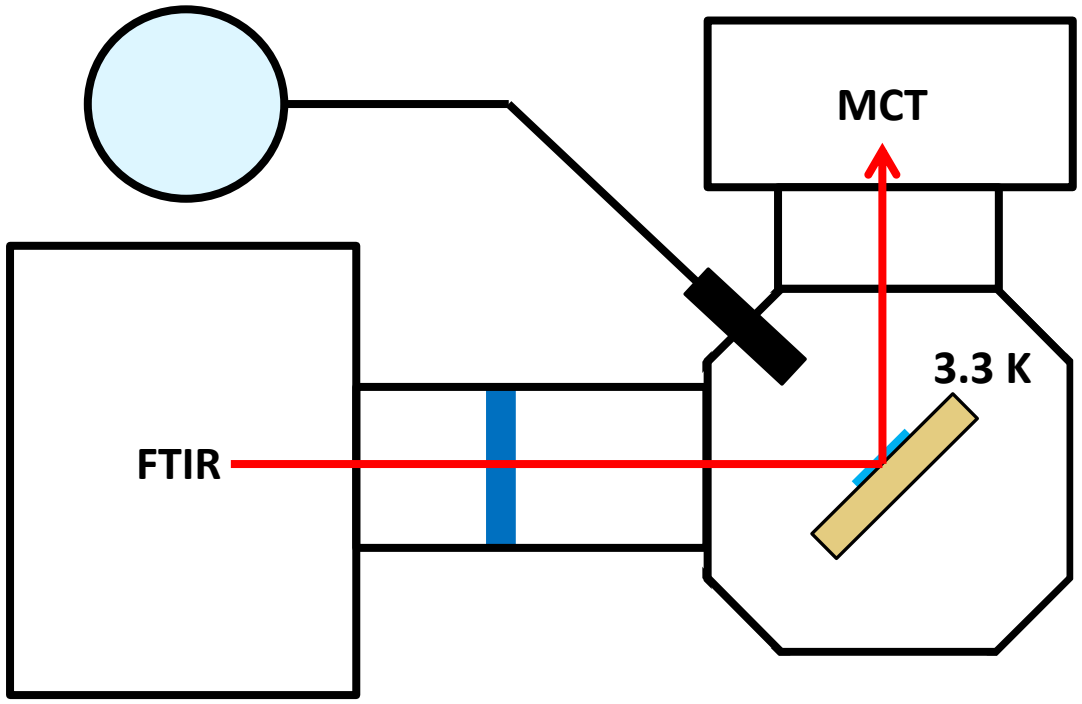

10 hr (~11 mmol/hr)

200 scans (0.25 cm^{-1} resolution)

Experimental Spectra

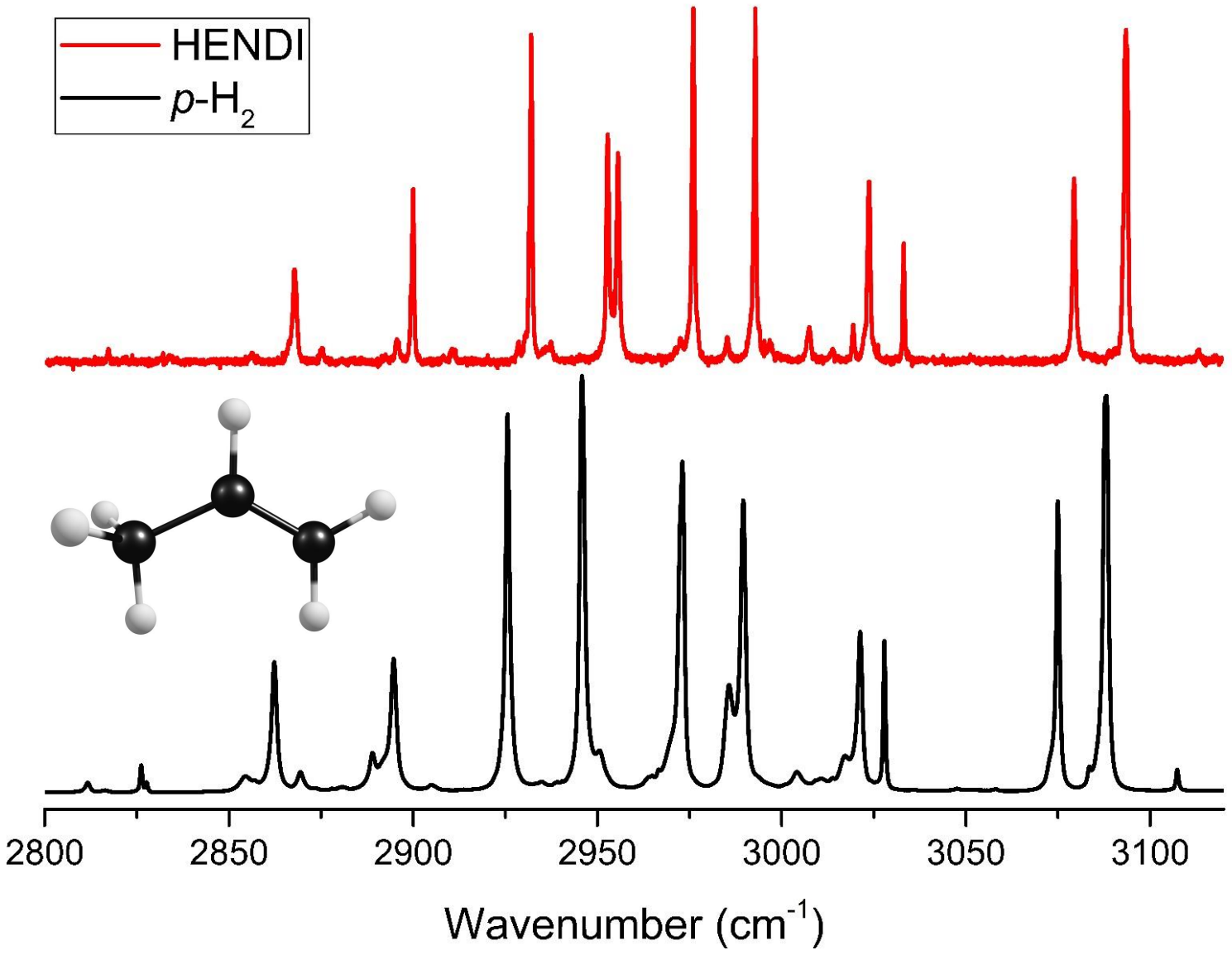

Experimental Spectra

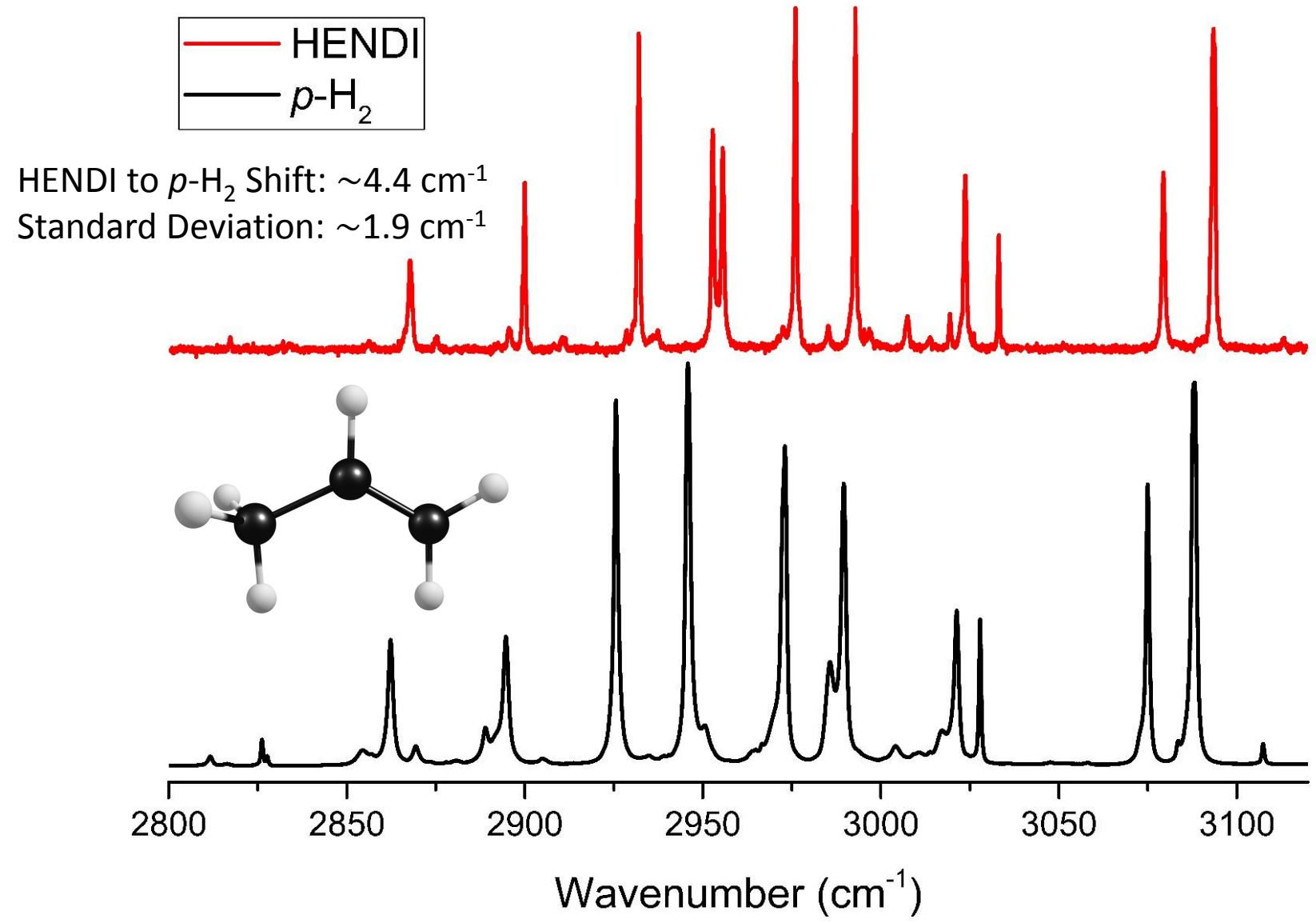

Experimental Spectra

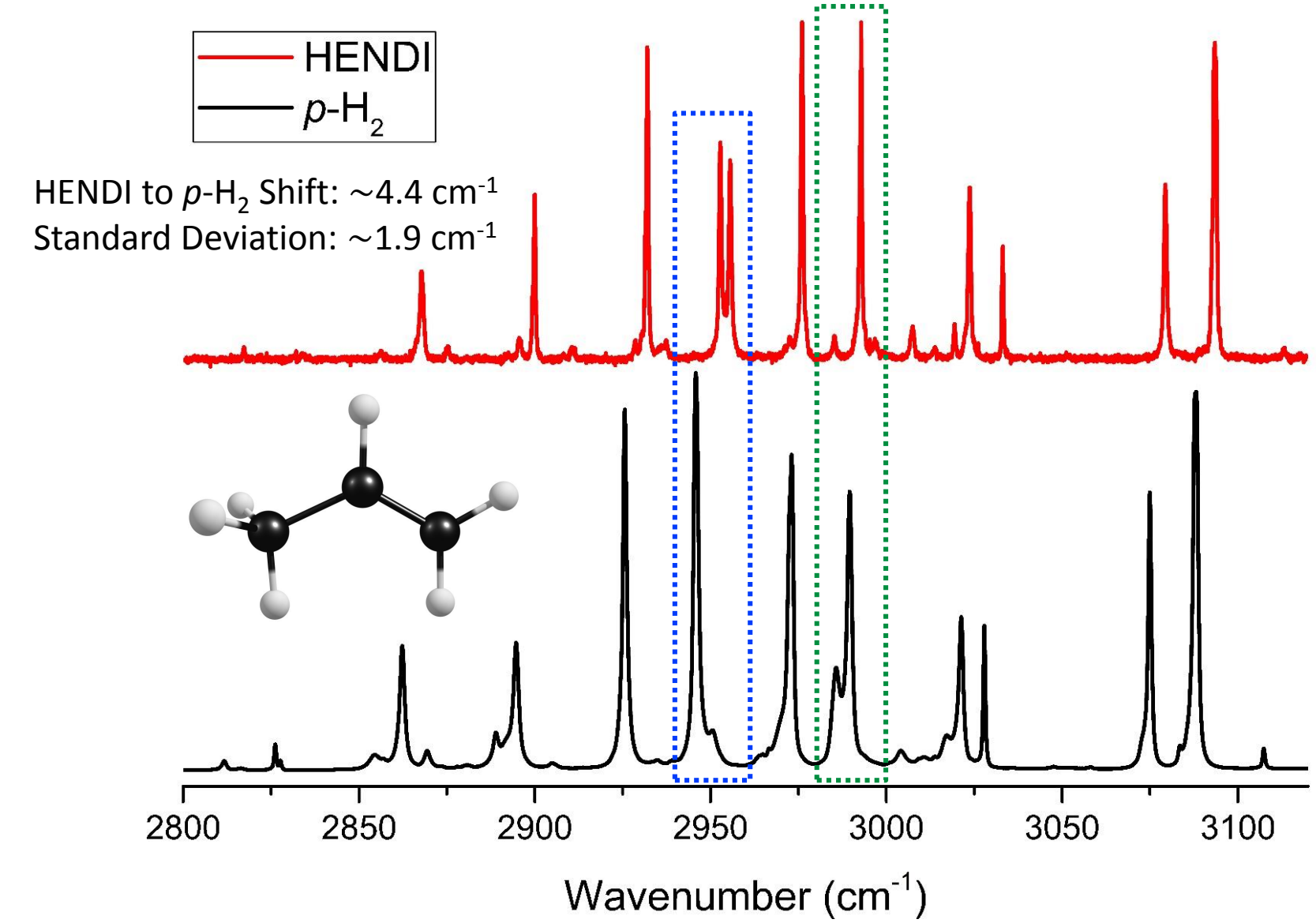

Comparison to Theory

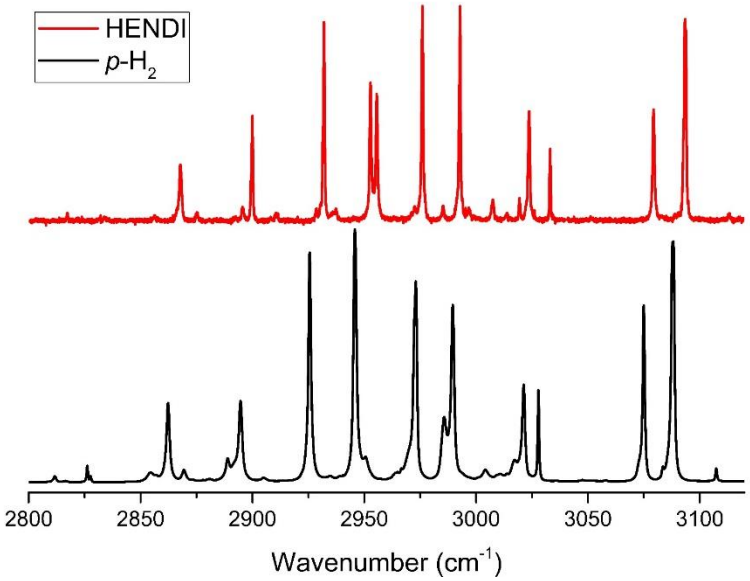

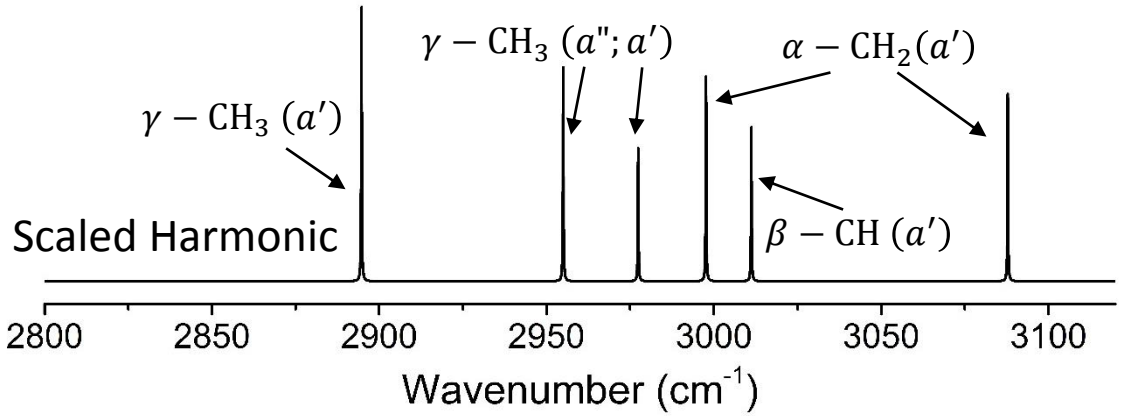

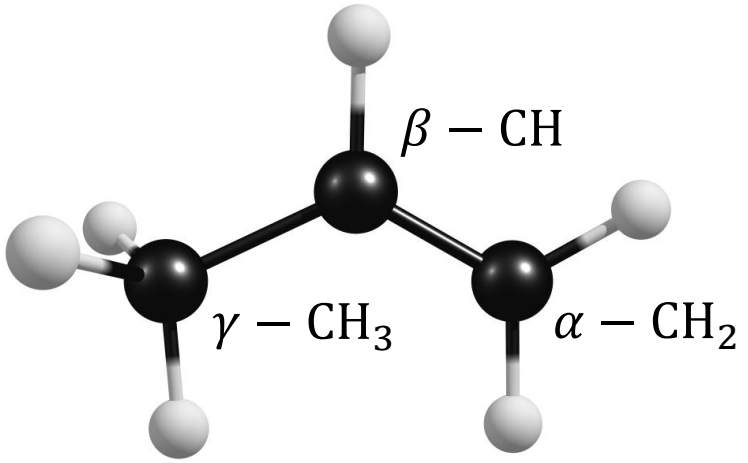

Comparison to Theory

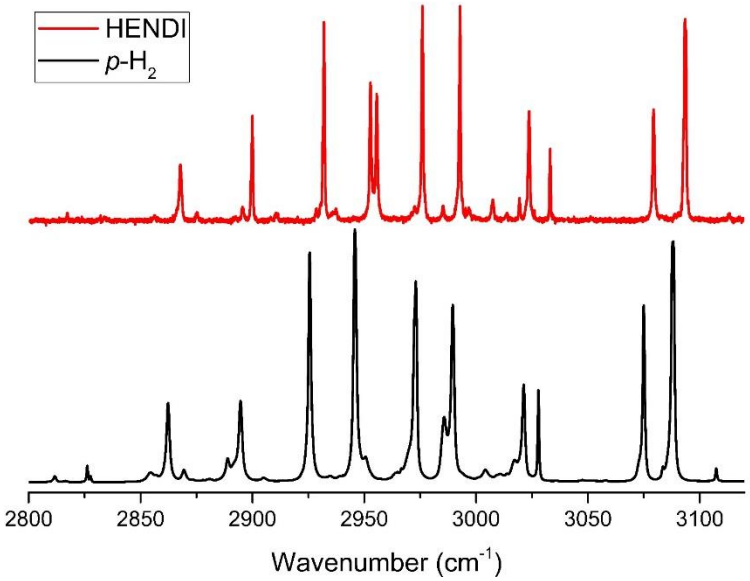

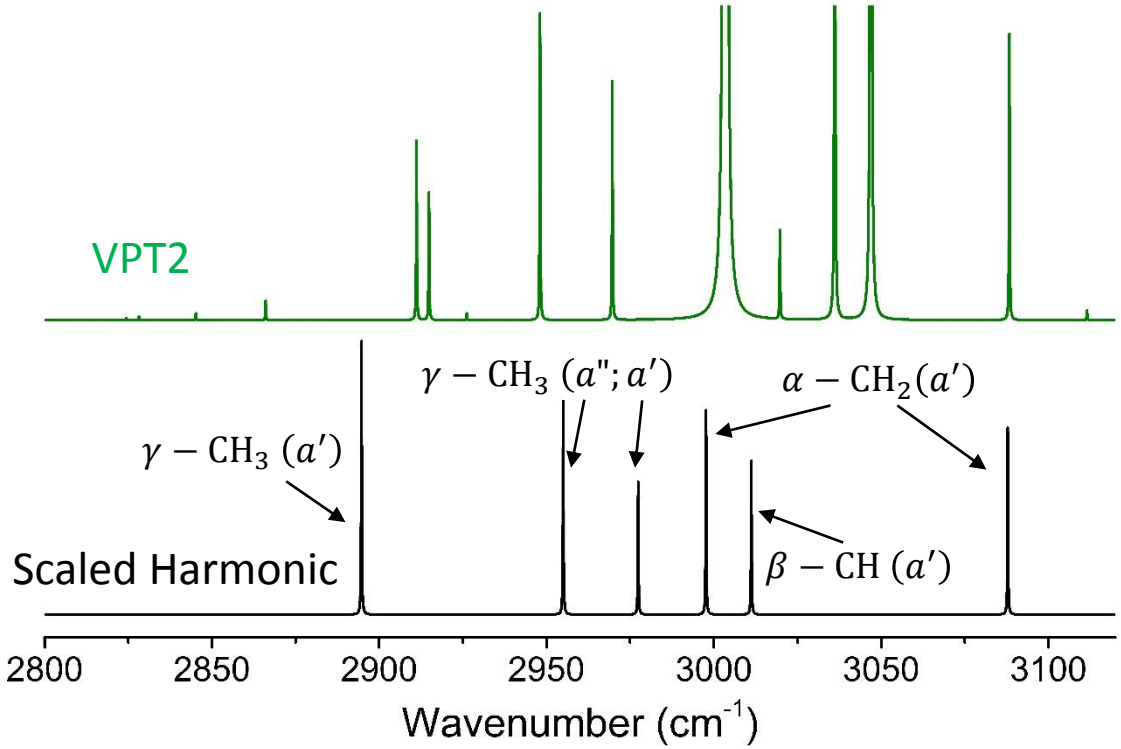

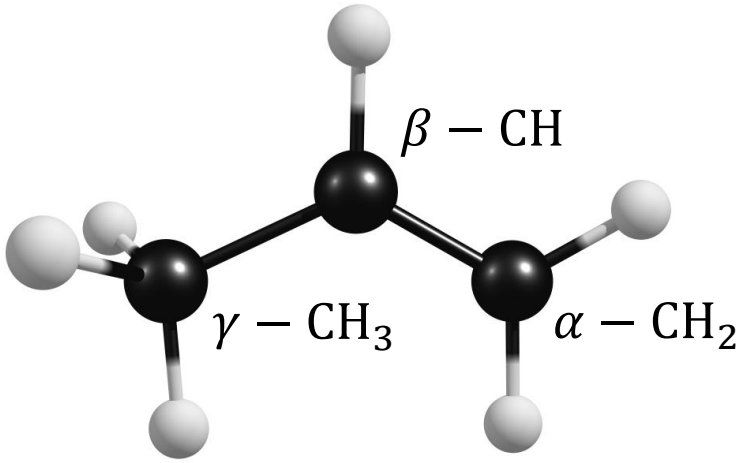

Comparison to Theory

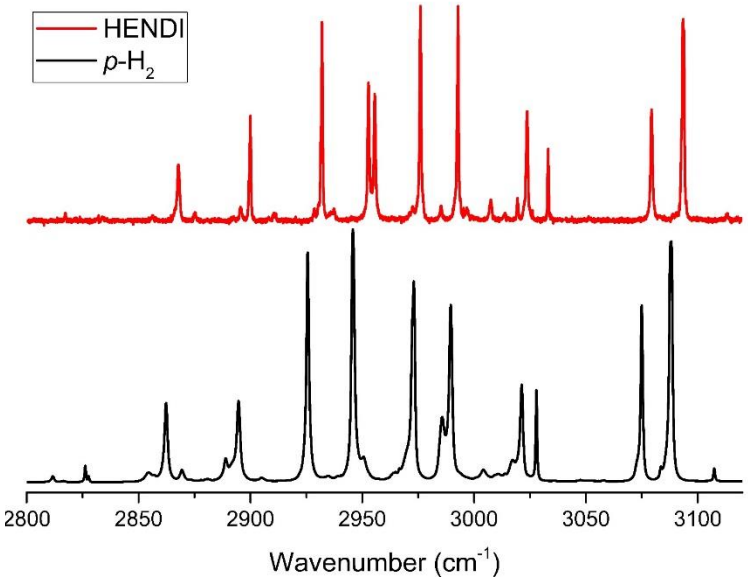

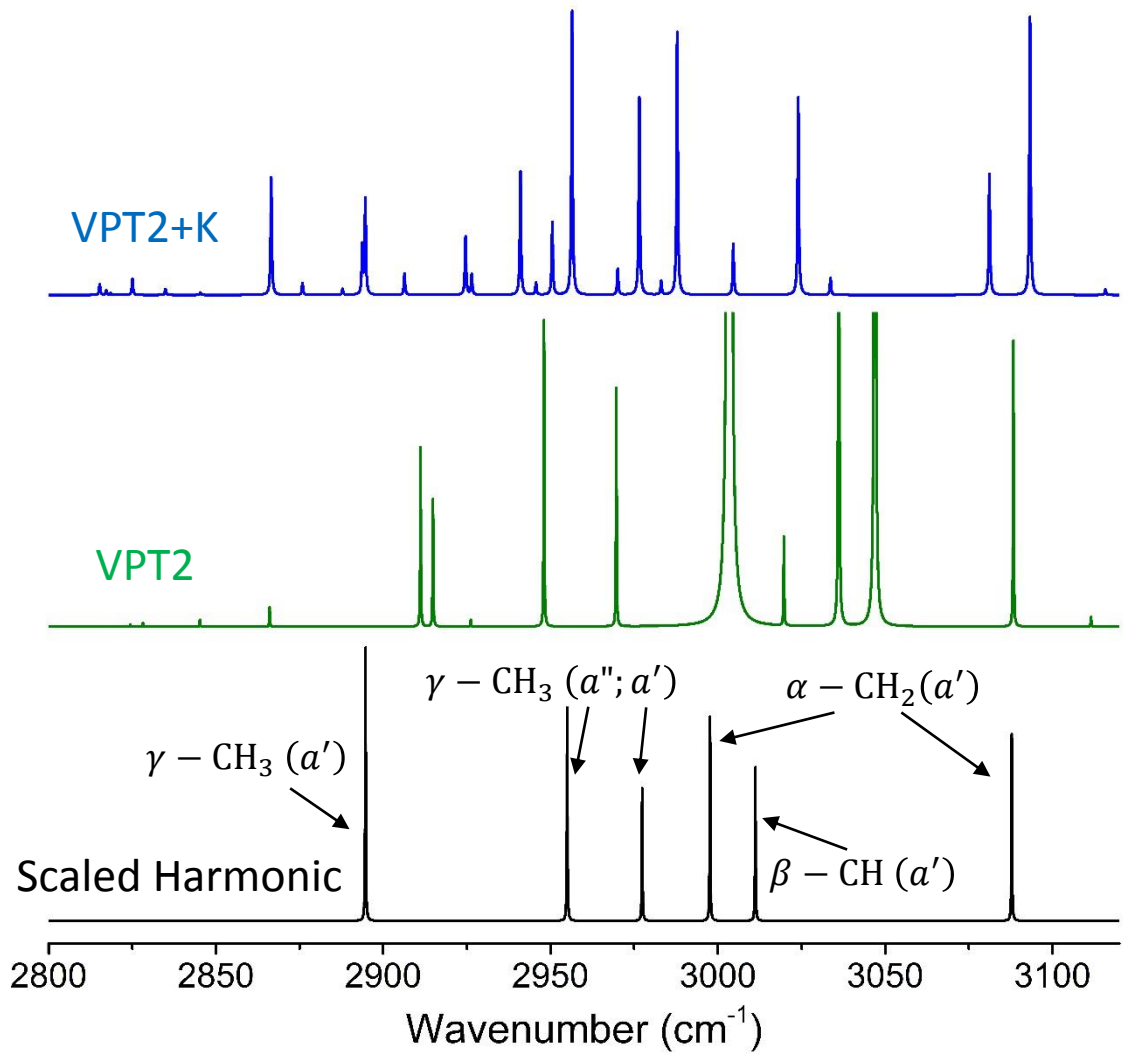

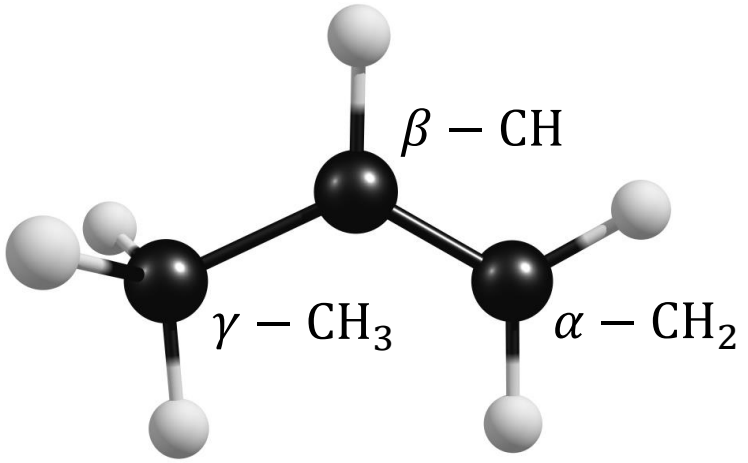

Comparison to Theory

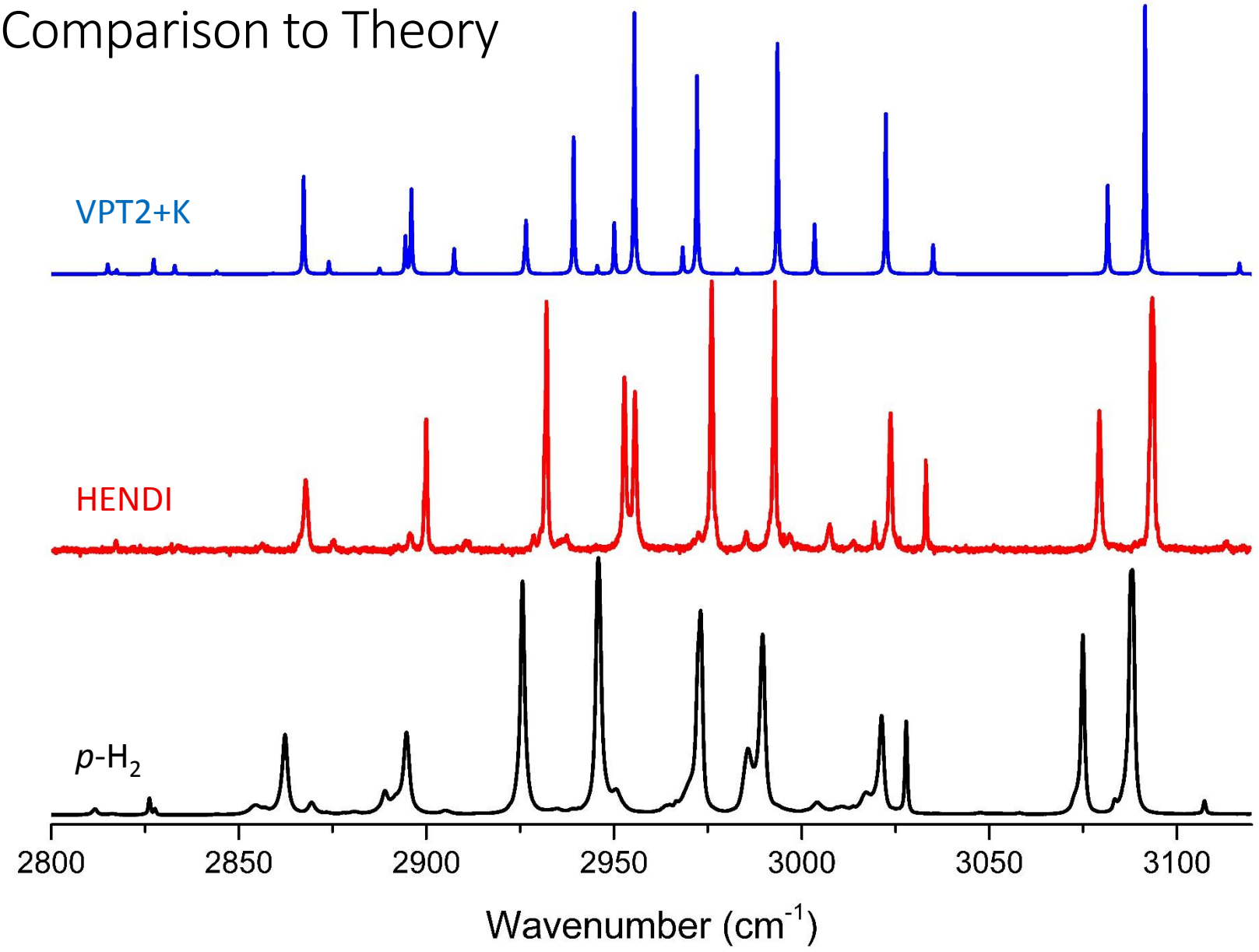

Comparison to Theory

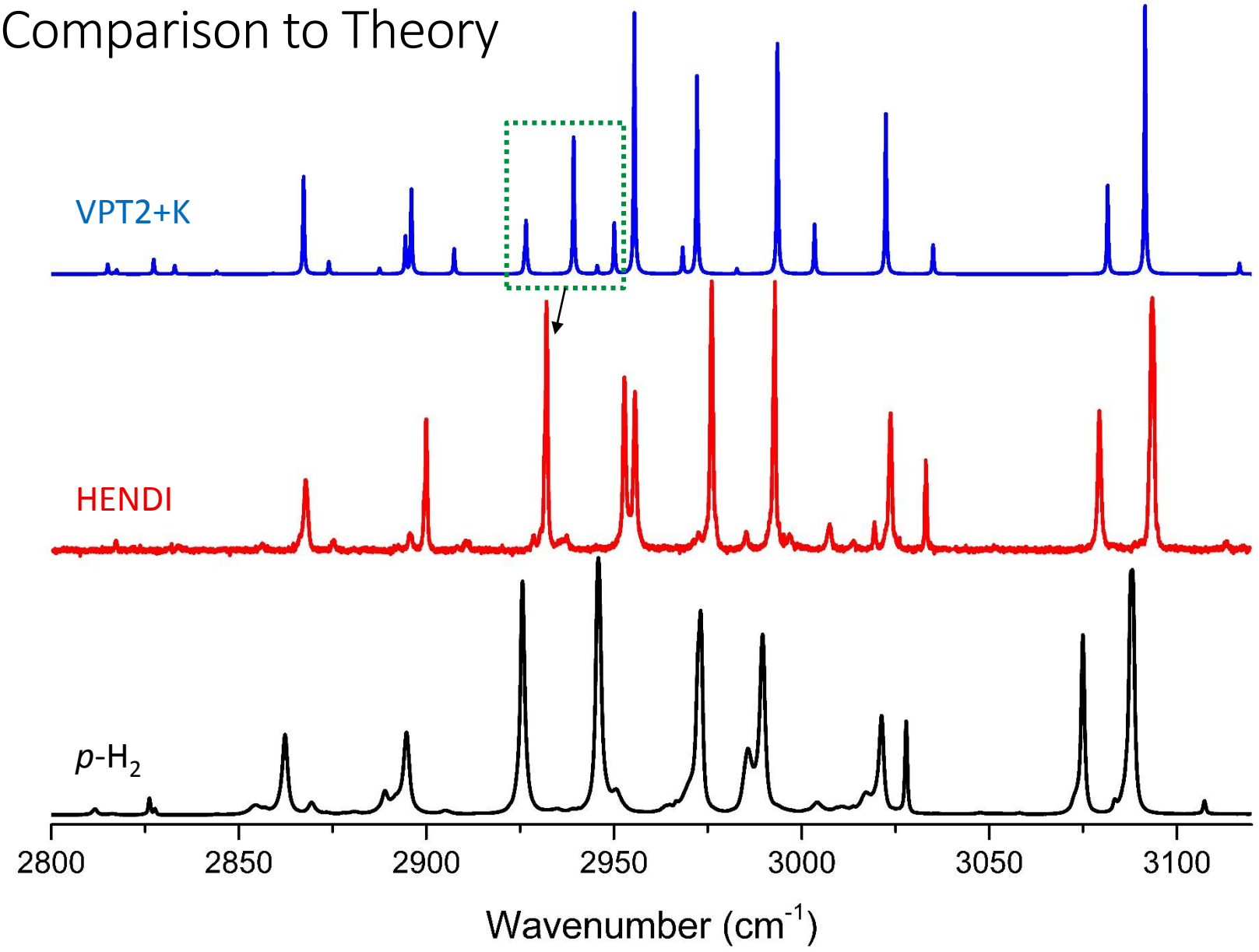

Comparison to Theory

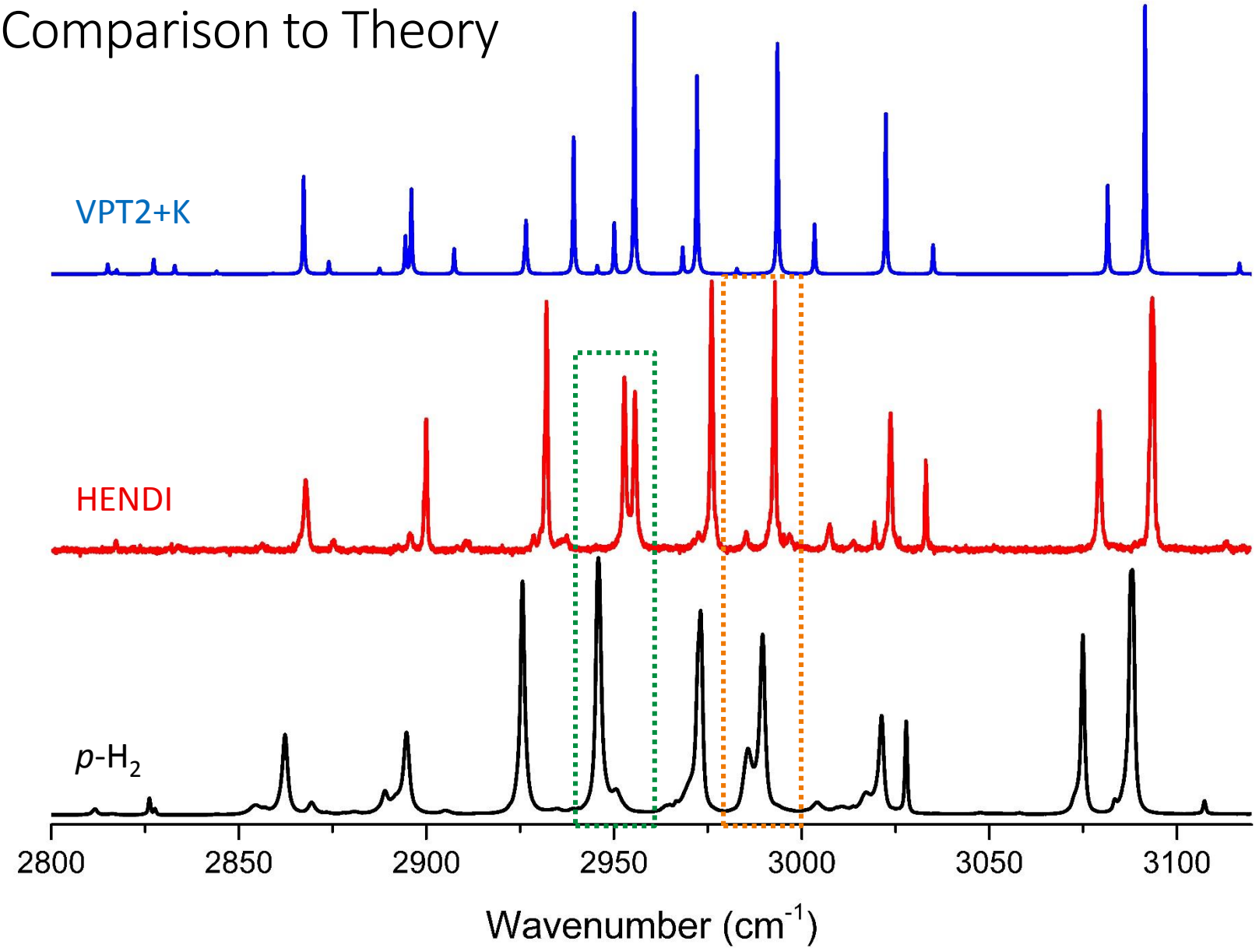

Comparison to Theory

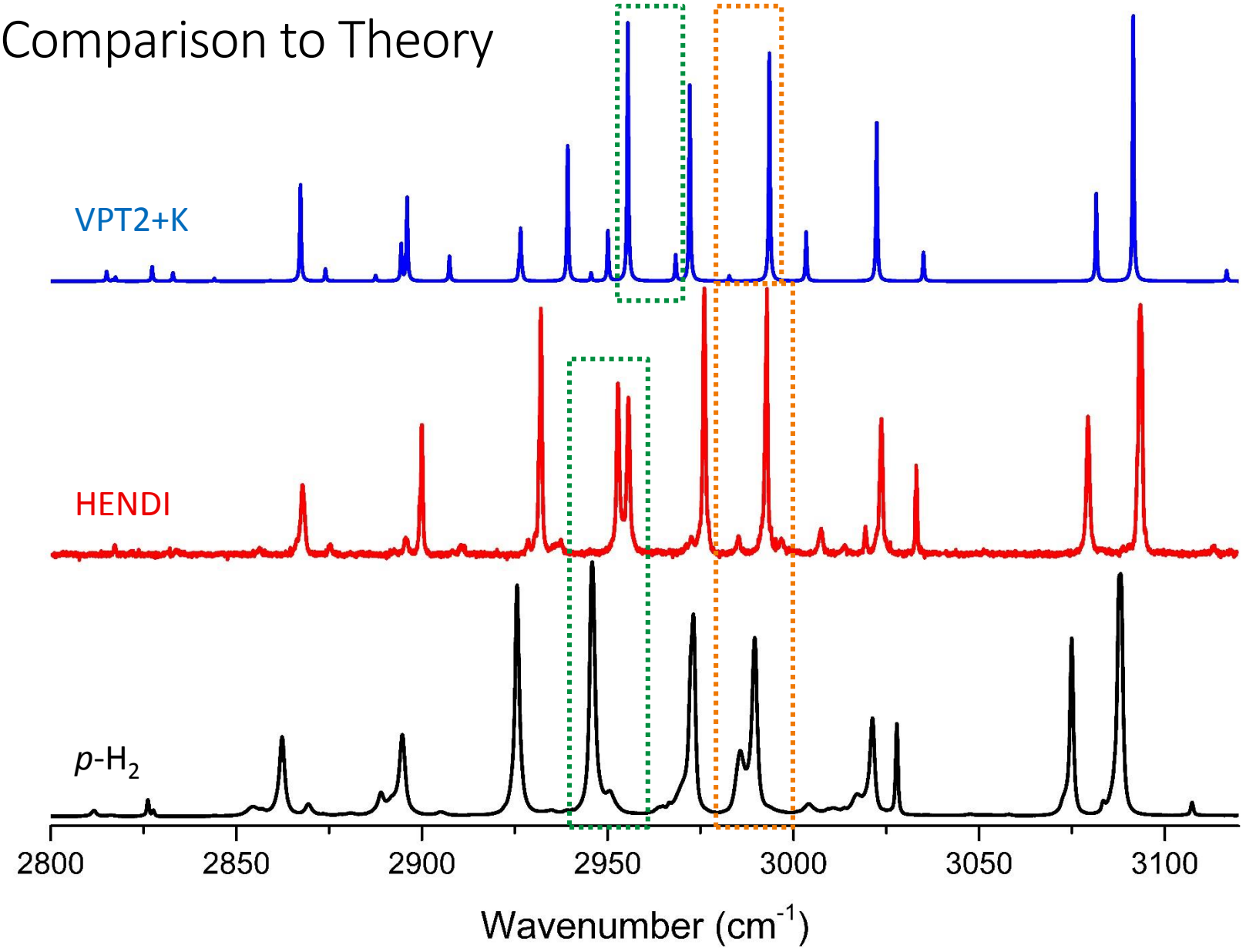

Comparison to Theory

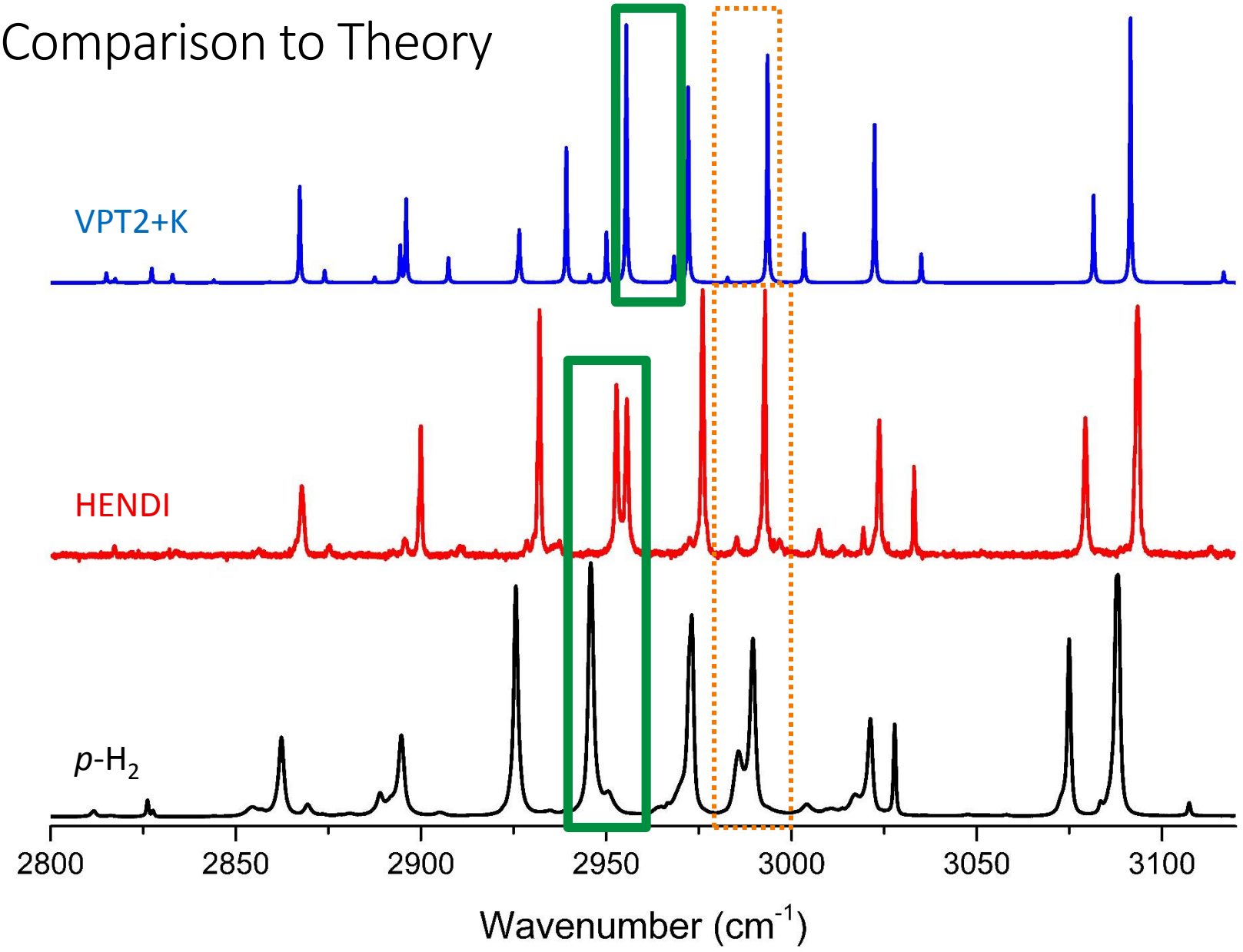

Comparison to Theory

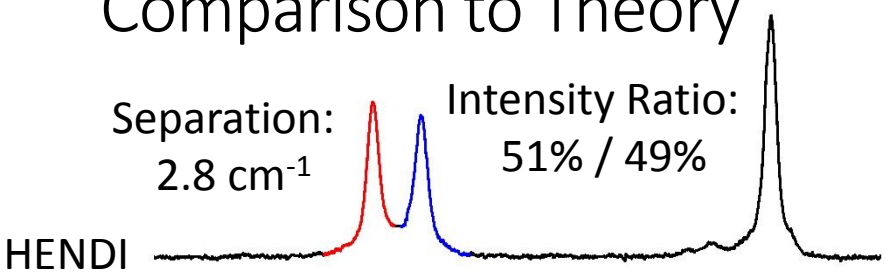

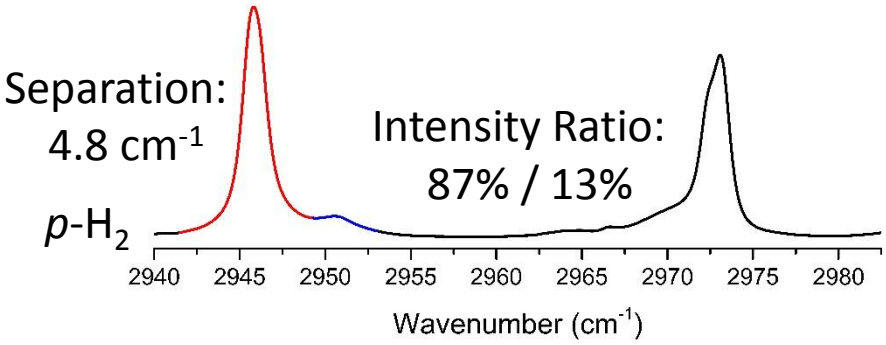

Comparison to Theory

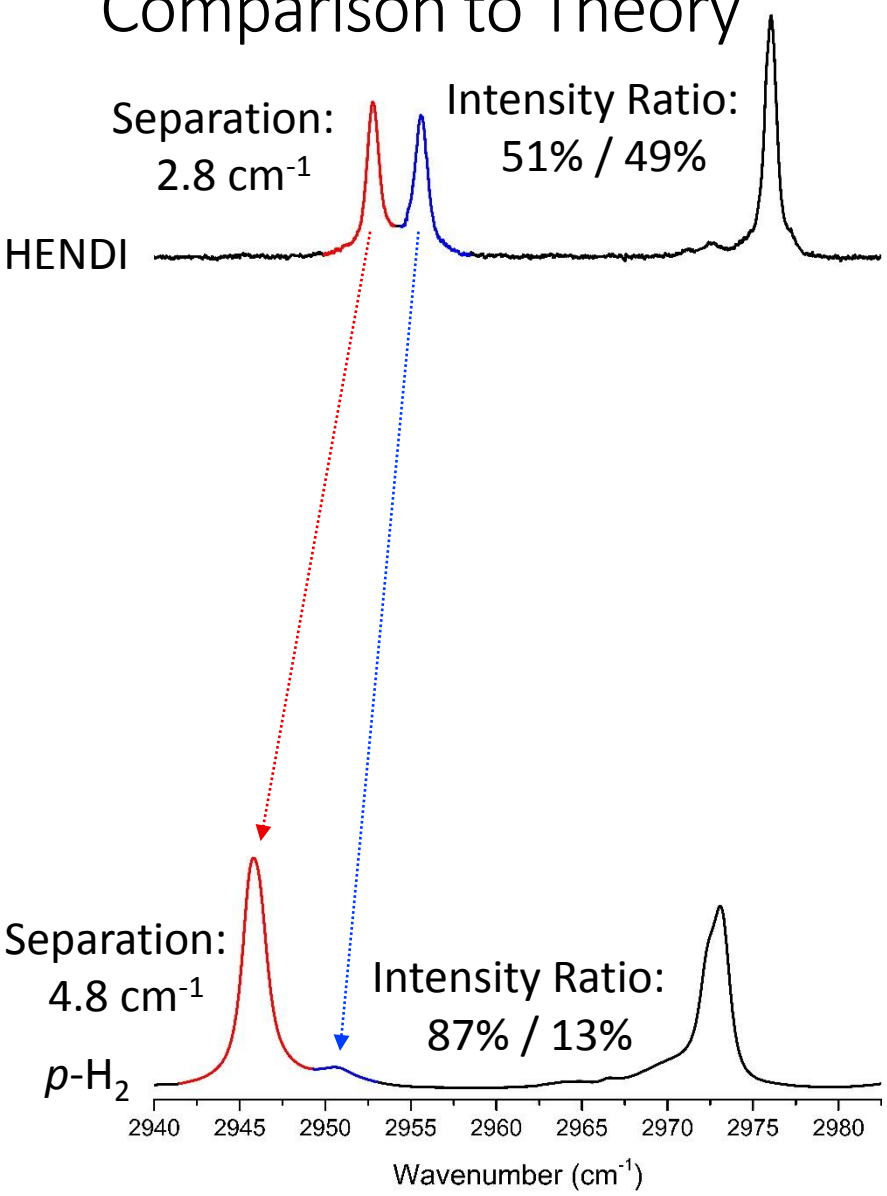

Comparison to Theory

$$\begin{matrix}\langle \text{bright}| \\ \langle \text{dark}|\end{matrix} \begin{pmatrix} 2954.19 & 1.40 \\ 1.40 & 2954.21 \end{pmatrix}$$

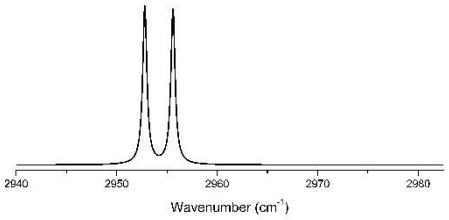

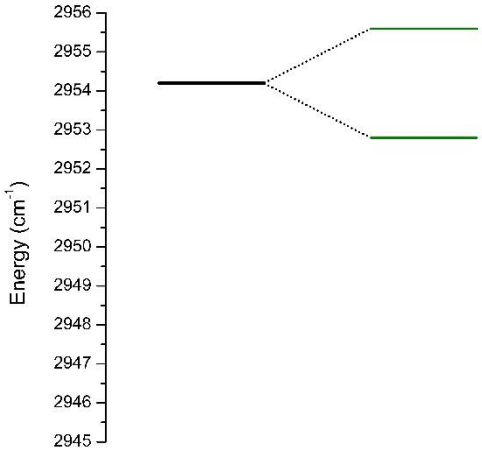

HENDI

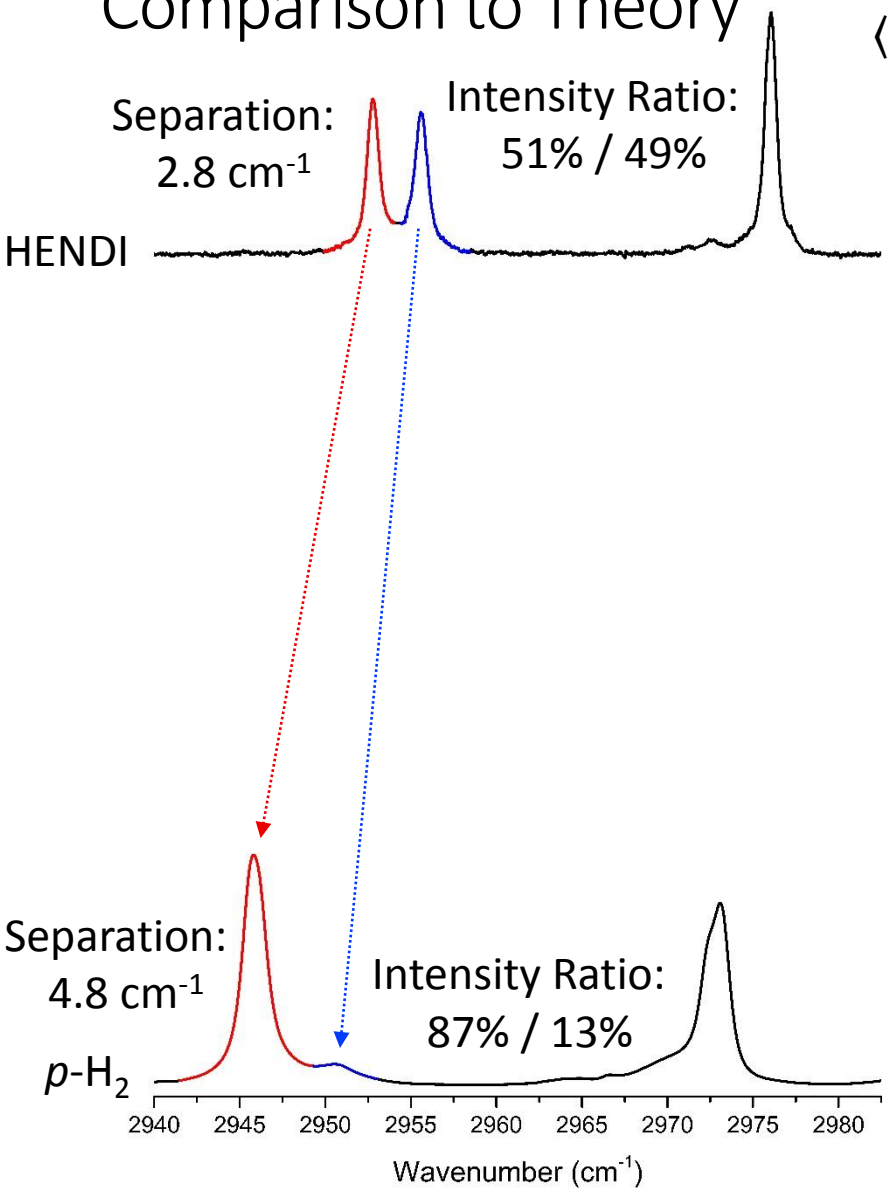

Comparison to Theory

$$\begin{matrix}\langle\text{bright}| \\ \langle\text{dark}|\end{matrix}\begin{pmatrix}2954.19 & 1.40 \\ 1.40 & 2954.21\end{pmatrix}$$

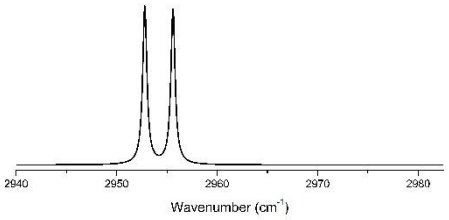

Separation:
2.8 cm^{-1}

Intensity Ratio:
51% / 49%

HENDI

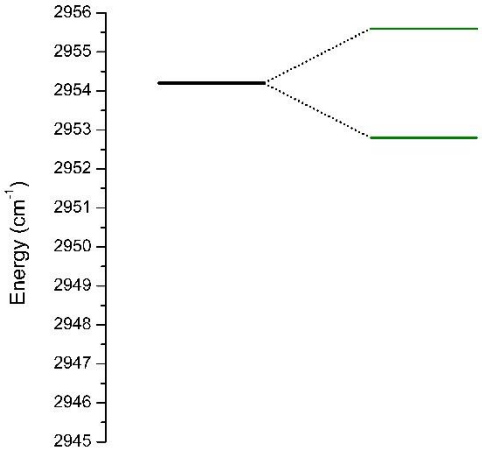

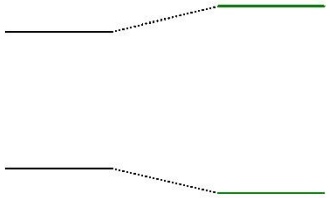

HENDI

p-H_2

Separation:
4.8 cm^{-1}

Intensity Ratio:
87% / 13%

p-H_2

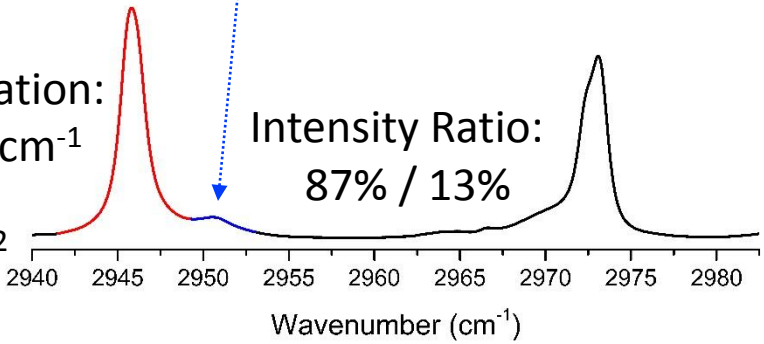

$$\begin{matrix}\langle\text{bright}| \\ \langle\text{dark}|\end{matrix}\begin{pmatrix}2946.50 & 1.62 \\ 1.62 & 2950.03\end{pmatrix}$$

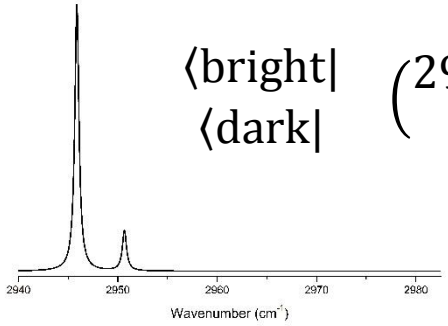

Comparison to Theory

$$\begin{matrix}\langle\text{bright}| \\ \langle\text{dark}|\end{matrix}\begin{pmatrix}2954.19 & 1.40 \\ 1.40 & 2954.21\end{pmatrix}$$

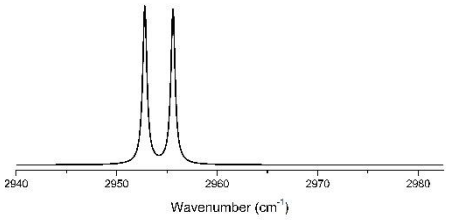

Separation:
2.8 cm^{-1}

Intensity Ratio:
51% / 49%

HENDI

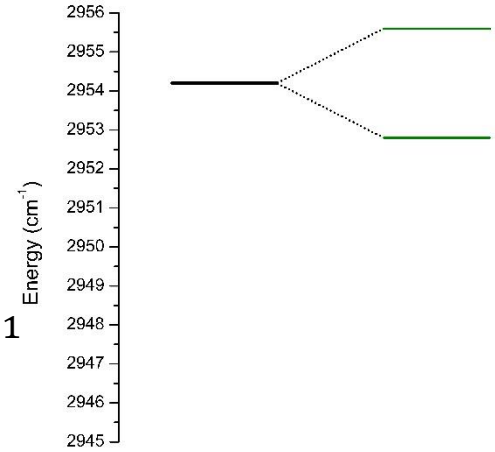

$$\Delta \text{ bright} = -7.7 \text{ cm}^{-1}$$
$$\Delta \text{ dark} = -4.2 \text{ cm}^{-1}$$
$$\Delta \text{ coupling} = 0.22 \text{ cm}^{-1}$$

HENDI

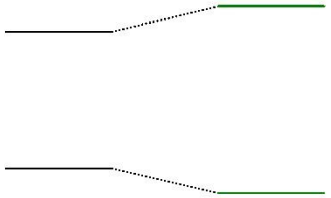

p-H_2

Separation:
4.8 cm^{-1}

Intensity Ratio:
87% / 13%

p-H_2

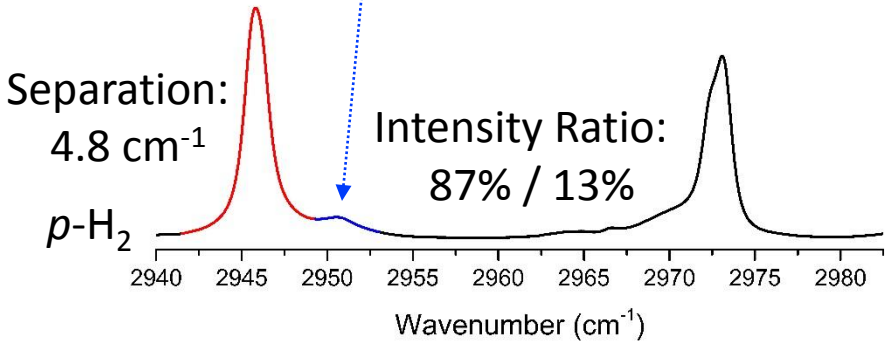

$$\begin{matrix}\langle\text{bright}| \\ \langle\text{dark}|\end{matrix}\begin{pmatrix}2946.50 & 1.62 \\ 1.62 & 2950.03\end{pmatrix}$$

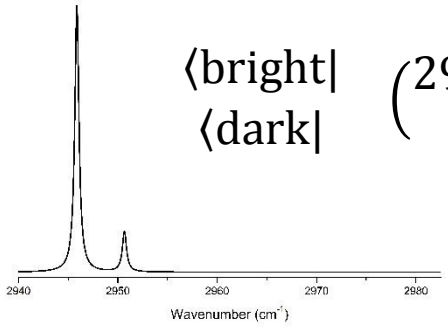

Comparison to Theory

$$\begin{matrix}\langle\text{bright}| \\ \langle\text{dark}|\end{matrix}\begin{pmatrix}2954.19 & 1.40 \\ 1.40 & 2954.21\end{pmatrix}$$

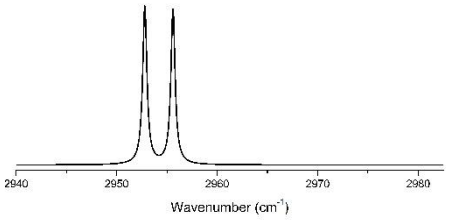

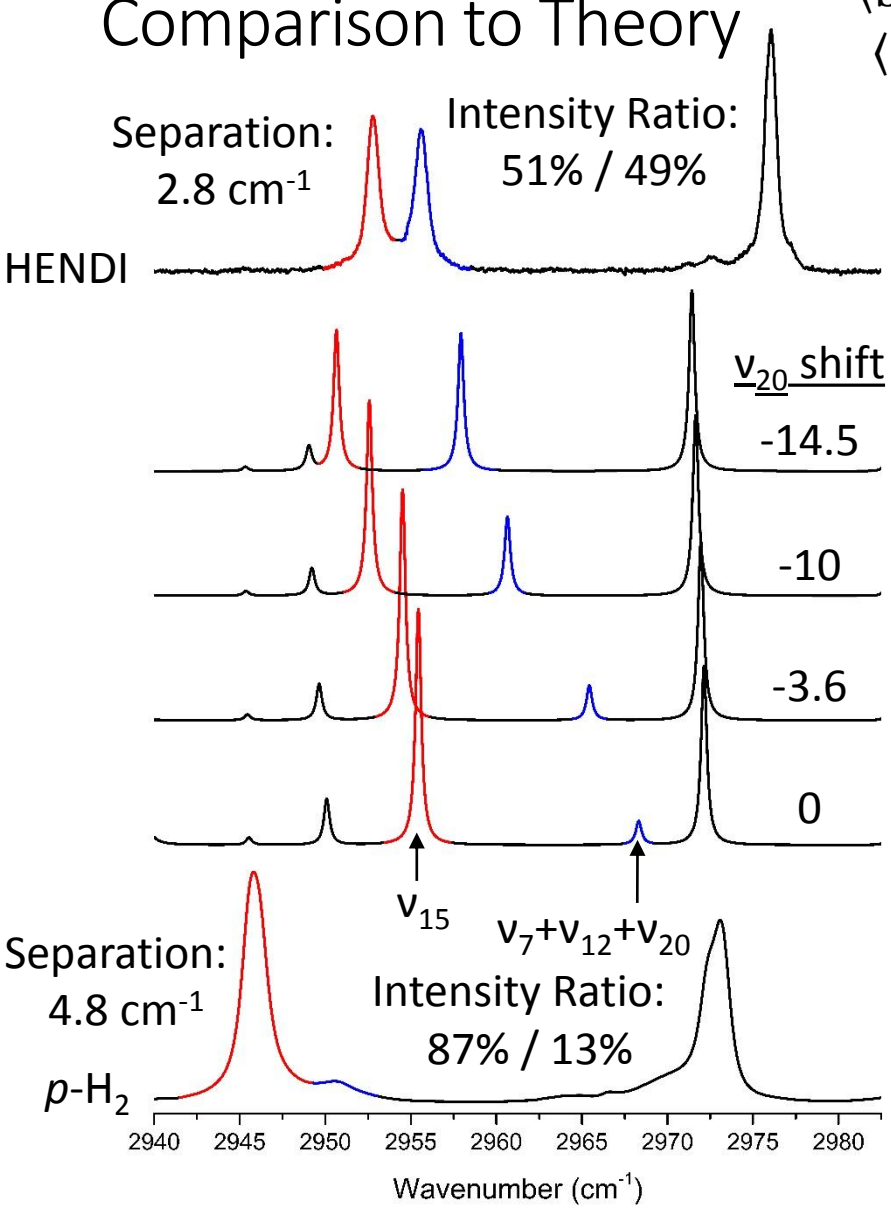

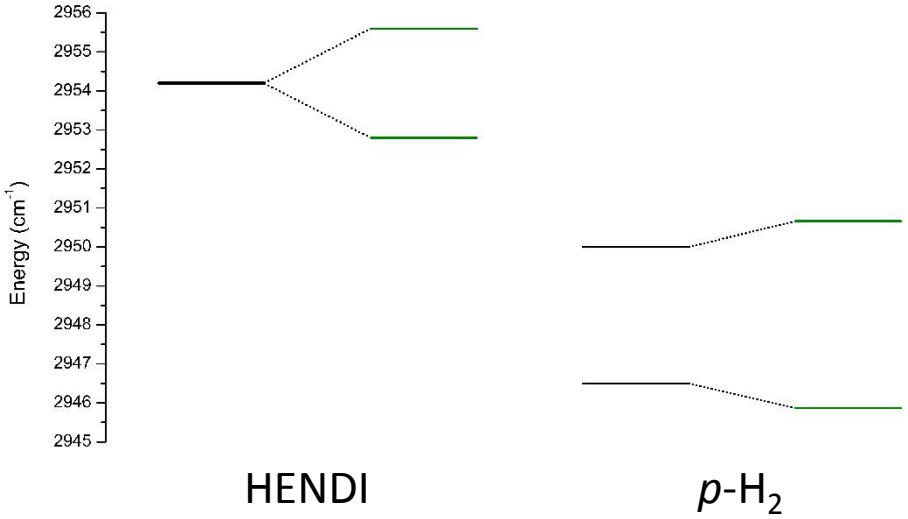

$$\begin{matrix}\langle\text{bright}| \\ \langle\text{dark}|\end{matrix}\begin{pmatrix}2946.50 & 1.62 \\ 1.62 & 2950.03\end{pmatrix}$$

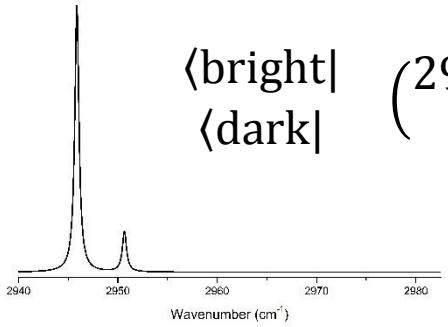

Comparison to Theory

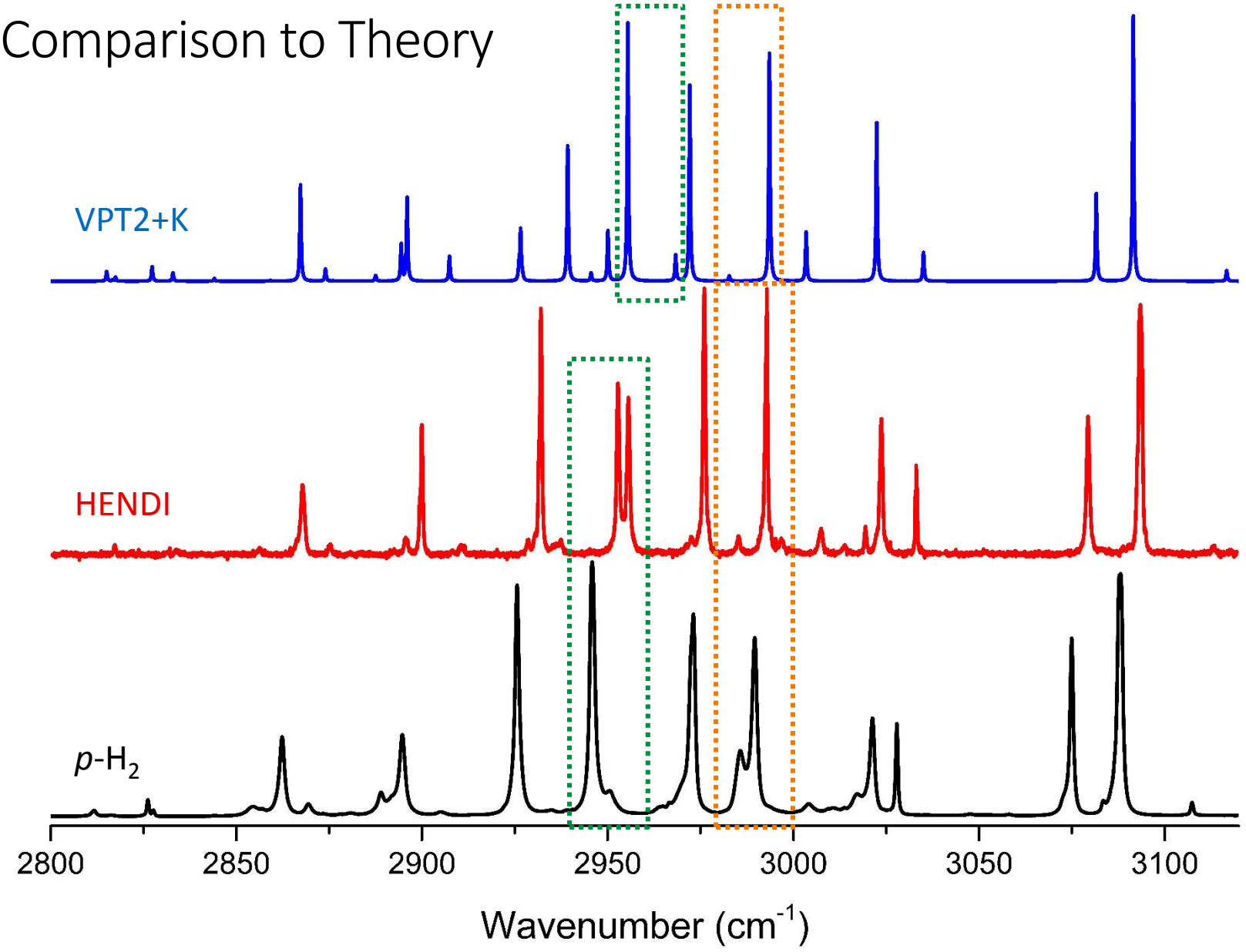

Comparison to Theory

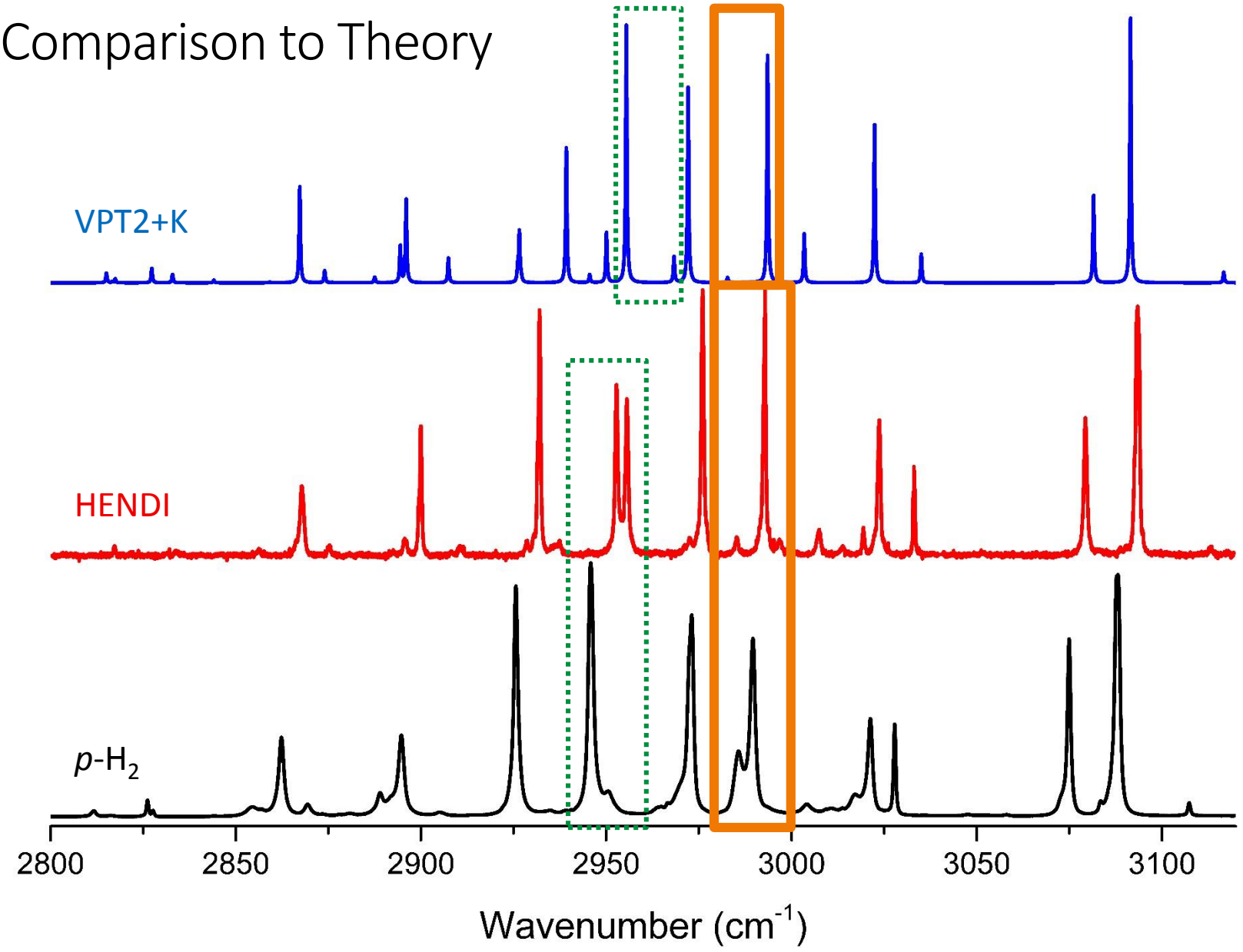

Comparison to Theory

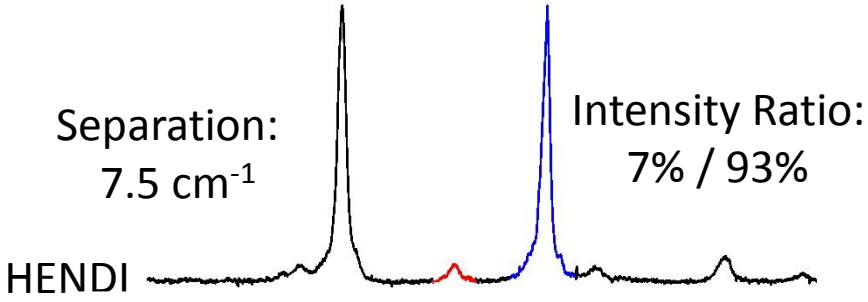

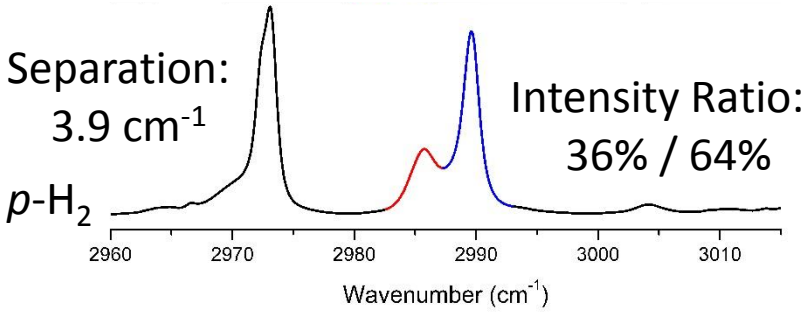

Comparison to Theory

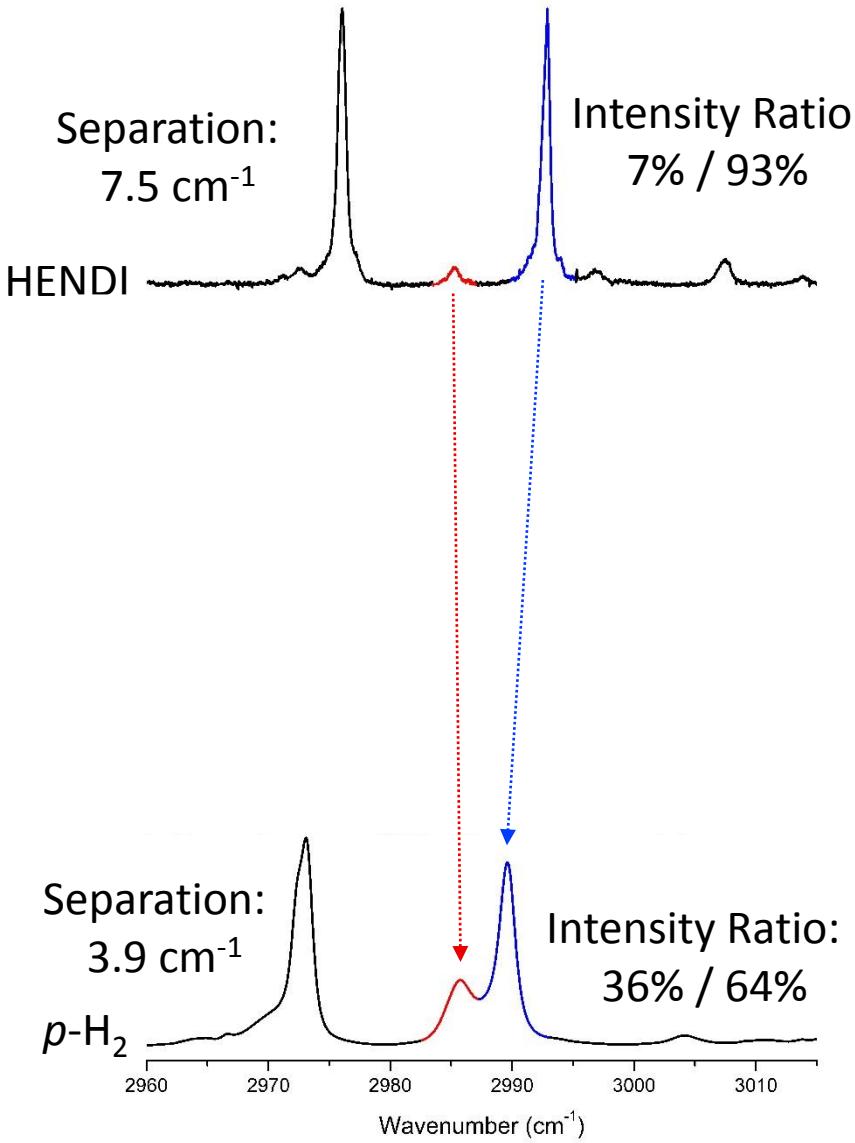

Comparison to Theory

$$\begin{matrix}\langle \text{dark}| \\ \langle \text{bright}|\end{matrix}\begin{pmatrix}2985.82 & 1.98 \\ 1.98 & 2992.24\end{pmatrix}$$

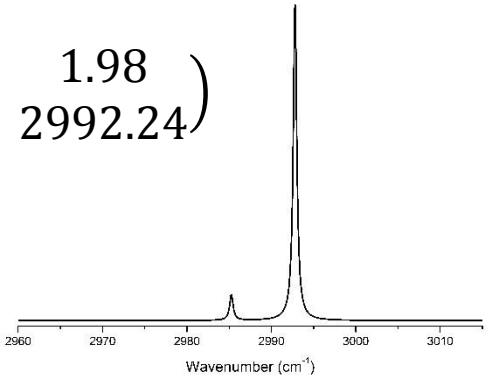

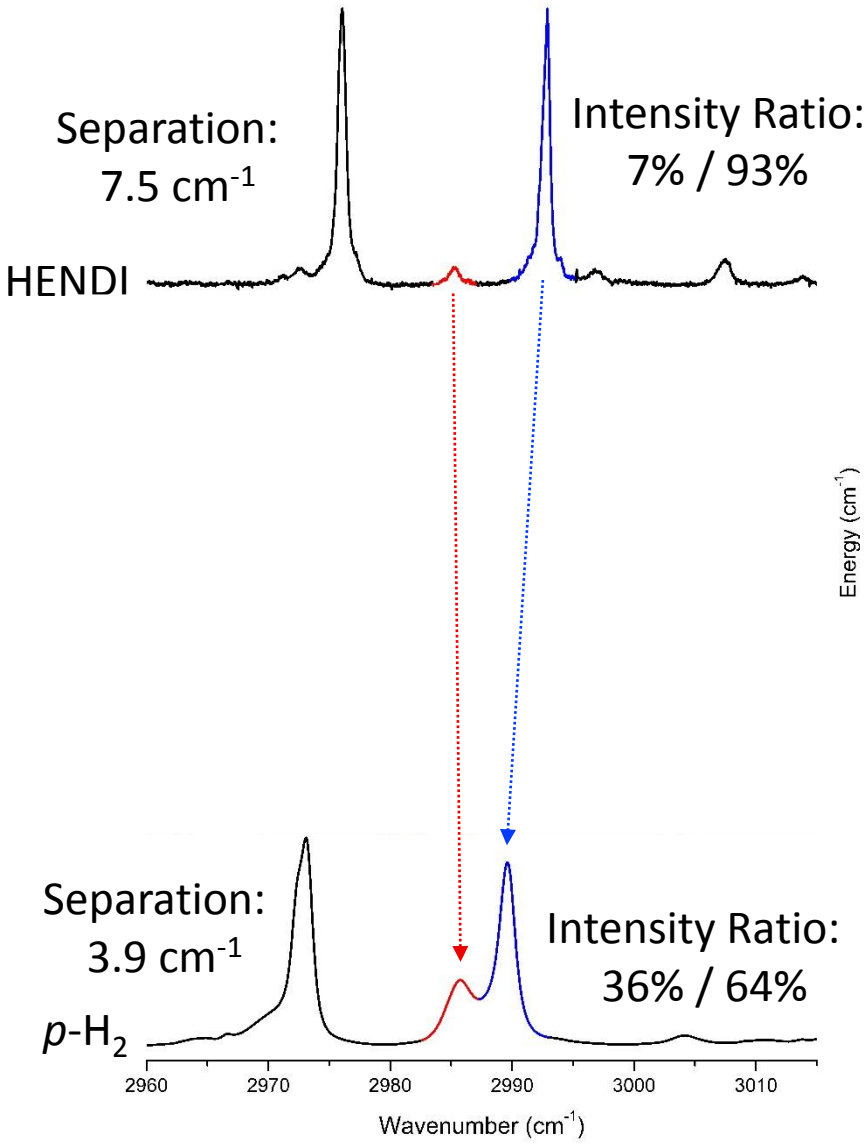

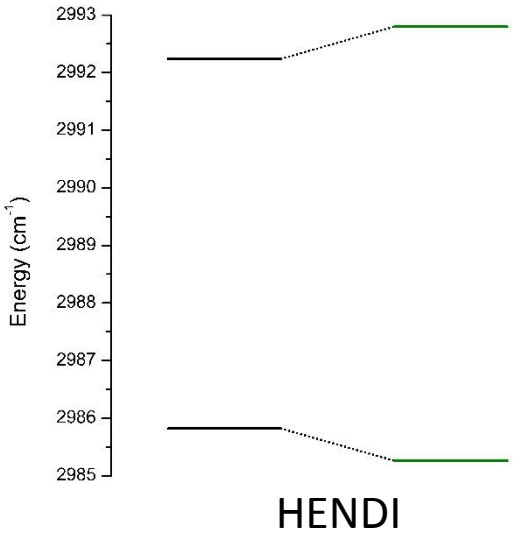

Comparison to Theory

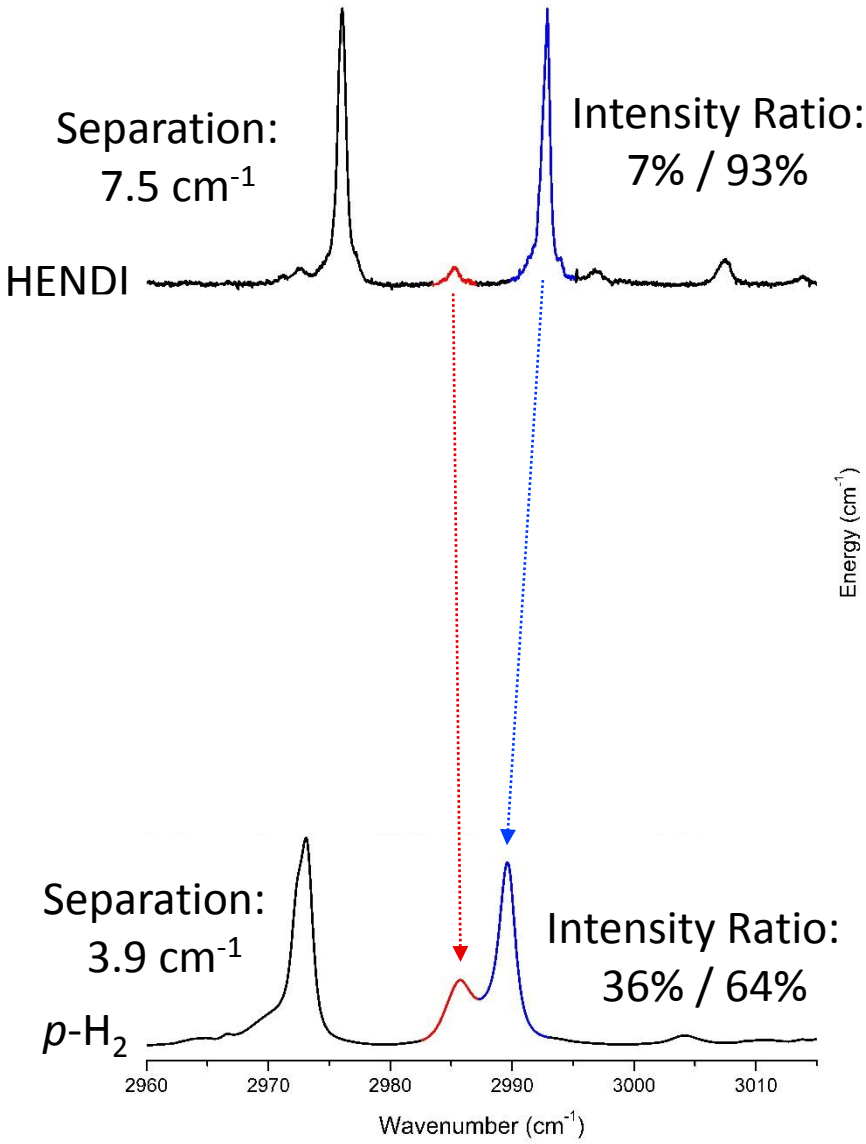

$$\begin{matrix}\langle\text{dark}| \\ \langle\text{bright}|\end{matrix}\begin{pmatrix}2985.82 & 1.98 \\ 1.98 & 2992.24\end{pmatrix}$$

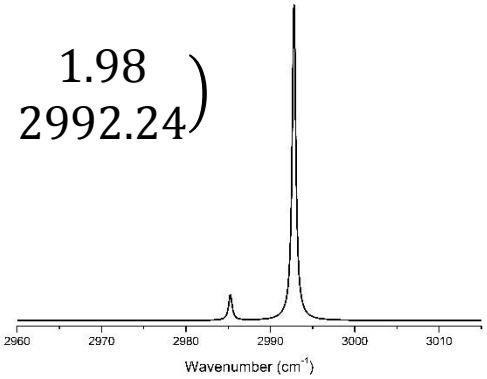

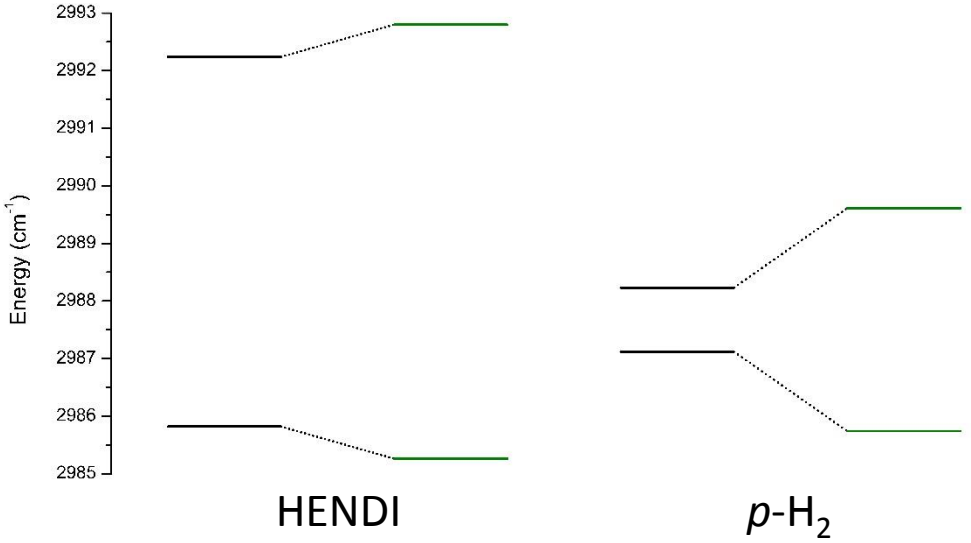

$$\begin{matrix}\langle\text{dark}| \\ \langle\text{bright}|\end{matrix}\begin{pmatrix}2987.12 & 1.85 \\ 1.85 & 2988.23\end{pmatrix}$$

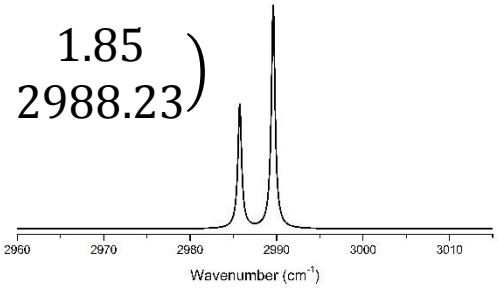

Comparison to Theory

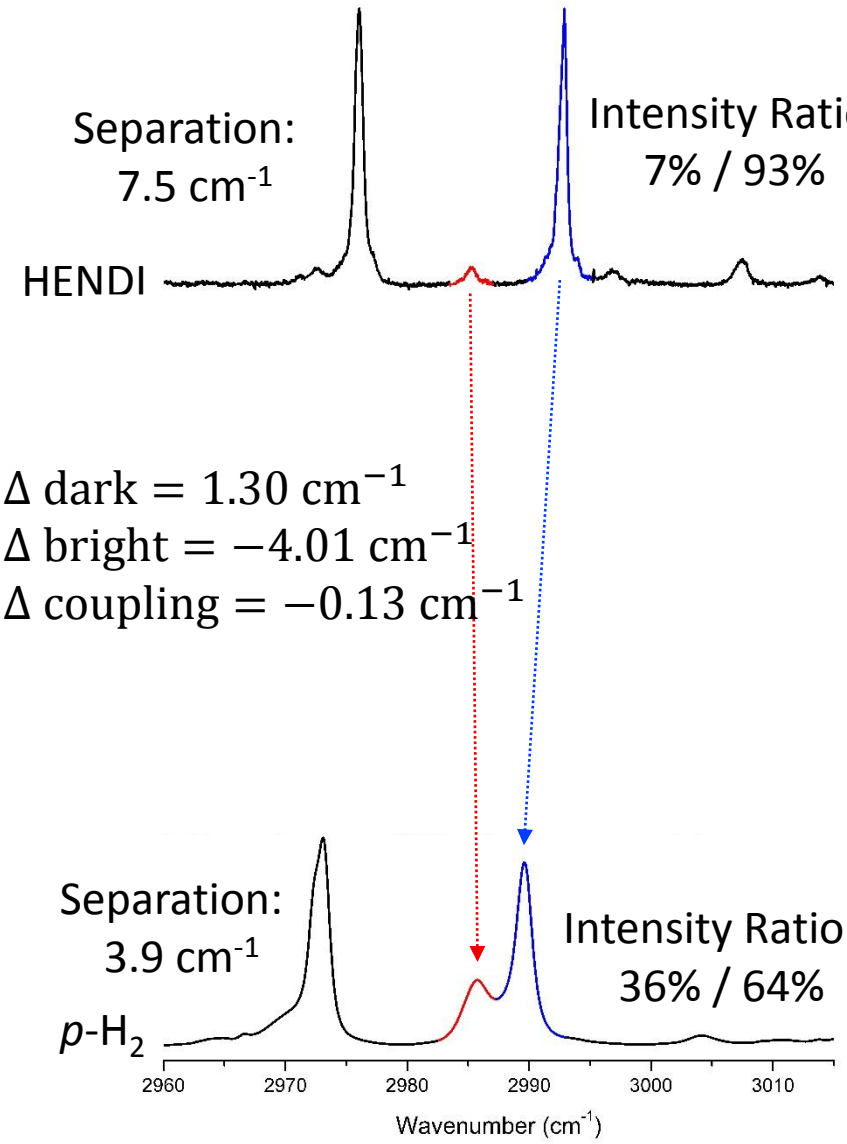

Δ dark $= 1.30\ \mathrm{cm}^{-1}$
Δ bright $= -4.01\ \mathrm{cm}^{-1}$
Δ coupling $= -0.13\ \mathrm{cm}^{-1}$

$$\begin{matrix} \langle \text{dark}| \\ \langle \text{bright}| \end{matrix} \begin{pmatrix} 2985.82 & 1.98 \\ 1.98 & 2992.24 \end{pmatrix}$$

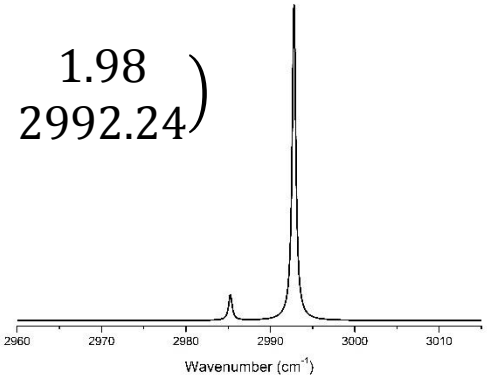

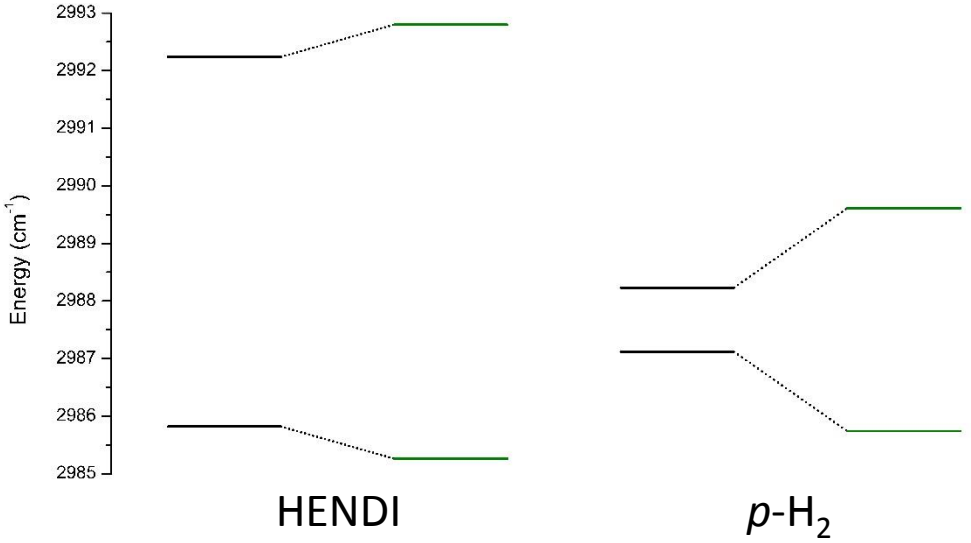

$$\begin{matrix} \langle \text{dark}| \\ \langle \text{bright}| \end{matrix} \begin{pmatrix} 2987.12 & 1.85 \\ 1.85 & 2988.23 \end{pmatrix}$$

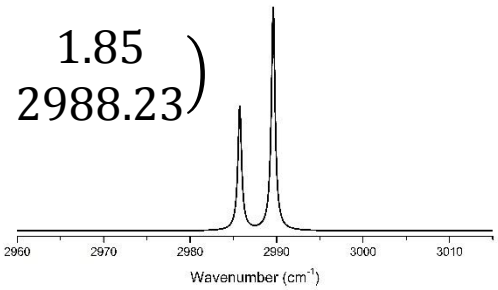

Comparison to Theory

$$\begin{matrix}\langle\text{dark}| \\ \langle\text{bright}|\end{matrix}\begin{pmatrix}2985.82 & 1.98 \\ 1.98 & 2992.24\end{pmatrix}$$

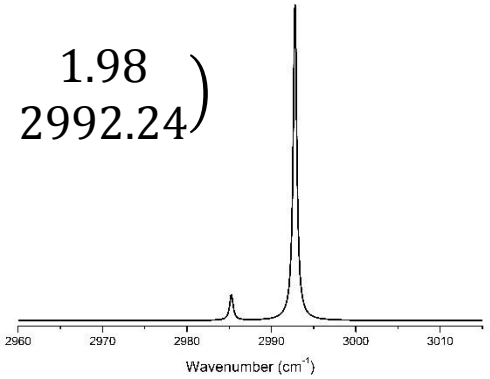

Separation:
7.5 cm^{-1}

Intensity Ratio:
7% / 93%

HENDI

$\nu_{12}+\nu_{14}+$
$\nu_{17}+\nu_{20}$

ν_3

ν_3 shift

0

-13.6

-18

-23

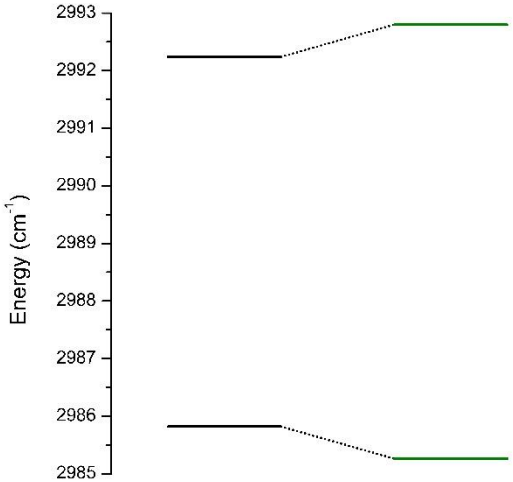

HENDI

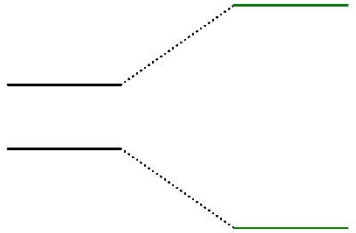

p-H_2

Separation:
3.9 cm^{-1}

Intensity Ratio:
36% / 64%

p-H_2

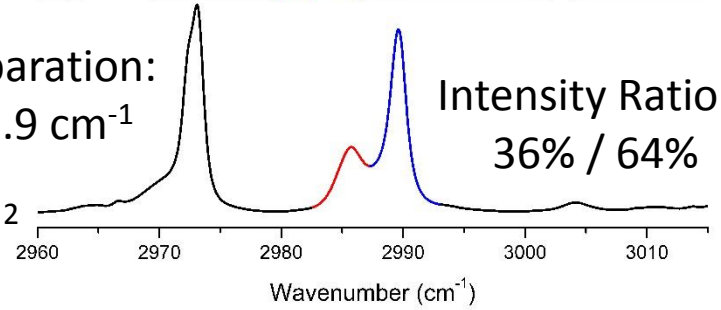

$$\begin{matrix}\langle\text{dark}| \\ \langle\text{bright}|\end{matrix}\begin{pmatrix}2987.12 & 1.85 \\ 1.85 & 2988.23\end{pmatrix}$$

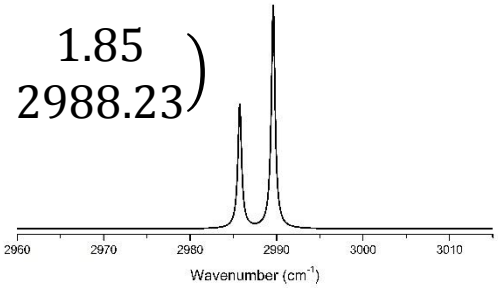

Hydrogen Addition to Propene

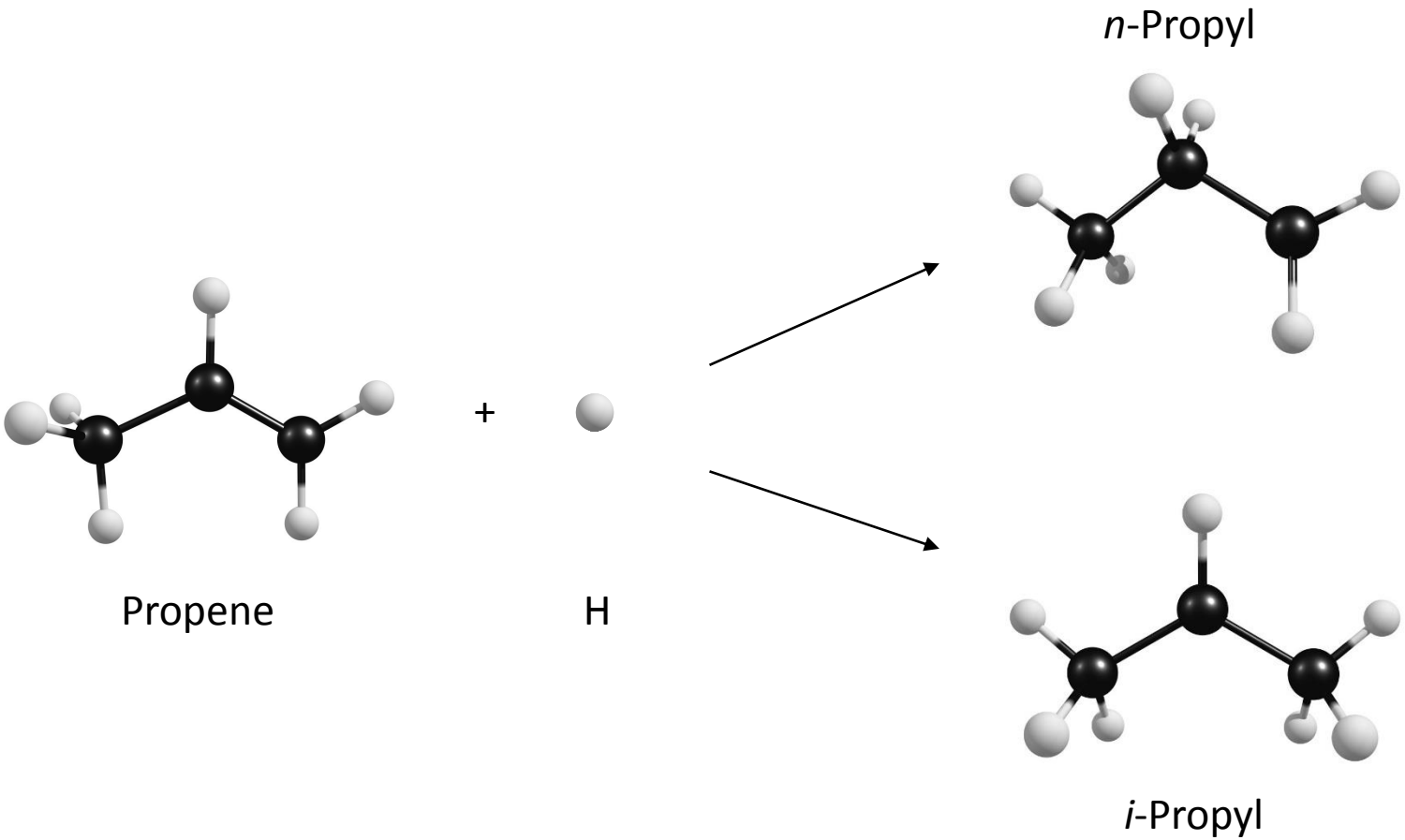

Hydrogen Addition to Propene

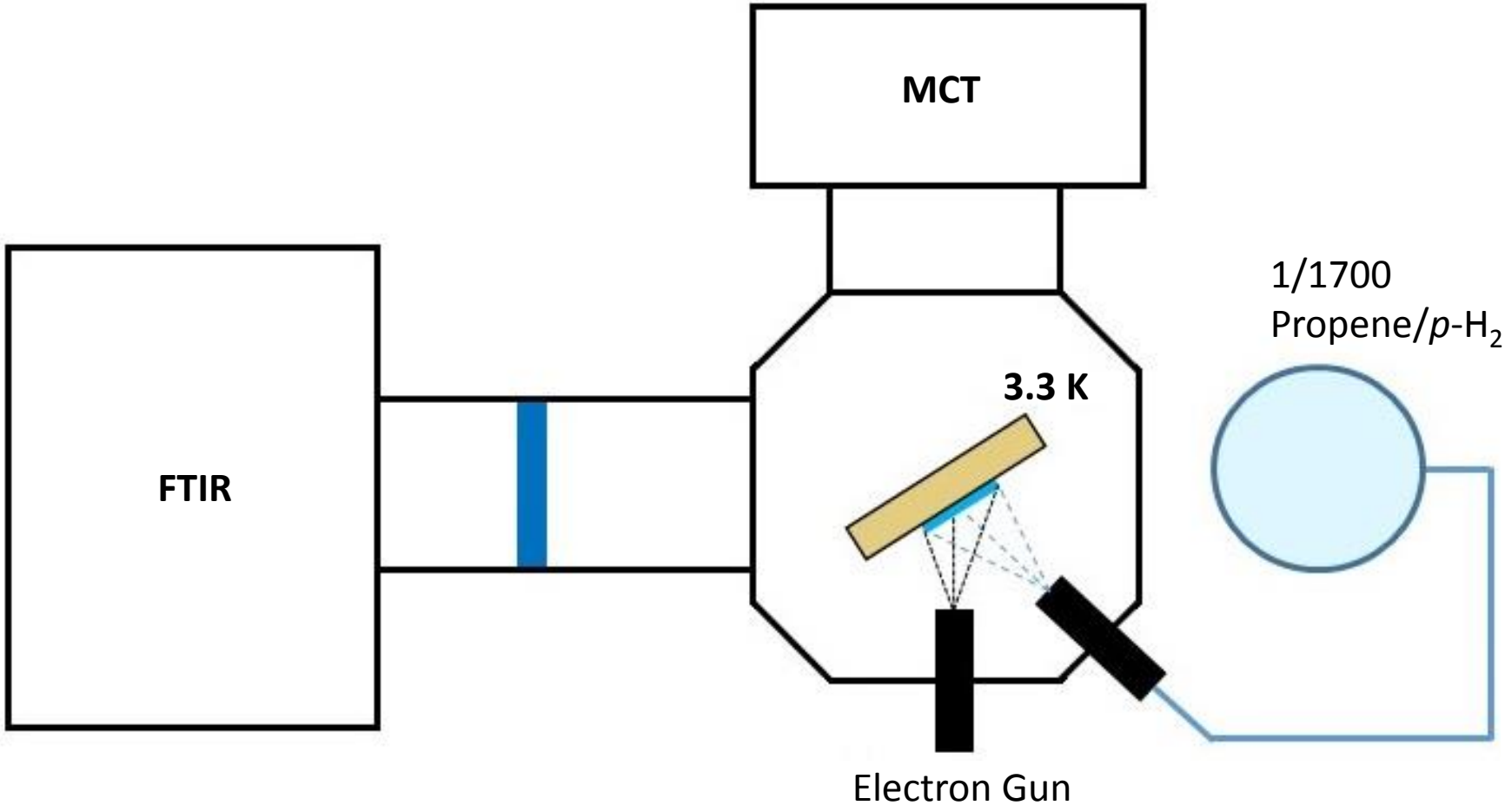

Hydrogen Addition to Propene

$$e^- + H_2 \rightarrow {H_2}^+$$

$${H_2}^+ + H_2 \rightarrow {H_3}^+ + H$$

$$e^- + {H_3}^+ \rightarrow H_2 + H$$

$$\text{Propene} + H \rightarrow \text{Propyl radical}$$

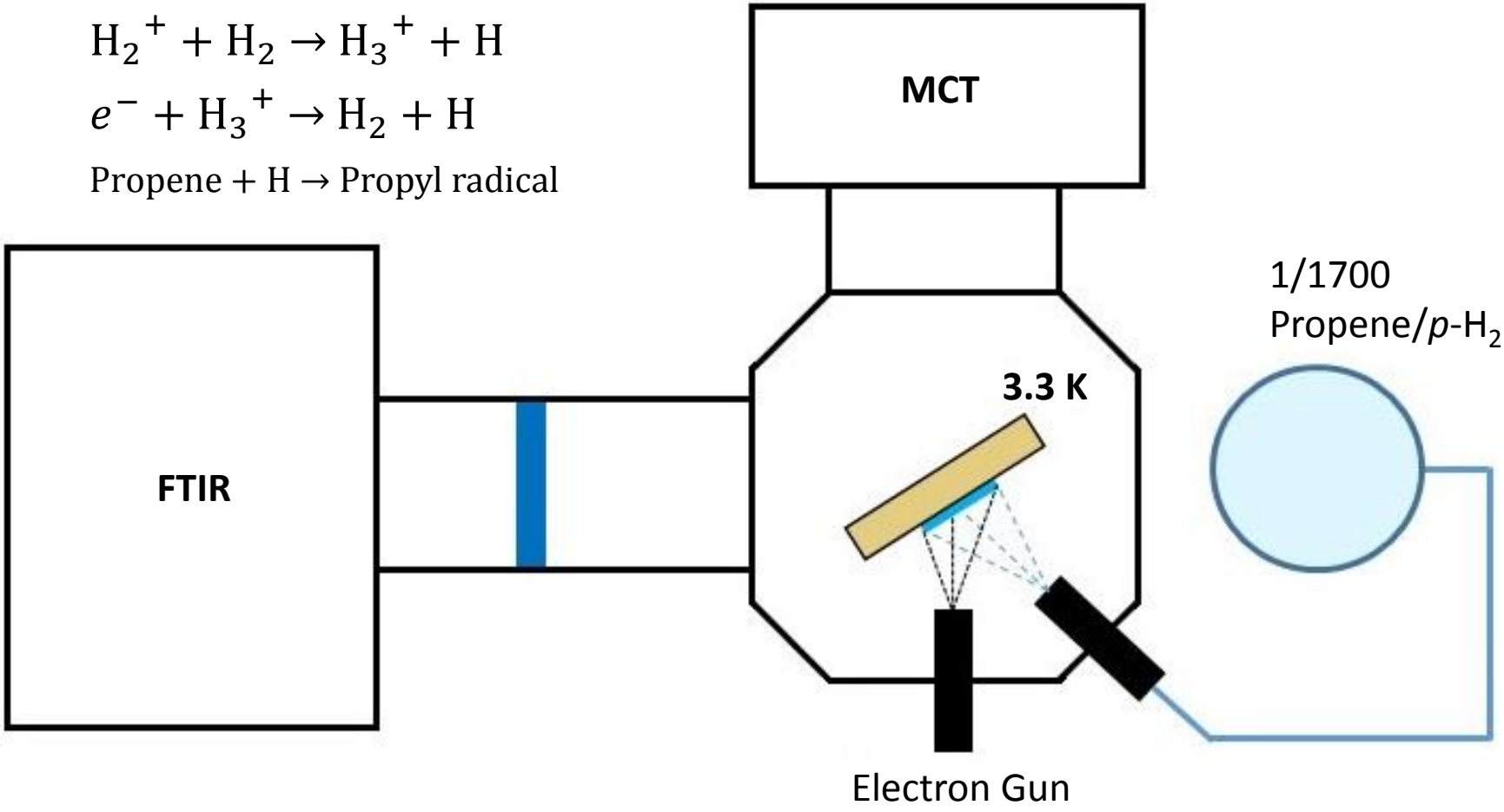

Hydrogen Addition to Propene

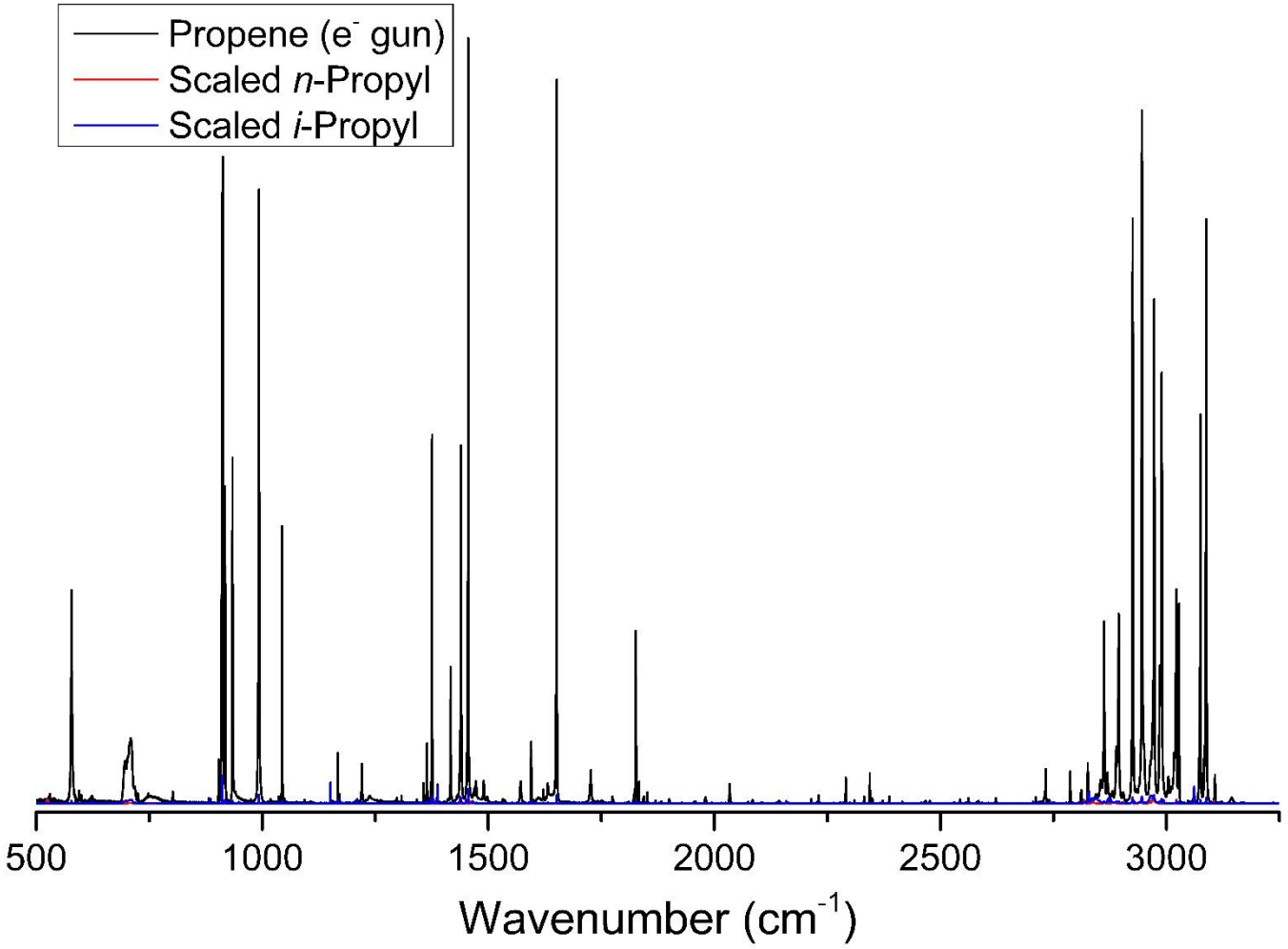

Hydrogen Addition to Propene

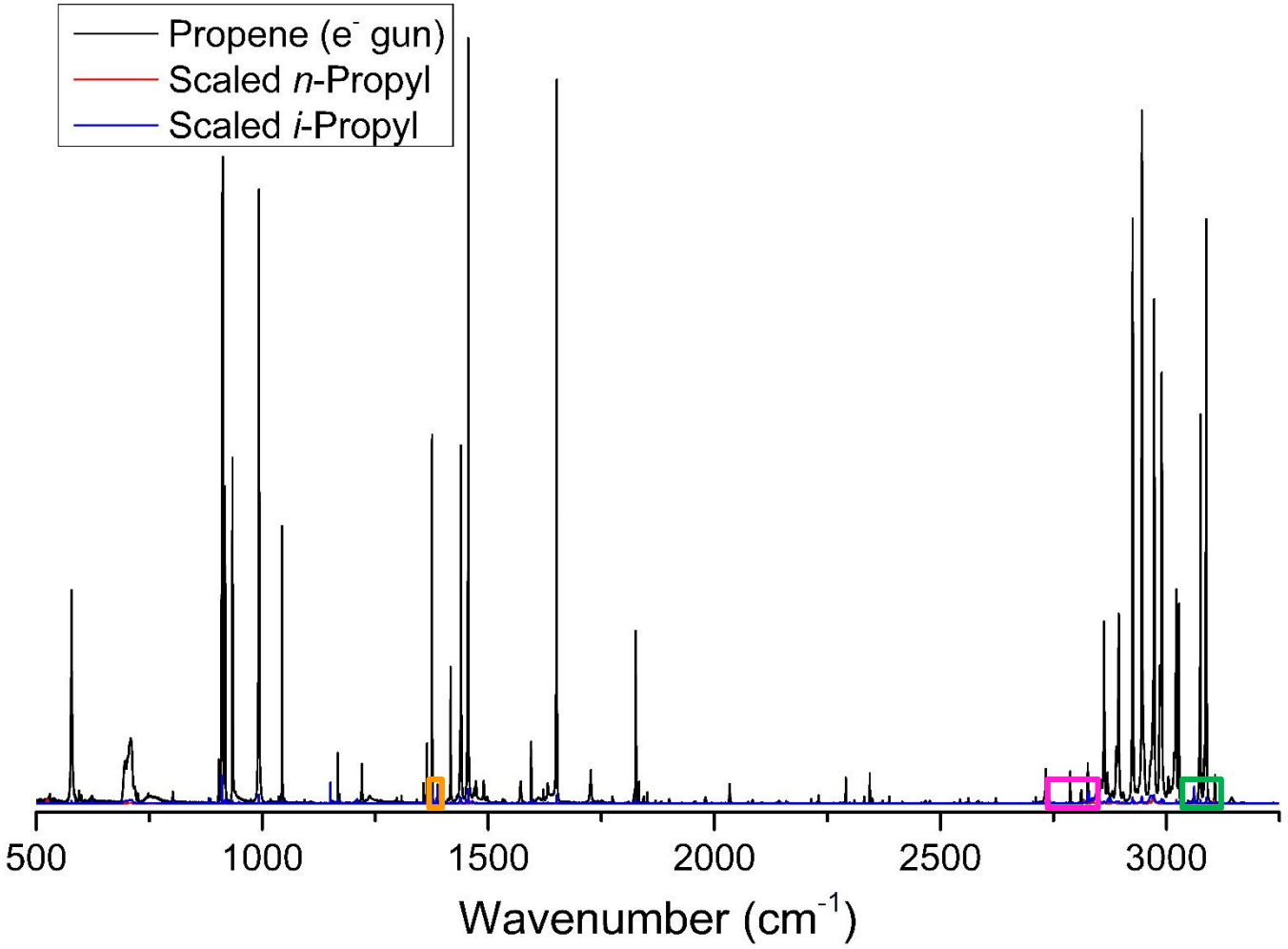

Hydrogen Addition to Propene

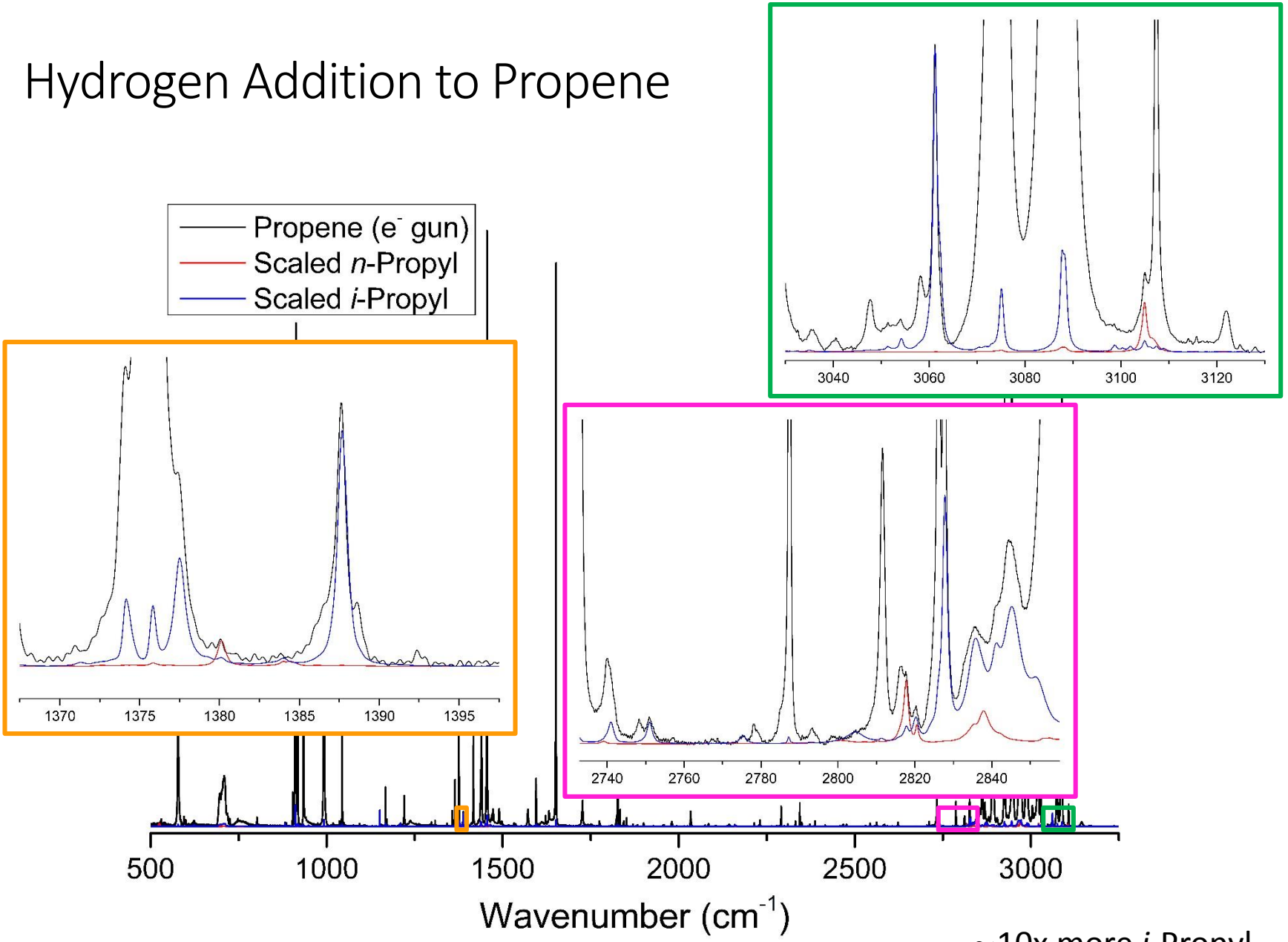

~10x more *i*-Propyl

Hydrogen Addition to Propene

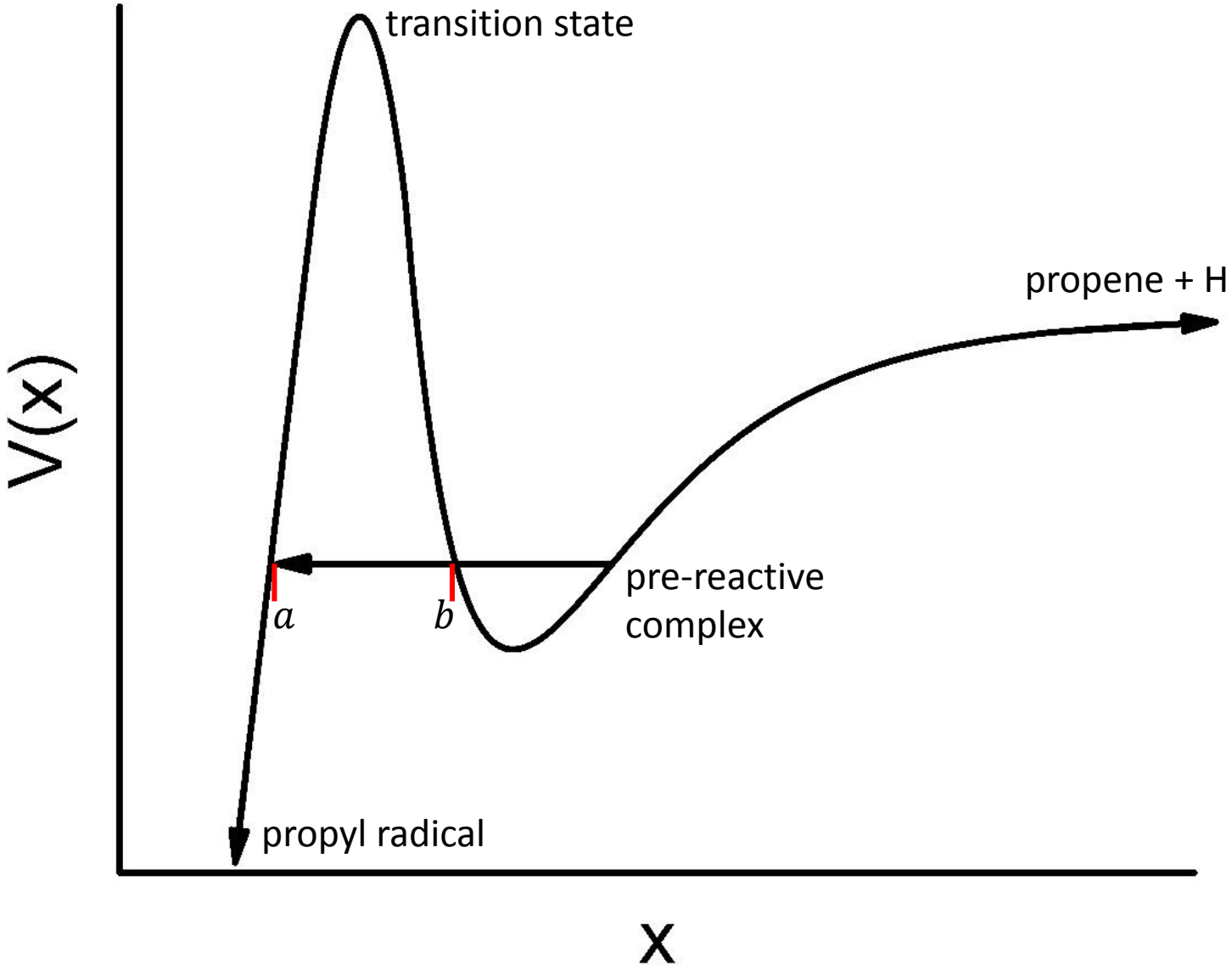

Hydrogen Addition to Propene

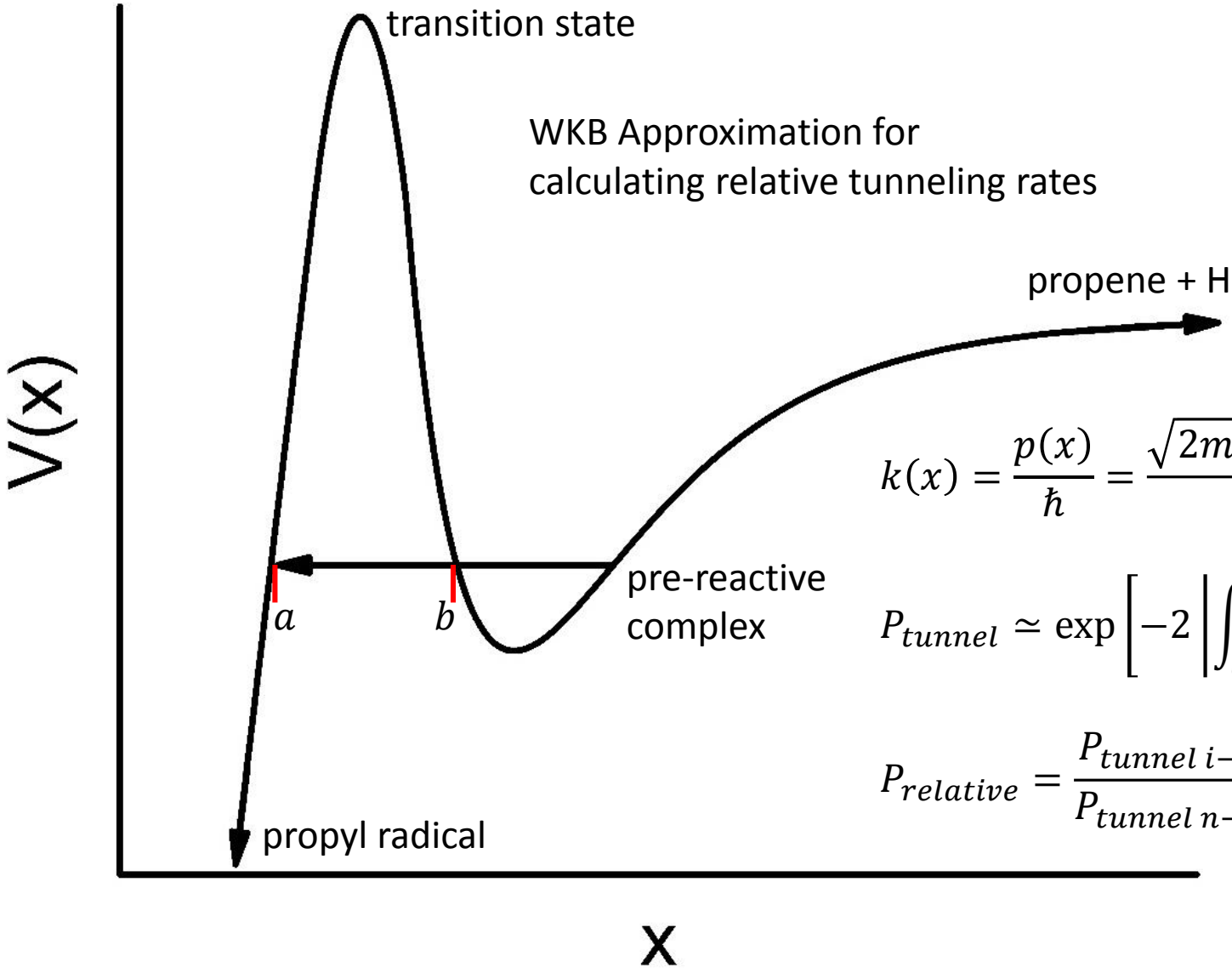

WKB Approximation for
calculating relative tunneling rates

$$k(x) = \frac{p(x)}{\hbar} = \frac{\sqrt{2m[E - V(x)]}}{\hbar}$$

$$P_{tunnel} \simeq \exp\left[-2\left|\int_a^b k(x)\,dx\right|\right]$$

$$P_{relative} = \frac{P_{tunnel\ i-Propyl}}{P_{tunnel\ n-Propyl}}$$

Hydrogen Addition to Propene

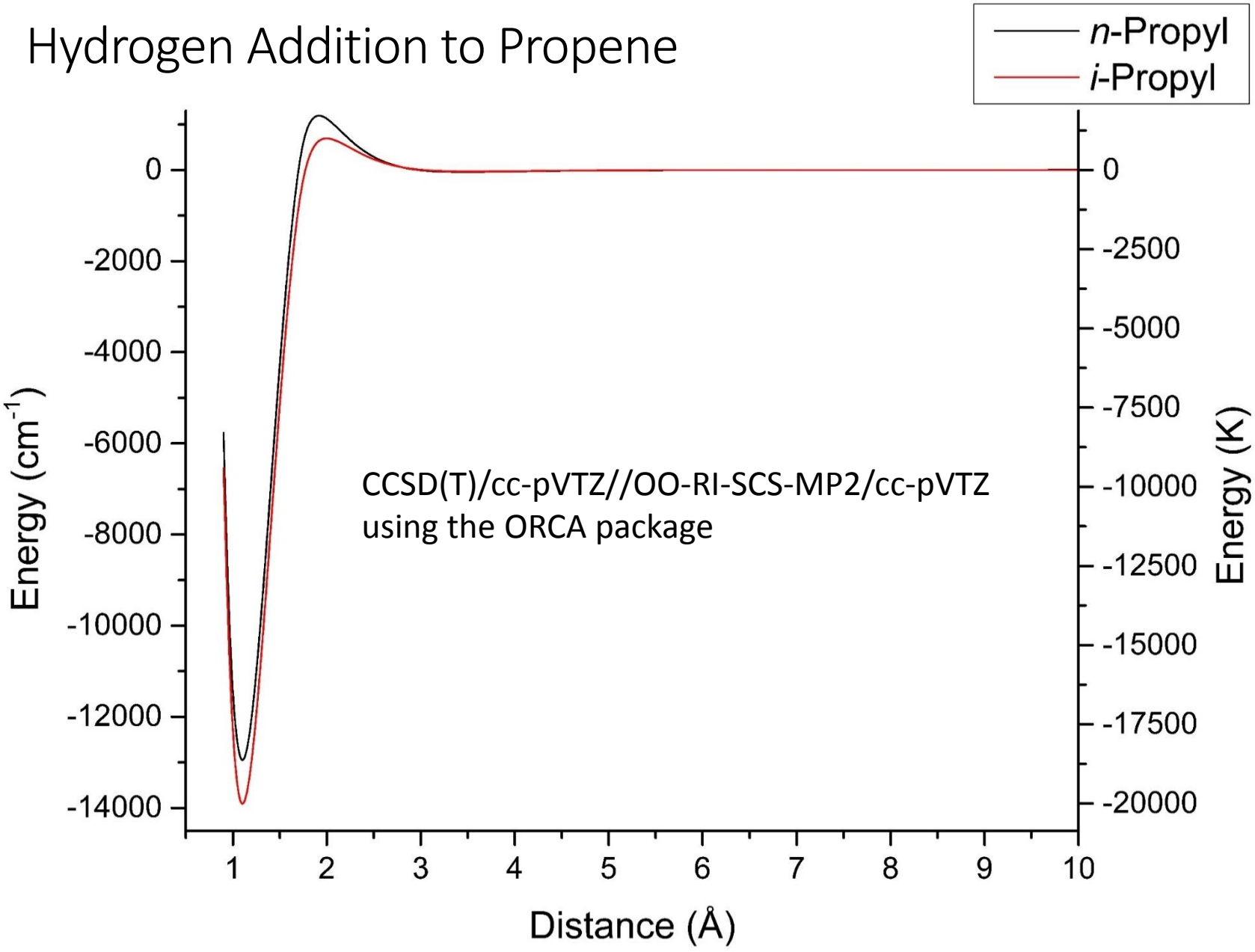

Hydrogen Addition to Propene

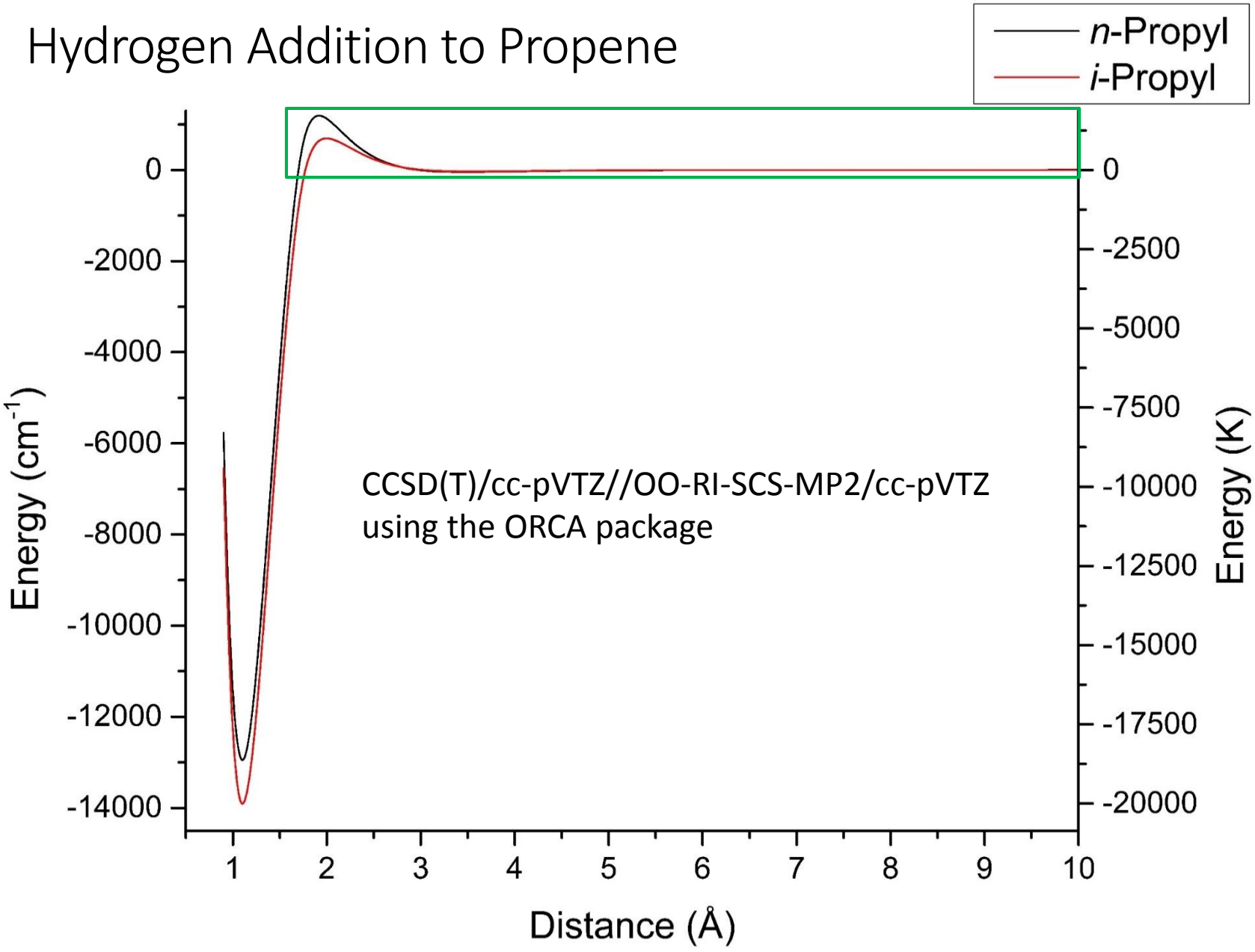

Hydrogen Addition to Propene

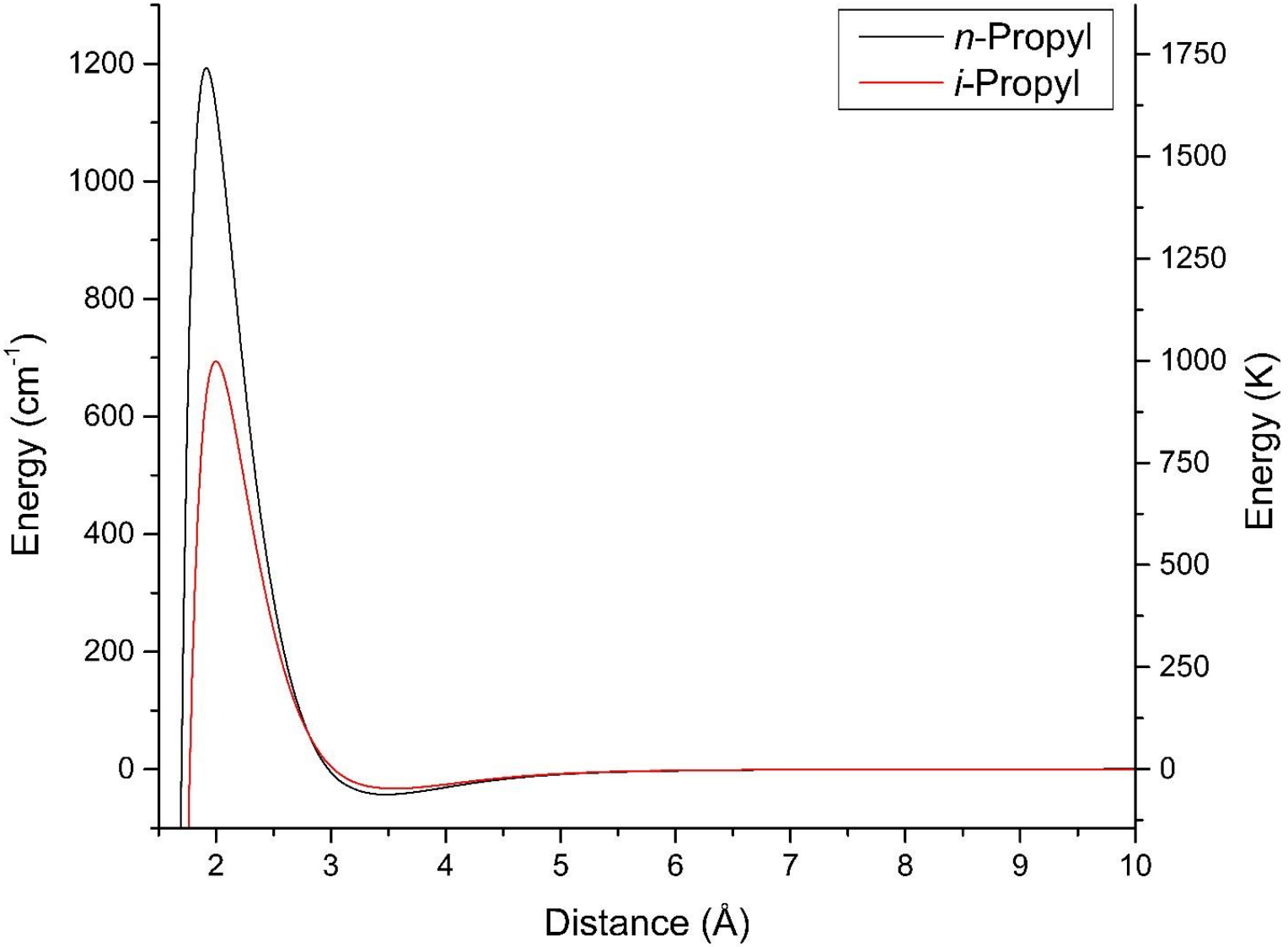

Hydrogen Addition to Propene

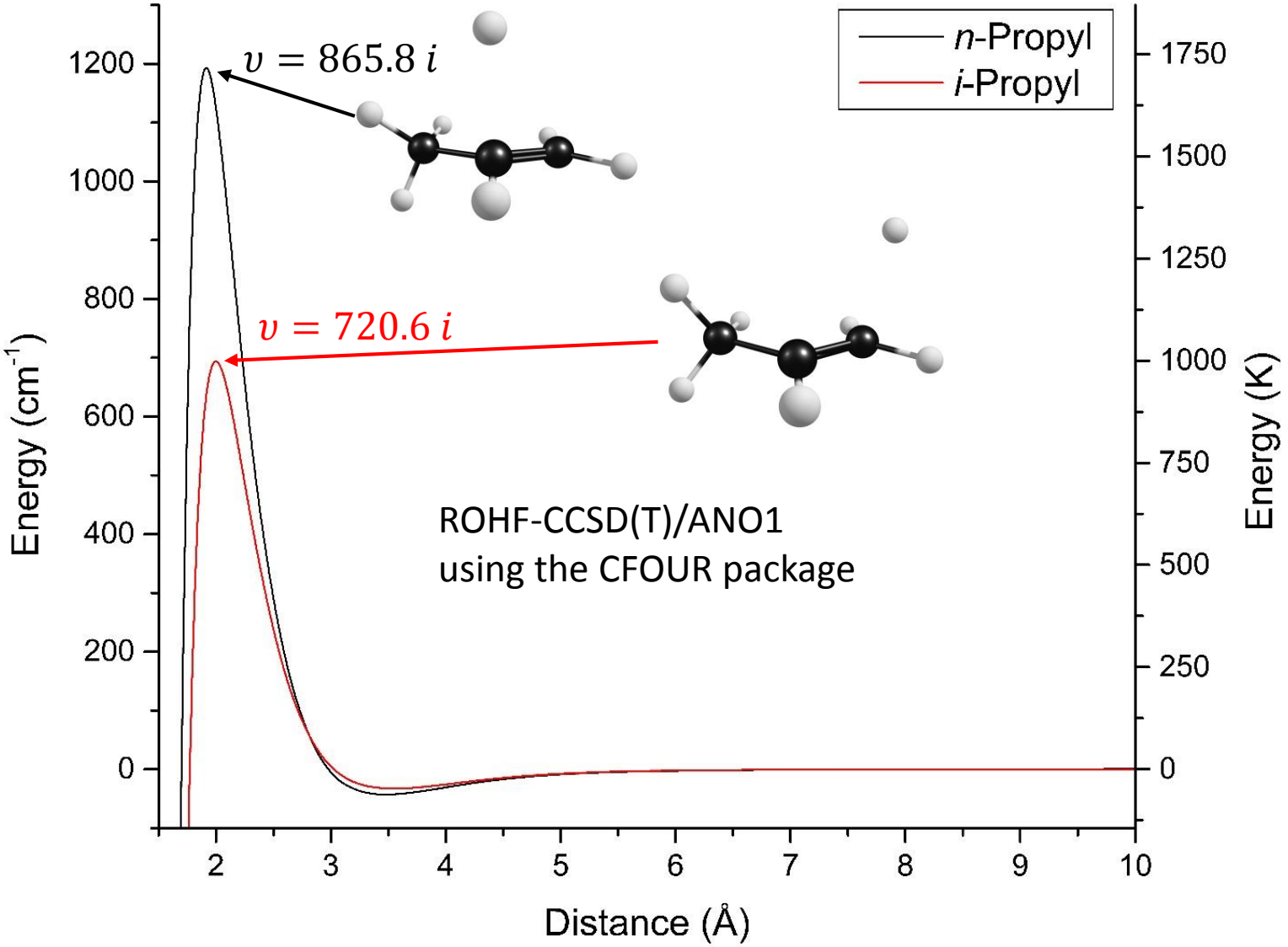

Hydrogen Addition to Propene

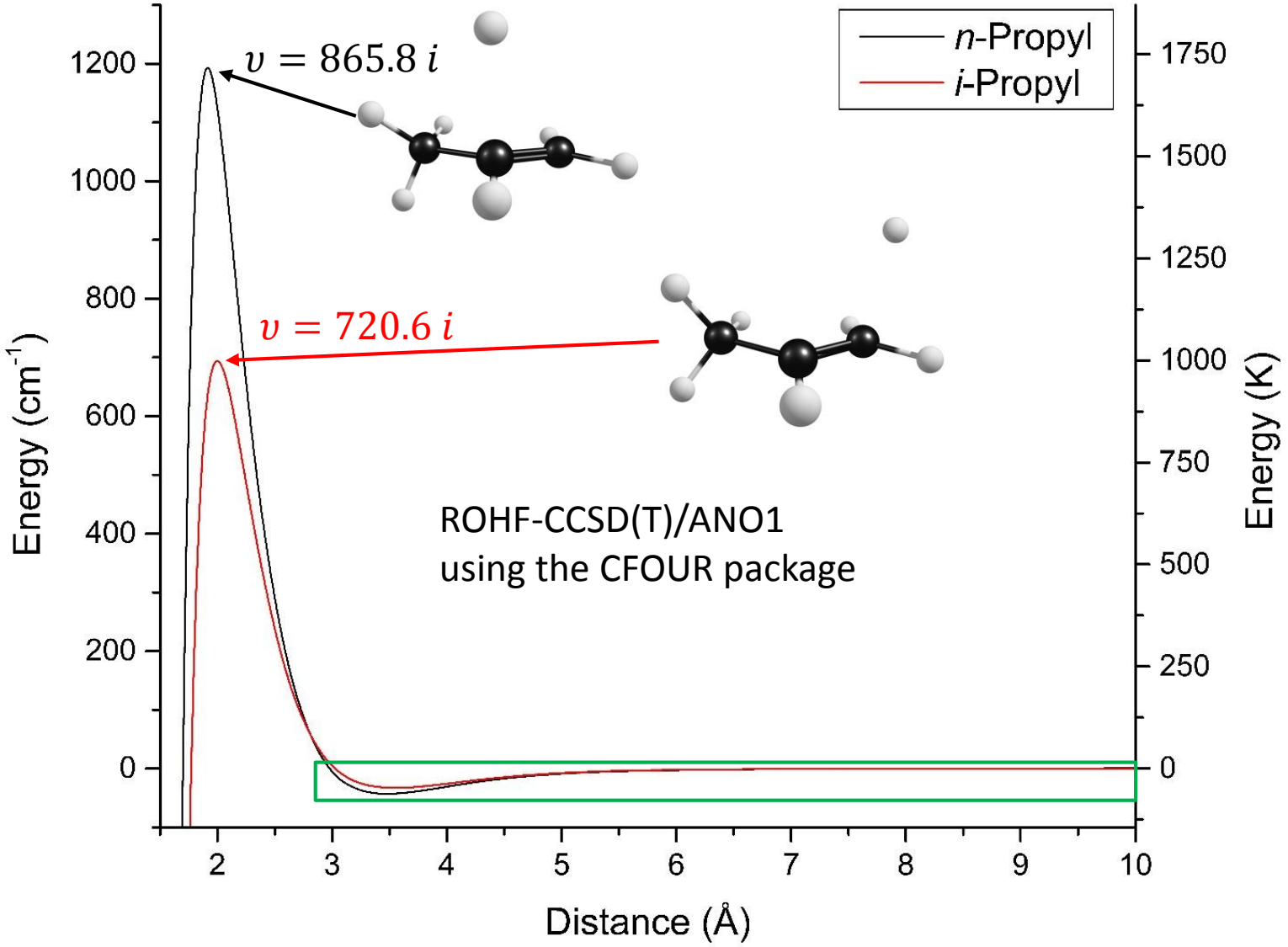

Hydrogen Addition to Propene

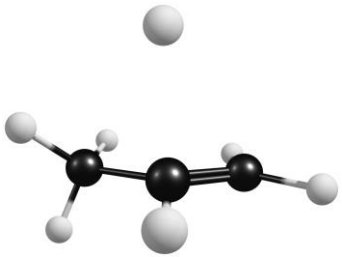

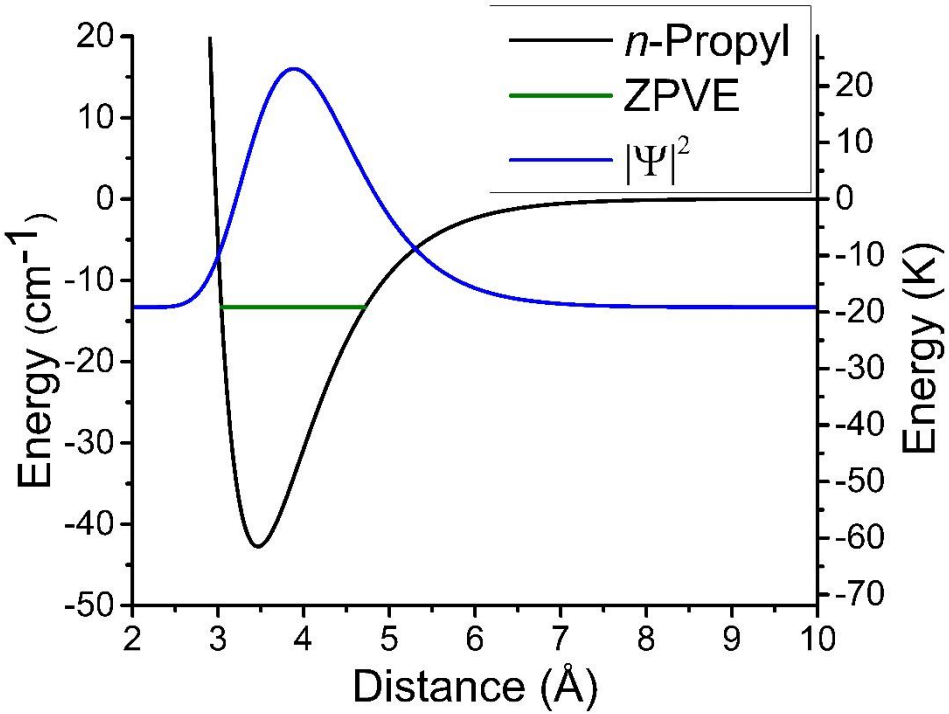

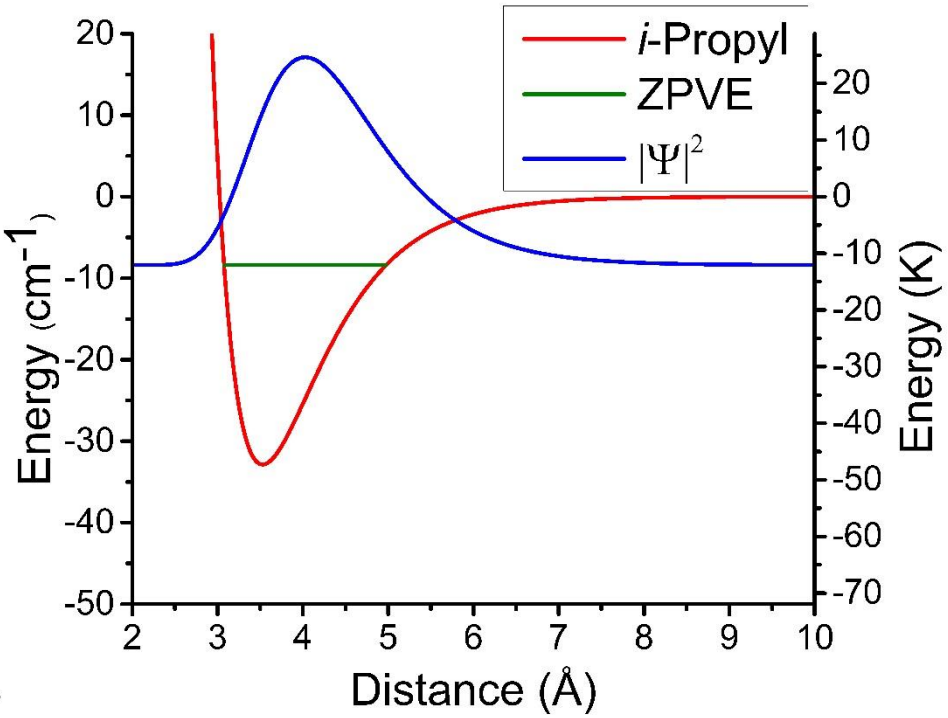

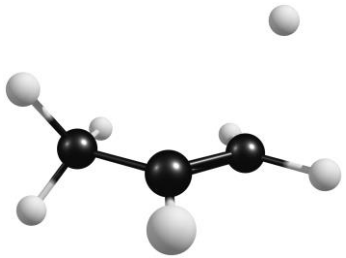

Hydrogen Addition to Propene

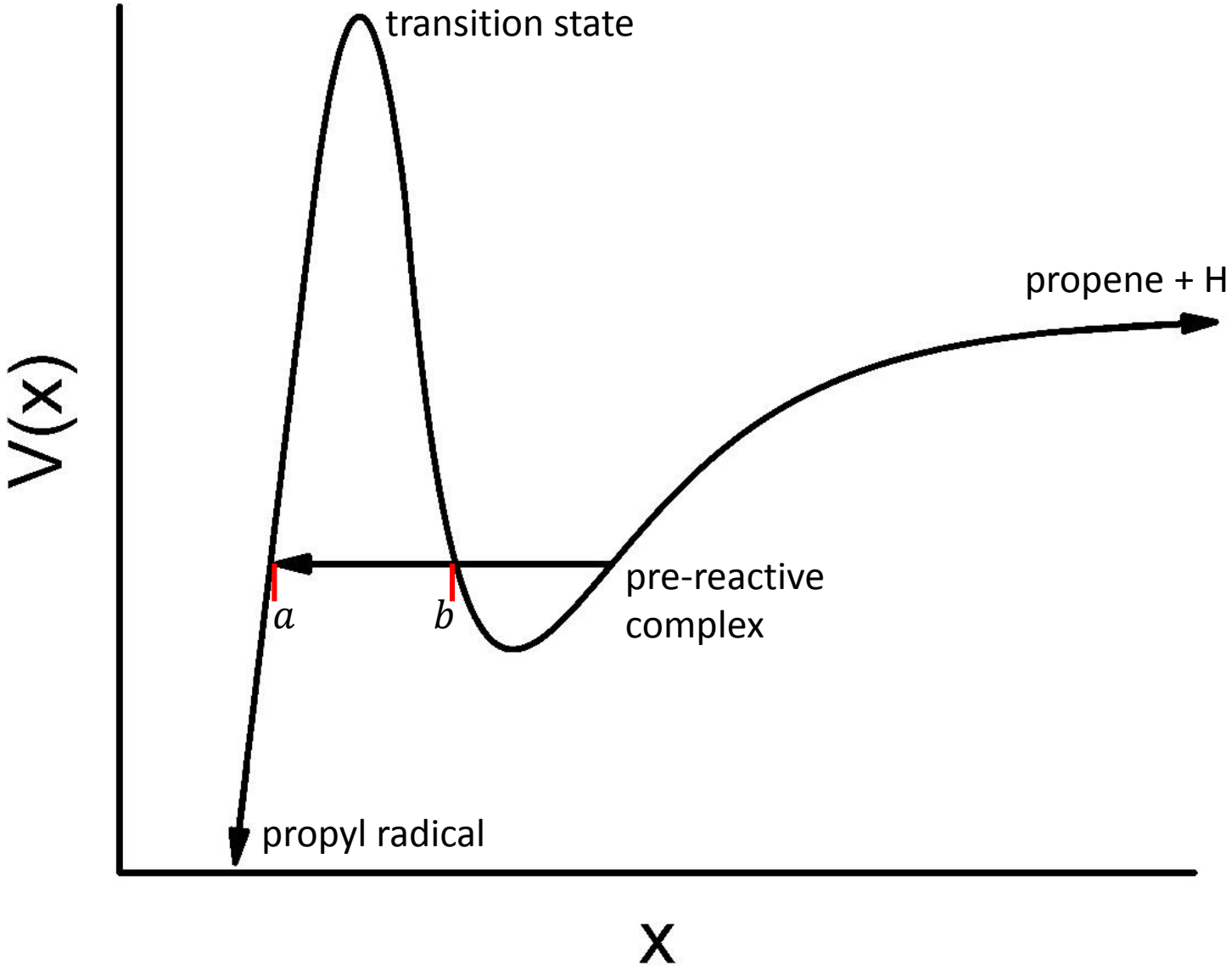

Hydrogen Addition to Propene

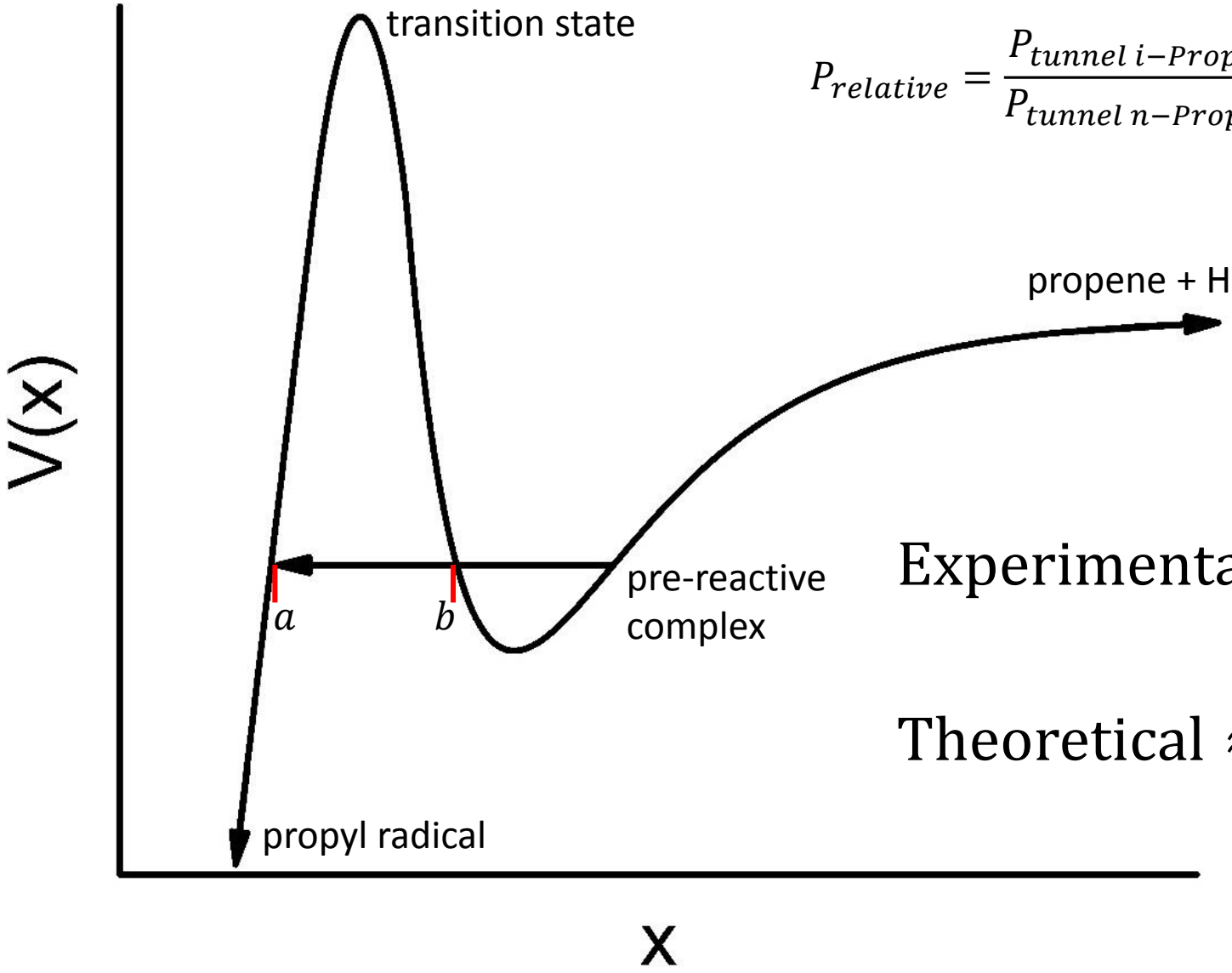

$$P_{relative} = \frac{P_{tunnel\ i-Propyl}}{P_{tunnel\ n-Propyl}}$$

$$\text{Experimental} \approx \frac{10}{1}$$

$$\text{Theoretical} \approx \frac{20}{1}$$

Conclusions

- We measured the spectrum of propene using two different experimental methods
- We observed significantly different intensity ratios in two regions of the spectra
- These differences were determined to arise from very weakly and indirectly coupled modes that only interact and share intensity when they are very close in energy, and any slight matrix perturbation can shift them into or out of resonance, inducing or removing intensity borrowing

- We measured the hydrogen addition to propene tunneling rates in a *p*-H_2 matrix
- Theoretical predictions for the relative tunneling rates mostly agree with experimental measurements

Funding/Support

U.S. DEPARTMENT OF ENERGY

Office of International Education
UNIVERSITY OF GEORGIA

Graduate School
UNIVERSITY OF GEORGIA

科 技 部

Ministry of Science and Technology

國立交通大學
National Chiao Tung University

Support:

U.S. Department of Energy, Office of Science (BES-GPCP)
U.S. National Science Foundation
The University of Georgia, Office of International Education
The University of Georgia, Graduate School
The Ministry of Science and Technology of Taiwan
The Ministry of Education of Taiwan
National Chiao Tung University

Acknowledgements

Dr. Yuan-Pern Lee

Dr. Gary Douberly

Dr. Karolina Haupa
Dr. Jay Amicangelo
Kelly Tseng
Peter Chen
The rest of the Lee group

Peter Franke
Joseph Brice
Alaina Brown
The rest of the Douberly group

Thank you for your attention

Propene Harmonic Frequencies

		ANO1		ANO2		
		Freq	Int	Freq	Int	Mode Type
ν_1	A'	3234.0	14.4	3233.4	13.0	α-CH_2 antisymmetric C-H stretch
ν_2	A'	3155.8	11.5	3153.1	10.7	β-CH C-H stretch
ν_3	A'	3141.6	13.6	3138.9	14.2	α-CH_2 symmetric C-H stretch
ν_4	A'	3117.3	11.0	3117.7	9.2	γ-CH_3 antisymmetric C-H stretch
ν_5	A'	3030.8	19.6	3031.1	19.1	γ-CH_3 symmetric C-H stretch
ν_6	A'	1695.0	9.5	1696.6	10.7	α-β C=C stretch
ν_7	A'	1498.0	12.8	1501.0	13.2	γ-CH_3 antisymmetric C-H bend
ν_8	A'	1451.8	1.2	1454.2	1.2	α-CH_2 C-H bend
ν_9	A'	1406.1	1.5	1408.9	1.5	γ-CH_3 symmetric C-H bend
ν_{10}	A'	1320.5	0.2	1322.1	0.1	β-CH C-H bend
ν_{11}	A'	1191.5	0.2	1194.0	0.1	in-phase α-CH_2 + γ-CH_3 rock
ν_{12}	A'	941.5	3.2	942.8	3.1	out-of-phase α-CH_2 + γ-CH_3 rock
ν_{13}	A'	929.4	1.9	932.1	2.0	β-γ C-C stretch
ν_{14}	A'	419.2	0.9	420.3	0.9	C-C-C bend
ν_{15}	A"	3093.6	16.8	3094.2	14.9	γ-CH_3 antisymmetric C-H stretch
ν_{16}	A"	1484.6	6.3	1487.8	6.3	γ-CH_3 antisymmetric C-H bend
ν_{17}	A"	1067.4	2.6	1068.8	2.6	γ-CH_3 rock
ν_{18}	A"	1018.6	13.0	1018.0	12.6	β-CH H wag
ν_{19}	A"	929.7	38.8	929.5	38.3	α-CH_2 C-H wag
ν_{20}	A"	583.3	11.0	583.7	11.0	β-CH C wag
ν_{21}	A"	201.9	0.4	203.8	0.4	γ-CH_3 methyl torsion

Propene + H Scan Multireference Character

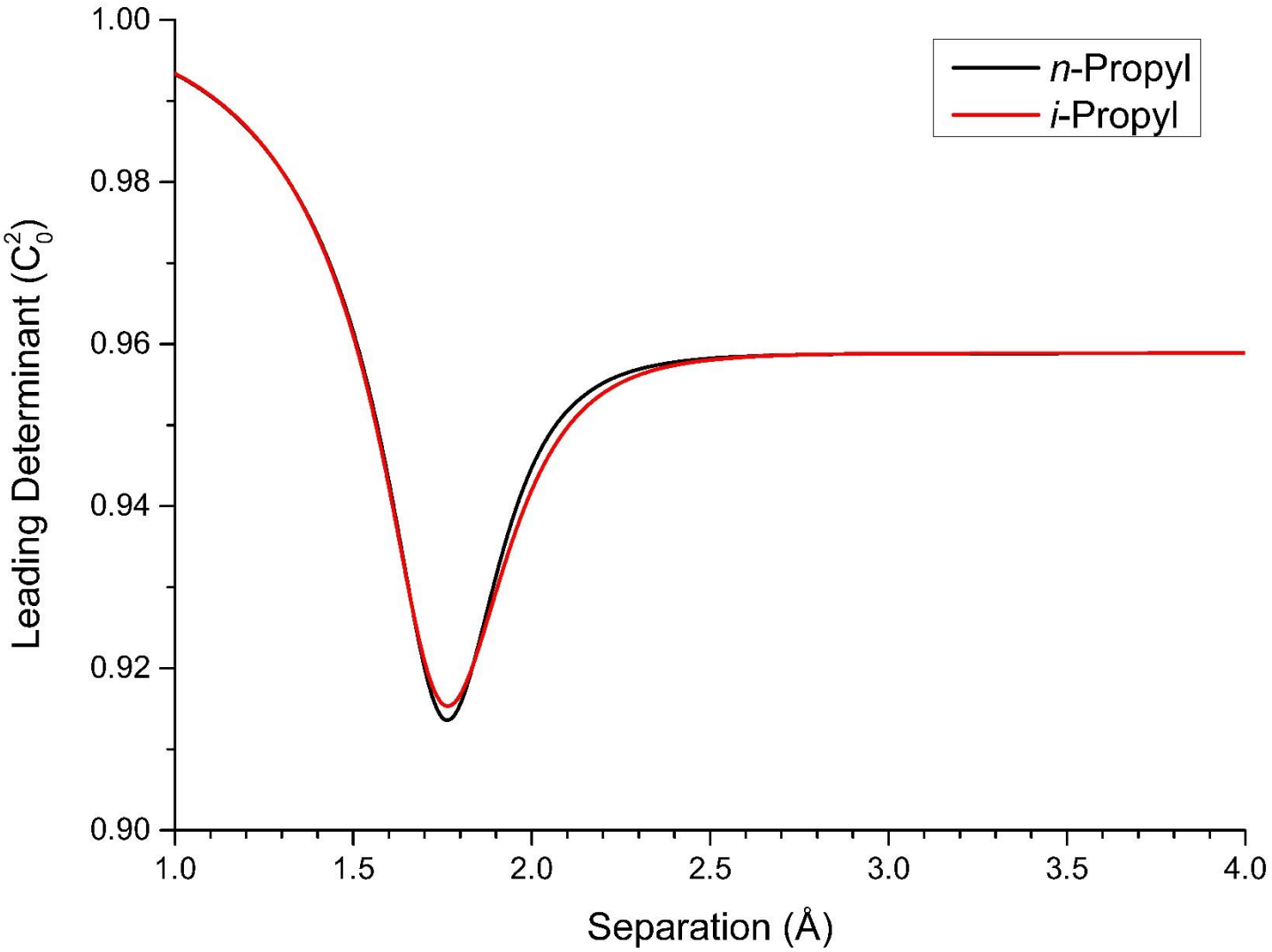

p-H_2 Matrix Isolation Experimental Details

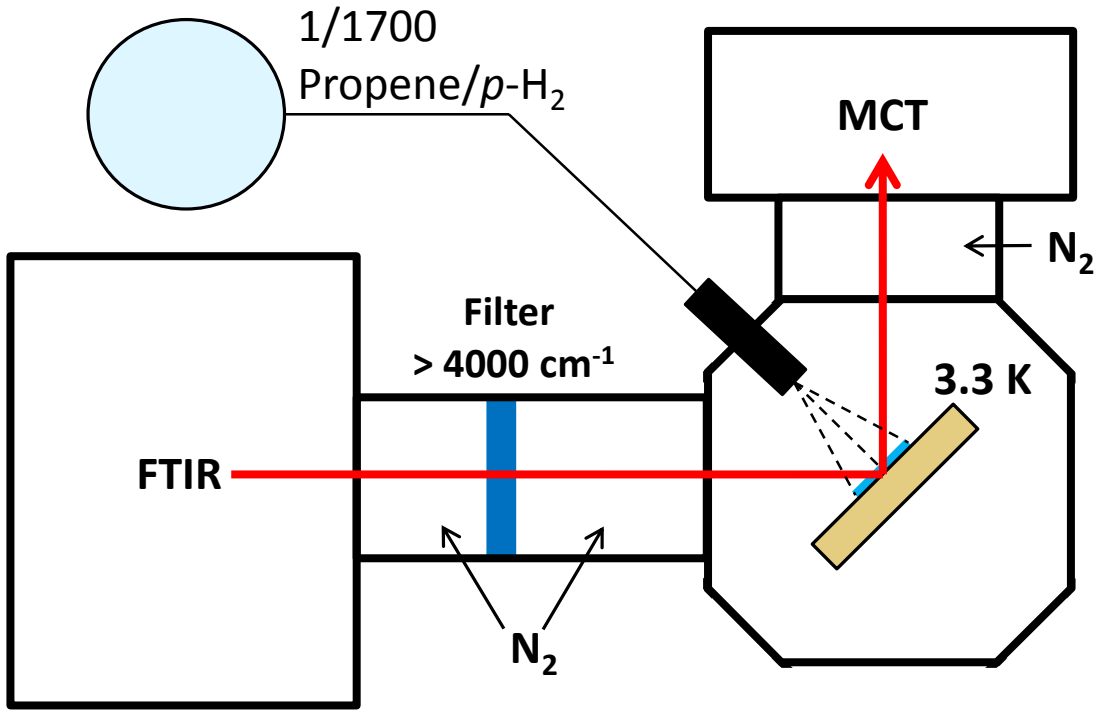

Bruker Vertex 80v FTIR
KBr Beamsplitter
Range: 4000 – 400 cm^{-1}
Resolution: 0.25 cm^{-1}
200 scans

IR filter: Spectrogon LP-2500
cut-off wavelength ~2.4 µm
(~4200 cm^{-1})

L-N_2 cooled MCT detector

Matrix mirror: 1 in diameter
gold coated copper plate
Deposition time: 10 hr
Gas flow rate: ~4 sccm
(~11 mmol/hr)

Production of *p*-H_2 Details

Fe_2O_3 catalyst
Temperature: 12.9 $\pm$ 0.5 K
Final concentration of *o*-H_2:
$\sim$400 – 600 ppm

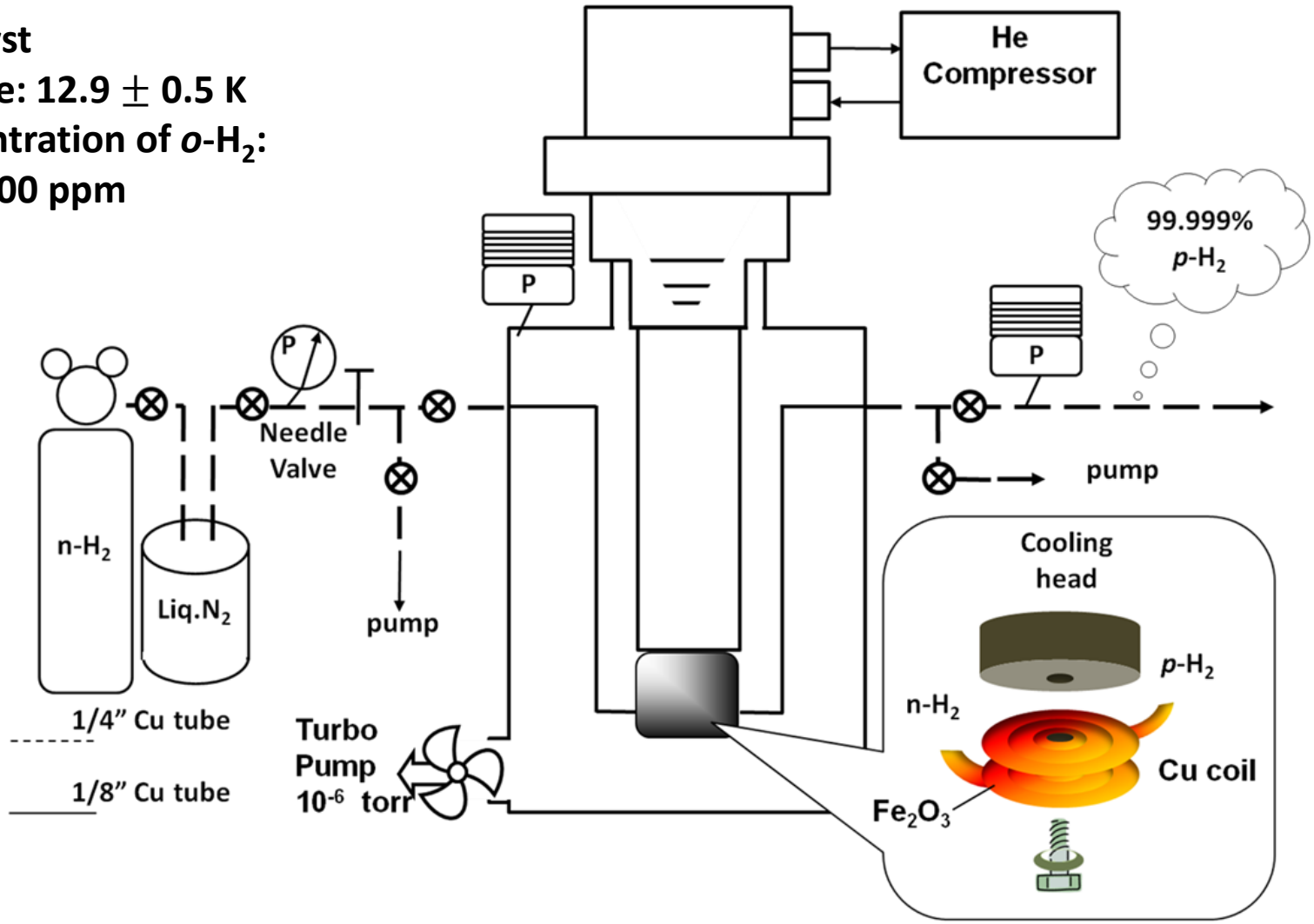

Basic quantum physics of solid *p*-H_2

Fermion (^{1}H Nuclear spin I = $\frac{1}{2}$) ➡ ψ_{total}: anti-symmetric

$$\psi_{total} = \psi_e \, \psi_v \, \psi_r \, \psi_n$$

ψ_r	ψ_n
Odd J Anti-symmetric Ground State: $J = 1$	Symmetric ***ortho*-H_2**
Even J Symmetric Ground State: $J = 0$	Anti-symmetric ***para*-H_2**

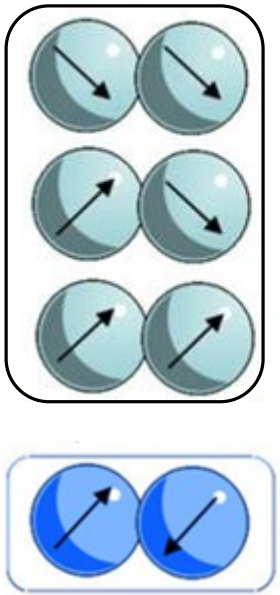

The ratio of *o*-H_2:*p*-H_2 is 3:1 @ R.T. and 0:1 @ 0 K

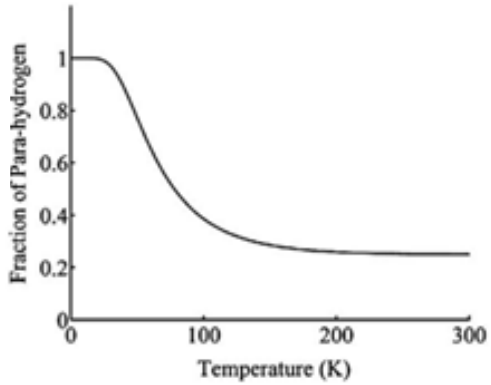

1. Equilibrium fraction of para-hydrogen as a function of temperature.

Benefits of *p*-H_2 as Matrix Host

No dipole moment

J = 0 rotational state is occupied
spherically symmetric charge distribution

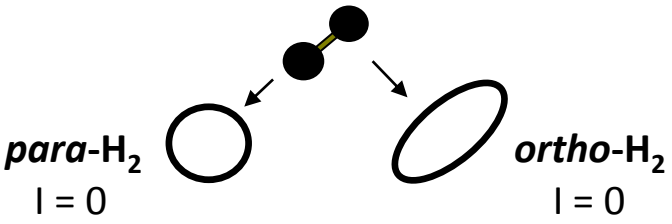

Ar and Ne have fcc and hcp crystal structures

p-H_2 only has an hcp crystal structure

The host-guest interaction in *p*-H_2 is weaker than in rare gas matrices

	***p*-H_2**	**Ne**	**Ar**
Lattice Constant (Å)	3.78	4.47	5.31
Zero-Point Amplitude Motion	18%	9%	5%
Zero-Point Lattice Vibration (Å)	0.68	0.42	0.27

p-H_2 has a high thermal conductivity

	***p*-H_2**	**Fe**	**Ar**
Thermal Conductivity (W cm^{-1} K^{-1})	0.72	0.68	0.04

Benefits of large ZP vibrational motion in *p*-H_2

	***p*-H_2**	**Ne**	**Ar**
Lattice Constant (Å)	3.78	4.47	5.31
Zero-Point Amplitude Motion	18%	9%	5%
Zero-Point Lattice Vibration (Å)	0.68	0.42	0.27

The amplitude of the zero-point lattice vibrations of *p*-H_2 is a substantial fraction of the spacing between nearest H_2 molecules.

The matrix is considered to be ***'soft'***.

Crystal defects around guest species are expected to be repaired automatically.

Brings homogeneity to *p*-H_2 matrix.

Reduces the possibility of having *multiple trapping sites* and leads to reduced *inhomogeneous broadening of lines* of the guest molecules.

Benefits of large ZP vibrational motion in *p*-H_2

	***p*-H_2**	**Ne**	**Ar**
Lattice Constant (Å)	3.78	4.47	5.31
Zero-Point Amplitude Motion	18%	9%	5%
Zero-Point Lattice Vibration (Å)	0.68	0.42	0.27

Some guest molecule rotation possible

CO, CH_4, H_2O, and HCl:
slightly hindered rotation in solid *p*-H_2

Larger species:

Some internal rotation (torsion) feasible: CH_3OH

Some rotation about a single axis: CH_3F

Such rotations not observed in noble-gas matrices

Matrix cage effect

Inert-gas matrices

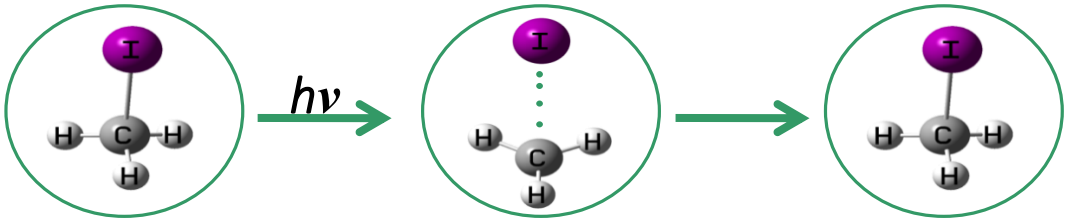

Diminished cage effect

p-H_2 matrix

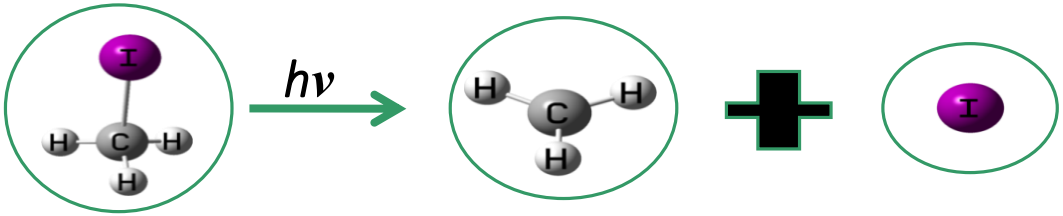

Introduction to VPT2+K

VTP2 with explicit treatment of Fermi and Darling-Dennison Resonances

$$\begin{pmatrix} \Omega_{10_2} & \frac{\phi_{10,10,7}}{4} & \frac{1}{2\sqrt{2}}K_{10,10;11,8} & D_{10,10;10,8} \\ \frac{\phi_{10,10,7}}{4} & \Omega_{7} & \frac{\phi_{11,8,7}}{2\sqrt{2}} & \frac{\phi_{10,8,7}}{2\sqrt{2}} \\ \frac{1}{2\sqrt{2}}K_{10,10;11,8} & \frac{\phi_{11,8,7}}{2\sqrt{2}} & \Omega_{11_18_1} & D_{11,8;10,8} \\ D_{10,10;10,8} & \frac{\phi_{10,8,7}}{2\sqrt{2}} & D_{11,8;10,8} & \Omega_{10_18_1} \end{pmatrix}$$

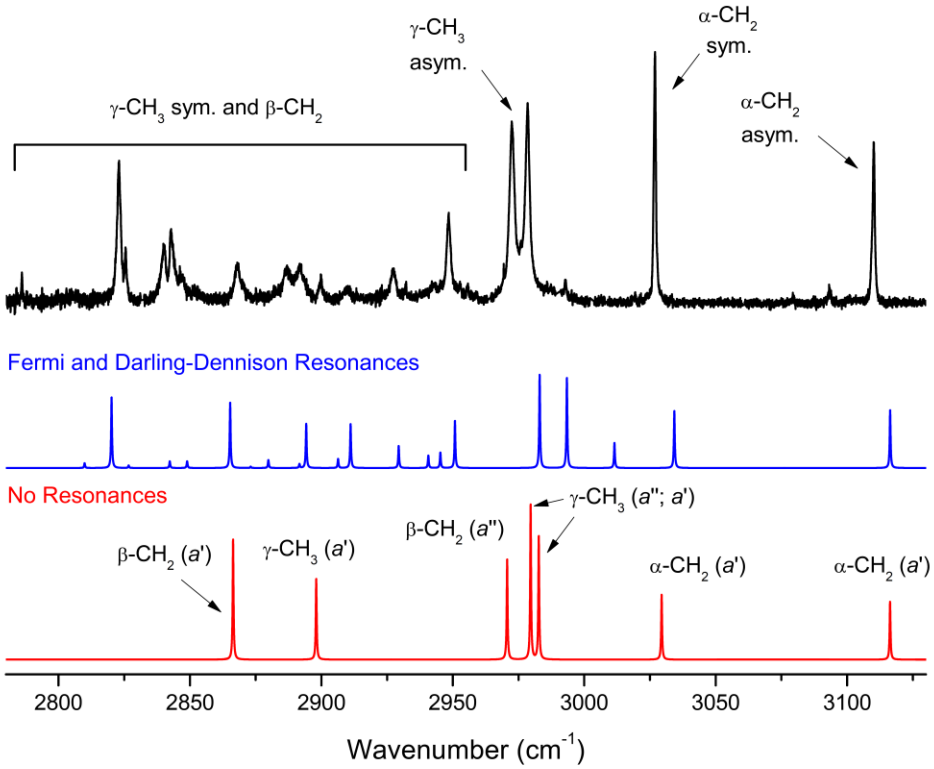

The VPT2+K method was applied using "semi-diagonal" quartic force fields computed at the CCSD(T) level of theory with the ANO1/ANO2 basis sets, using the CFOUR package. Our implementation of VPT2+K entails a full treatment of the vibrational problem with VPT2 (red trace) followed by deperturbation of the strong interactions between CH stretch fundamentals and CH bend overtones/combinations. The strong interactions are then treated explicitly via diagonalization of an effective Hamiltonian (small example provided above), yielding a theoretical spectrum that accounts for both Fermi and Darling-Dennison type resonance interactions (blue trace). The propene effective Hamiltonian contained 61 vibrational states. Electrical harmonicity was assumed (i.e. the harmonic intensities of the bright CH stretch fundamentals was distributed into the dark states proportional to the squares of their eigenvector coefficients).

Lockheed-Martin Aculight ARGOS continuous-wave mid-infrared optical parametric oscillator lasers (cw mid-IR OPOs).

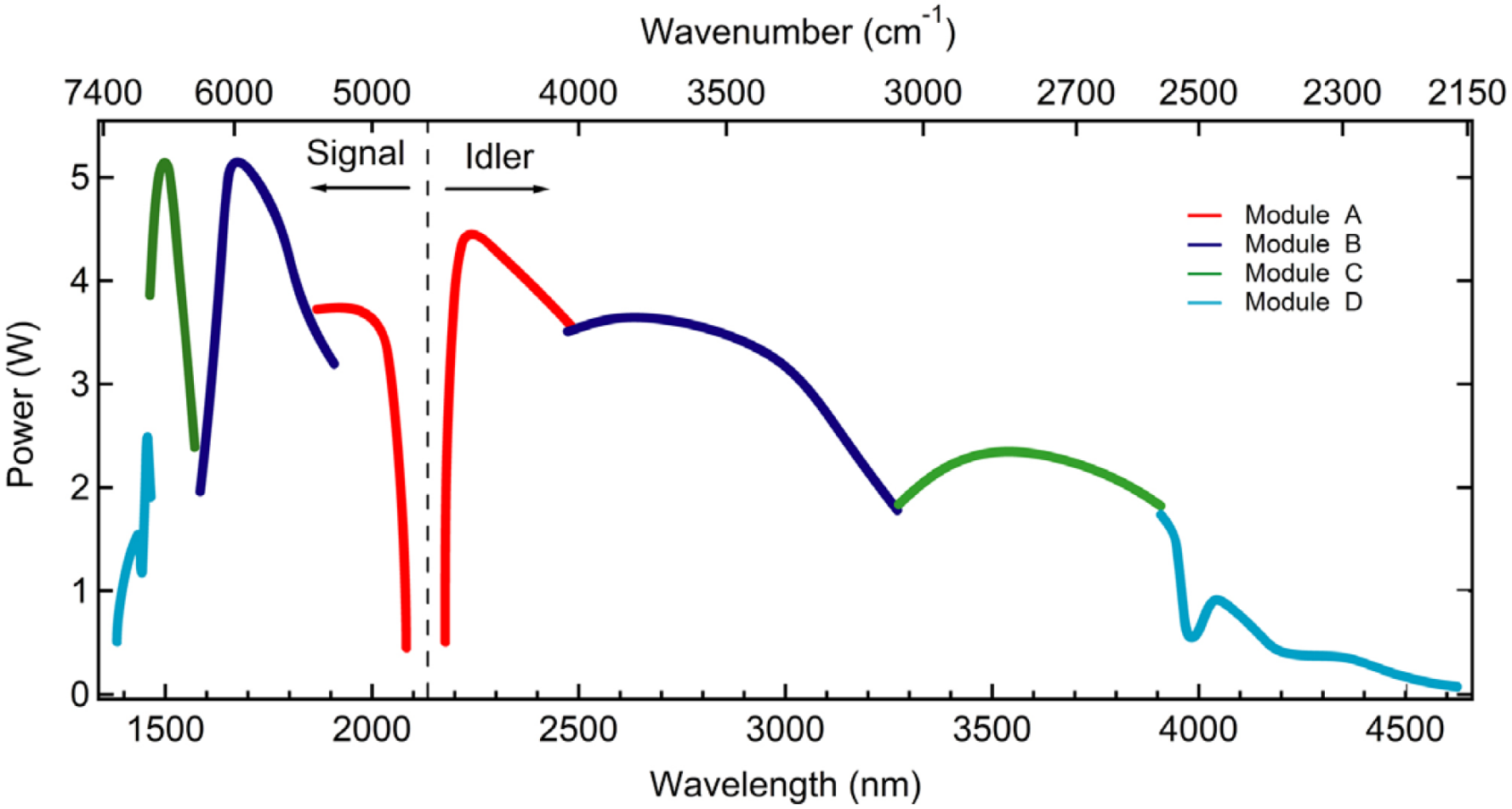

Typical Power vs. Wavelength for Model 2400-SF-15

(http://www.lockheedmartin.com/content/dam/lockheed/data/ms2/documents/aculight/Argos_Model_2400_SF_Series_Brochure.pdf)